ELASTIC SETTLEMENT PREDICTION OF CEMENT-TREATED CLAYEY GROUND IN SMALL STRAIN MECHANICAL BEHAVIOR

ムハンマド, アクマル, プテラ

ELASTIC SETTLEMENT PREDICTION OF CEMENT-TREATED CLAYEY GROUND IN SMALL STRAIN MECHANICAL BEHAVIOR

MUHAMMAD AKMAL PUTERA

JULY 2022

KYUSHU
UNIVERSITY

Doctoral Thesis

ELASTIC SETTLEMENT PREDICTION OF CEMENT-TREATED CLAYEY GROUND IN SMALL STRAIN MECHANICAL BEHAVIOR

By

MUHAMMAD AKMAL PUTERA

Supervised by

PROF. NORIYUKI YASUFUKU

Graduate School of Engineering

Department of Civil and Structural Engineering

Faculty of Engineering

Kyushu University

July 2022

ACKNOWLEDGMENT

After an intensive period of my doctoral study, I am writing this dissertation has had a significant impact on me. I would like to reflect on the people who have supported me so much throughout this period.

I would like to express my distinct appreciation and sincere gratitude to my supervisor Prof. Noriyuki YASUFUKU, for his patience, motivation, enthusiasm, endless encouragement, immense knowledge, and guidance throughout my doctoral journey in Japan. He has always been available to support and encourage me, make him a very great supervisor. He inspired me about the geotechnical engineering in fundamental things, in elemental testing, and taught us to improve our critical thinking to find the originality and applications. Thank you for your kindness and for accepting me three years ago, this experience will enhance my research ability and always remind me for never be enough to think deeper about anything.

I would like to express my gratefulness to all members of examining committee, Prof. Hideki SHIMADA, and Prof. Kiyonobu KASAMA for their treasured time, attentive evaluation, and valuable comments on my works.

I would also like to address my thanks to Assoc. Prof. Ryohei ISHIKURA for his precious guidance and valuable advice during my research and writing process of this dissertation. My grateful appreciation is also addressed to Assoc. Prof. Ahmad RIFA'I for his patient and kindness in guiding me and always gives me precious advice during my research works.

Thousand of appreciation also goes to Assistant Prof. Adel ALOWAISY for his crucial contribution, worth guidance and valuable advice during my research work. I would also like to thank and acknowledge with much appreciation to the academic

and technical staff in Geotechnical Engineering Laboratory, both past and present, Mrs. Aki ITO. Special thanks and appreciation also go to Mr. Michio NAKASHIMA for his great assistance and technical support in the laboratory testing. My special gratitude is given to present and past research members in Geotechnical Engineering Laboratory for their friendship and support throughout my time at Kyushu University.

I would also like to take this opportunity to express the profound gratitude of my sincere heart to my beloved parents and family for their love, wise counsel, and always be my all ears with patience. I miss you all.

Finally, fight the big challenges and great opportunities will come afterward.

Thank you very much!

AKMAL

Fukuoka, 2022.

ABSTRACT

Among other developing countries, Indonesia is developing its infrastructure, including a High-Speed Railway (HSR) project (maximum speed of 300 km/h) that is expected to connect the Jakarta and Surabaya cities, extending for 700 km. Along the railway, the lowland area is comprised mainly of clayey soil extending for a depth of 10-15 m on average. The clayey soil is characterized by high compressibility index and liquid limit, which exhibits settlement behavior. The engineering properties, mainly the compressibility index and liquid limit, are similar to the natural Ariake clayey distributed around the Ariake sea. Therefore, it was adopted for testing in this research. The maximum allowable settlement can be divided into two categories based on the Japanese railway standard for HSR, ranging from 10 mm to 30 mm. Proper railway structures such as ballastless tracks are usually considered to reduce the settlement potential. Despite the track structure, the subsoil mechanical properties often require improvement to limit the railway's settlement. Using Cement-Treated Soil (CTS) is a low cost-technique with high stiffness improvement in a short time. Thus, it is considered a reliable cheap technique, especially for developing countries. Through this study, settlement behavior mainly within elastic conditions was investigated considering the actual low vertical stress near-zero displacement on the ground surface. However, in reality, the accumulation of stress with time might cause elastoplastic settlement of the ground. Furthermore, anticipating and observing the mechanical behavior of CTS is associated with remarkable uncertainties, especially for the small-strain ranges within the elastic and elastoplastic conditions. In addition, optimizing laboratory mechanical behavior (Shear strength) testing using small-strain tools can improve the accuracy under small-strain ranges. The results are expected to be a simple tool for estimating the optimum mixing ratio for cement-treated soils in small-strain ranges.

To achieve the aims of this thesis, several objectives were formulated, including optimizing laboratory testing using triaxial testing equipped with axial and radial

local displacement transducer and bender element. The optimization process of this apparatus differs in its features and testing procedure, which were then compared to the conventional strain measurement in triaxial testing. The reliability and applicability of the proposed configuration and test procedure for the small strain range were confirmed experimentally. Furthermore, the optimum mixing ratio of the CTS under small strain ranges was studied. The investigation considered various parameters such as the cement content, curing period, and confining pressure. Finally, a prediction model of the elastic settlement under dynamic loading considering the curing period based on the mechanical properties of CTS was proposed. Several influence factors were considered in many ways to enhance the accuracy of this empirical method, such as CTS stiffness, curing period, depth of embedment, and vertical loading of the structure.

Chapter 1, Introduces the new development project of Indonesia HSR on Java Island. It is planned to be constructed in the Lowland area, making it susceptible to settlement-related problems, where a ground improvement to ensure the reliability of the railway structure is necessary. The proposed aim and its vital role in reducing the settlement behavior, original contributions, and the framework of the thesis are represented.

Chapter 2 provides a brief literature review illustrating the research carried out in relation to the scopes considered in this thesis. The chapter is divided into three main sections where the first section discusses the recent experimental and field investigation methods for determining the mechanical behavior in clayey soil ground. Furthermore, the second and third sections deal with the mechanical behavior and state of the art of elastic settlement prediction.

Chapter 3 presents the optimization of experimental testing of CTS in triaxial testing using the small-strain tools. The small-strain axial LDT, radial LDT and BE device were utilized for testing. This chapter also explains the testing procedure, including testing setup and configuration of the devices to ensure high accuracy

measurements within the elastic zone. Finally, the elastic to elastoplastic characteristics can be determined using the proposed testing methodology.

Chapter 4 presents the mechanical behavior of CTS in large to small-strain ranges subjected to the confining pressures, curing period, and cement content using triaxial testing. Considering the degradation stiffness modulus during the static shearing process with low shearing speed, it is necessary to use LDTs with the triaxial testing to ensure accurate results. Furthermore, a formula for estimating the mechanical properties of CTS in small strain ranges has been proposed using a power function that considers the confining pressures and cement content.

Chapter 5 focuses on the elastic settlement prediction of CTS as a shallow ground improvement. This chapter mainly discusses the influence of dynamic train loading on the behavior of the CTS layer. Also, to enhance the prediction method considering the strict allowable settlement for high-speed railways, the influence of displacement factor and rigidity index factor of CTS is proposed and included in the prediction model. Finally, the elastic settlement can be predicted by simply extrapolating the settlement with time using a power function, focusing mainly on the operation phase. In addition, the prediction model can be used to determine the optimum mixing ratio needed at a specific curing period to satisfy the allowable settlement.

Chapter 6 summarizes the main findings of this thesis and delineates the remaining problem to be solved related to the practical and academic points of view. Furthermore, it defines goals for future research and scopes that need to be investigated subjected to the dynamic loading behaviors in laboratory testing.

TABLE OF CONTENT

LIST OF FIGURES

LIST OF TABLES

Chapter 1

Introduction

1.1 Indonesia high-speed railway project

A new national plan of the high-speed railway development in Indonesia was studied in 2012. The railway service will be connecting major cities i.e. Jakarta and Surabaya which approximately 700 km apart (JETRO, 2012). This route was planned to be constructed on the lowland area. The term of lowland covers a broad spectrum of lands affected by fluctuating water levels, in which human activities such as agriculture, industry and living are pursued or being proposed (Miura et al., 1994). In Java Island, lowland areas are located near shore waters, and they are covered by clayey soil as illustrated in Fig. 1.1. Clayey soil thickness based on field investigation was found to be around 10-15 m along the north Java Seas (Ranst et al., 2004). A development of high-speed railway structure on lowland areas has an inevitably challenge, especially in its construction techniques. To carry on the sustainable developments of high-speed railway on the problematic soils, the process has to follow strict requirements of settlement.

The regulation about high-speed railway settlement is considering several points, one of them is the vertical railway track irregularity. It considers the influence of train loading during serviceability, static loading from the structures itself, structure design procedure, weather, and geological condition. In Japanese railway design standards, the allowable settlement for post construction or during the serviceability is 10 mm/10 years (Kanazawa and Tarumi, 2010; Liu et al., 2011; Watanabe et al., 2021). As for the maximum allowable settlement during the serviceability is about

30 mm. That serviceability is considered to decide the maintenance time regarding the supporting ground of railway track. To be able to achieve the allowable settlement for substructures of railway track, it is necessary to improve the supporting ground by choosing the suitable method for ground improvement if the ground is lack of bearing capacity. Also, there are criteria subjected to the disaster region, in this case was pointed out to Japan which has similar geological conditions with Indonesia. This criterion is divided into the high potential of earthquake region, which is about 10 mm, and for low-to-middle region is considered 100 mm. Those requirements need to be strictly followed according to Japanese standards (Ando et al., 2021; Kanazawa and Tarumi, 2010). However, to meet the requirements of settlement behavior on high-speed railway, a proper structure must be ensured to match with lowland areas.

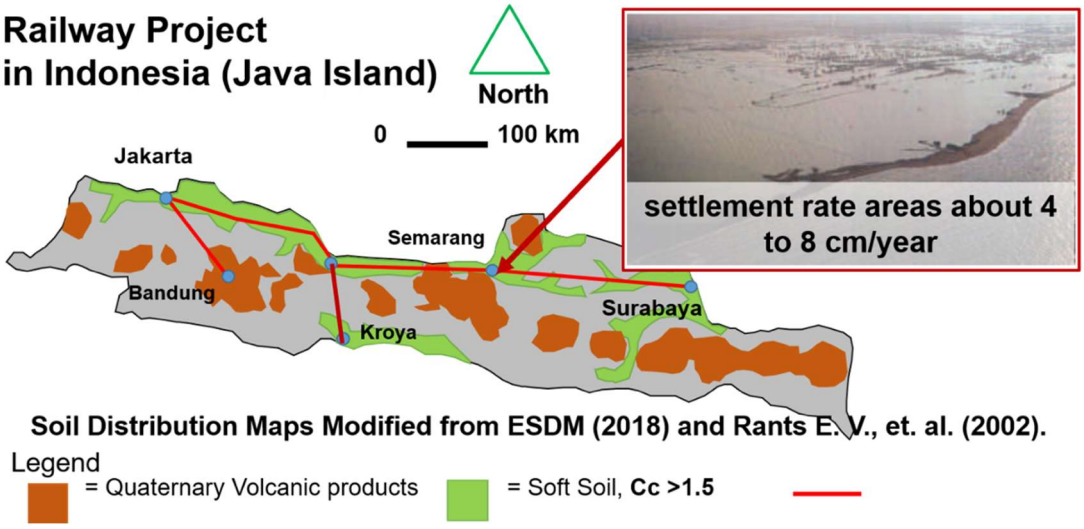

Fig. 1.1 Indonesia high-speed railway project with clayey soil distribution

1.2 Overview of High-speed railways structures design

The definition of high-speed railway structures in this research is dedicated only for operation of the high-speed train that can be specified under the ranges of maximum operation speed approximately about 210 km/h to 300 km/h (Alamaa, 2016). A brief description of the high-speed railway structures components consists of the ballasted and ballastless railway which described in the following paragraphs:

1.2.1 Ballasted railway

One of the conventional methods considered in this study is the ballasted embankment. This design has been used intensively for many countries. Indonesia have already had an experience to develop the national regular railway with this type of structures, which is explained under geotechnical engineering circumstances in Indonesia railway standards (SNI-8460-2017). Ballasted structures consist of an adequate embankment of ballast layer: crushed stone and gravel materials. Several advantages of this structure are it can distribute the contact forces from the axial load to maintain the track stability and keep the vertical stress on substructures at a tolerable level. Furthermore, ballasted track can contribute as a drainage layer, that can be defined by the material shape and compacted layer with granular material. It might be suitable structures to be adopted for non-cohesive soil distribution areas. However, in the clayey soil, there are some difficulties during maintaining the ballasted track, which leads to high maintenance costs (Lichtberger, 2011; Zhai et al., 2015). In addition, the deformation on ballasted track could be accumulated by increasing stress distribution, which in fact led to the progressive shear deformation and plastic deformation. Those are major problems that can influence the subgrade layer. By the time, the subgrade layer will be exposed to the natural ground level, as can be seen in Fig. 1.2.

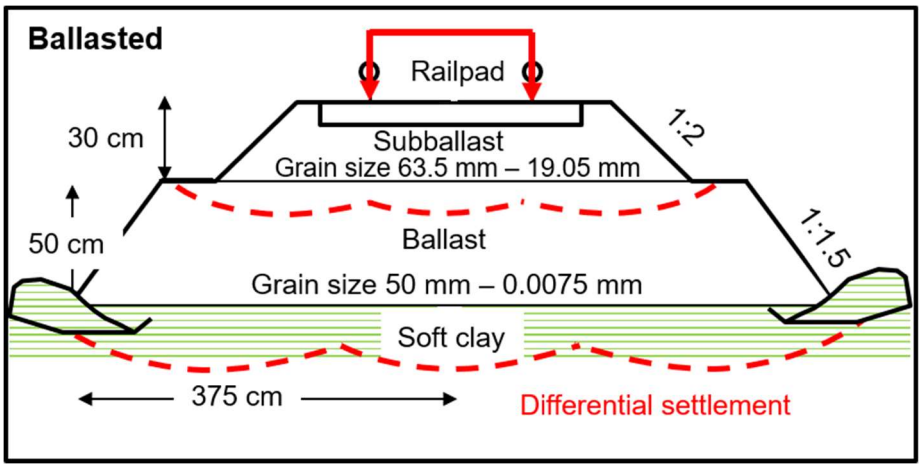

Fig. 1.2 Ballasted track for high-speed railway and regular train design

1.2.2 Ballastless railway

Nowadays, ballastless railway design has been developed in many research due to its durability regarding the long-term settlement effect under static and dynamic loading. In Japanese design standard for high-speed railway, the ballastless method is applied for high-speed train tracks. The structure is designed by considering an adjustment on the train load effect. The application of ballastless track which consists of slab track structure and concrete mixture can be easily found as it is usually produced on a large-scale basis. The manufacturing process has taken into account the static load during the construction phase and dynamic load during the serviceability phase (Liu et al., 2011). Ballastless track on natural ground application is shown in Fig. 1.3. It is a reasonable design for applying the structures on the clayey soil ground. Based on the perspective of its geometry, it can be conducted to optimizing the small working space areas and thin structures for high-speed railway track. However, the long-term strength consideration might be influenced due to the lack of bearing capacities of this structure. Furthermore, the maximum allowable settlement must be achieved for high-speed train development. The maximum displacement was considered in the mid-point and the below part of the structures, as illustrated by the bending curvature. That condition is remarkably caused by the lack of bearing capacity. This issue can be tackled by fitting the ground improvement technology to prevent the settlement behavior.

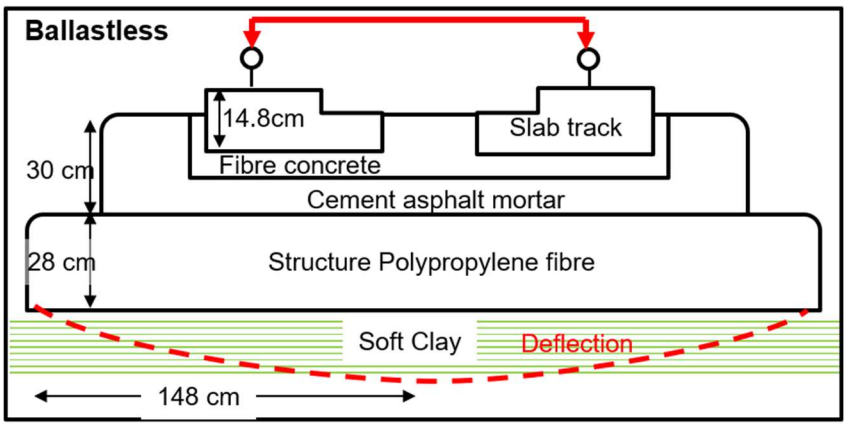

Fig. 1.4 Ballastless track for high-speed railway design

1.3 Ground Improvement Techniques

Such methods for improvement techniques especially in clayey soil at lowland areas has been developed since the late 20th century. For example, the improvement of a problematic soil behavior that deals with lack of shear strength, high compressibility index, hydraulic conductivity and liquefaction potential is one of the scopes that has been discussed. A comprehensive study of the settlement behavior is conducted by improving the problematic soils beneath the structures. An advanced technique was utilized at a certain point to decrease the variability of soil properties. That could comprise the improvement of bearing capacity on problematic soil layers, then adjusted the ground improvement technique to achieve a homogenous layer with higher bearing capacity (Evans et al., 2022; Kitazume and Terashi, 2013). However, the practical judgement recently was considering the effectivity of using a proper technique that can bring a cost-efficient result, especially for developing countries. The implementation of ground improvement techniques has several options as shown in Fig. 1.5.

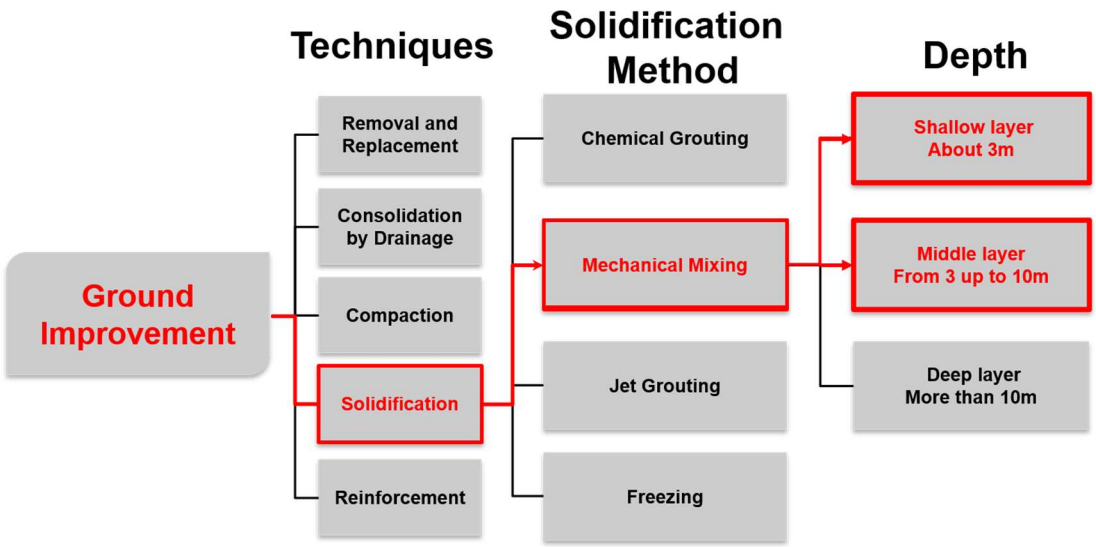

Fig. 1.5 Ground Improvement techniques of clayey soil layer

A key factor to pick a suitable technique for ground improvement in developing countries is the availability of machine or vehicle. An affordable machine is highly preferred for the construction process. Apart from that, the improvement techniques

are not applicable at certain condition due to the small working space and heavy weight of vehicle that can induce an immediate settlement. This study was focused on the solidification technique by mixing the natural soil ground to be a cement-treated soil. This technique has some advantages such as the affordable cost of vehicle, and the high strength improvement with short-term period of curing. In addition, according to the strict allowable settlement, a vehicle load of ground improvement is more reliable than the reinforcement technique by three point supporting pile driver. A comparison method can be seen in Table 1.1. Extensive and detailed of the solidification method was chosen by the target depth of cement-treated soil embedment layer.

Table 1.1 Comparison of ground improvement techniques

Ground Improvement Technique	Consolidation	Reinforcement	Compaction	Solidification
Material	PVD	Driven Pile	Sand	Portland Cement
Soil Types	Clayey soil	Clayey soil	Clayey soil	Clayey soil
	Organic Material	Sandy soil	Sandy soil	Sandy soil
		Organic Material	Organic Material	Organic Material
Vibration during installation	Medium	Heavy Vehicle	Heavy Vehicle	Lightweight to Heavy vehicle
Construction Period	A year	Months to years	Several weeks to months	Several weeks to months
Cost effective	Low	High	Middle	Middle to High
Strength increment	Low	High	Low-Middle	Middle to High

Reliable techniques to determine stiffness of mechanical properties were needed in advance to evaluate the cement treated soil mechanical behavior under strict allowable settlement of high-speed railway. Most researcher considered the field investigation to evaluate the mechanical behavior of cement-treated soils by using non-destructive method such as seismic wave velocity and destructive method such as cone penetration test (Archer and Heymann, 2015; Atkinson, 2000; Benz et al., 2009; Lee et al., 2009). In the meantime, a significant discrepancies result has been discovered between the in-situ and laboratory test. To enhance the accuracy in laboratory test, a method has been developed by using small strain ranges condition (Goto et al., 1991; Putera et al., 2021; Yamashita et al., 2009). Those techniques refer to a sophisticated technique, which has difficulties in identifying the laboratory result in small strain ranges.

In order to use the small strain measurement devices effectively on laboratory test, especially for cement-treated soil application, this research offers a developed technique of cement treated soils and its application for determining the settlement. In addition, when clayey soil with high plasticity is dominantly distributed in the shallow ground layer, that comprises around 50% influence of immediate or elastic settlement during the construction period and operation phase for applying continuously dynamic loads above natural ground structures (Fang and Daniels, 2006; Foye et al., 2008; Pantelidis and Gravanis, 2020). Consequently, researchers have studied the prediction method for elastic settlement of cement treated soils as a substructure, where it can be a practical solution in determining the efficient deployment process of the structure with regards to the embedment layer, optimum cement content and mechanical properties index based on laboratory testing.

1.4 Research Objectives and Original Contributions

This thesis is aimed to study the empirical method for elastic settlement prediction of cement-treated clayey soil in relation to the dynamic load in small strain ranges. Furthermore, this study was subjected to new high-speed railway development

project in Indonesia. To achieve the aims of this thesis, several objectives were formulated as follow:

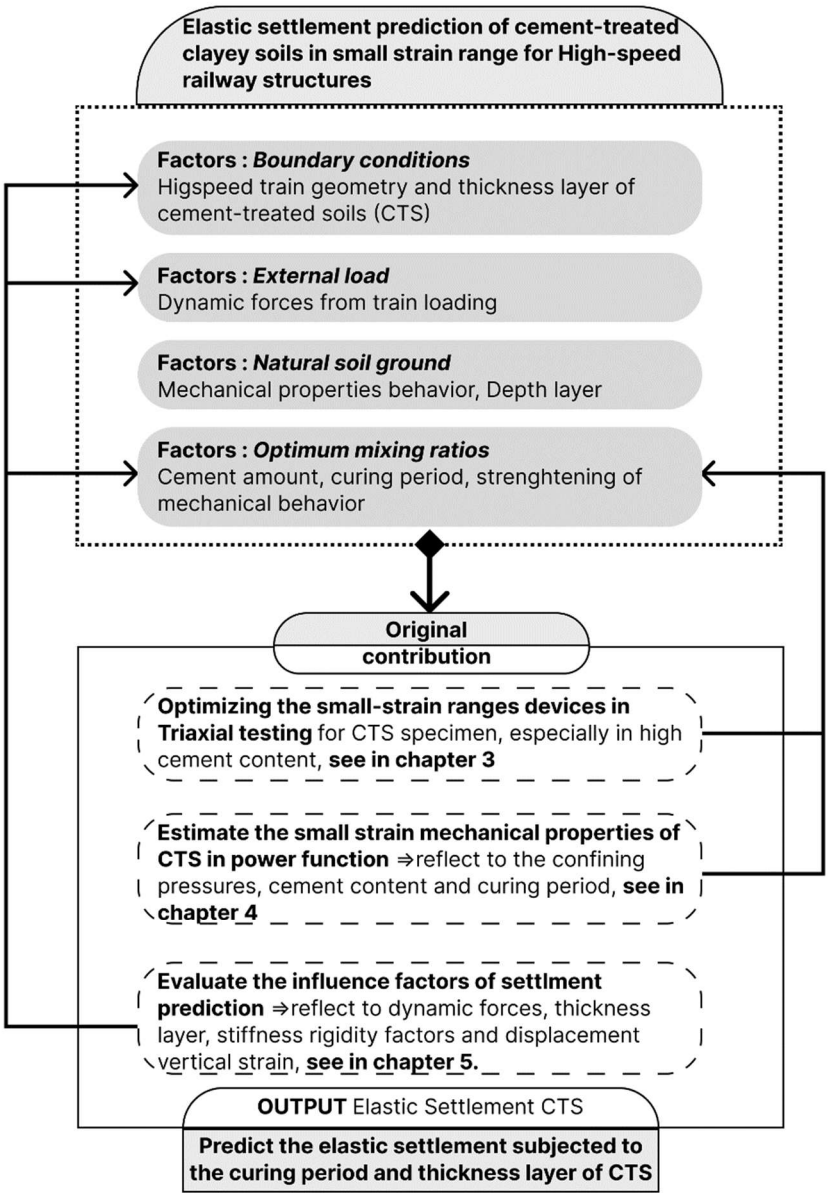

Fig. 1.6 Original contributions

To optimize the laboratory test under triaxial $\overline{CU}$ using axial and radial type of local displacement transducer and bender element. The optimization process of this apparatus differs in its features and testing procedure, which were then compared

to the conventional strain measurement in triaxial $\overline{CU}$ testing. The proposed configuration and test procedure were ensured to define a small strain mechanical behavior.

To investigate the stiffness modulus parameter of the cement-treated soils under small strain ranges. The investigation considered various parameters such as cement content, curing period and confine pressure. Based on those parameters, the stiffness modulus was determined as an influence that reflects the confine pressure.

To predict the elastic settlement of cement-treated soils due to dynamic loading and curing period. The analysis considered various dynamic loading and influence factors with boundary condition of ballastless railway track project. Their influence factors were considered in many ways such as cement treated soil subjected to stiffness parameter materials, curing period, depth of embedment and vertical strain of structure.

Furthermore, Fig. 1.6 illustrates some new findings obtained in this research to which are considered as the originality of this research.

1.5 Framework and outlines of thesis

To achieve the above-mentioned objectives and scopes, this thesis is organized in seven chapters, as presented in Fig 1.6 and briefly explained as follow:

Chapter 1 presents an introduction of the new development project of Indonesia high-speed railways in Java Island. That includes the current issues and motivation based on strict settlement regulation. This chapter also includes the original contributions of this study and the framework of the thesis are represented.

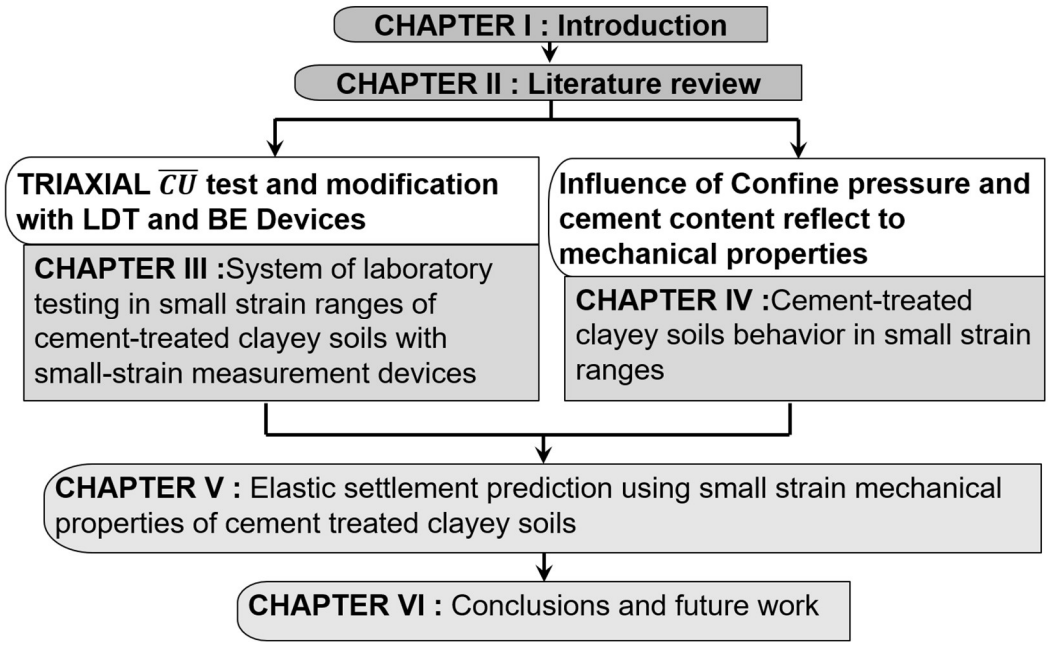

Fig. 1.7 Framework and thesis organization. (Flow chart)

Chapter 2 explains quality assurance and quality control (QA/QC) of the cement-treated soils due to field and laboratory testing in different time sequences. Based on QA/QC, it can be implied the necessary of laboratory testing especially for determining the initial stiffness due to small strain ranges. However, to provide the initial stiffness parameters of cement-treated soils, a good combination of devices should be chosen, especially in small strain ranges measurement. Using the axial-radial devices of local deformation transducer (LDT) and Bender Element (BE) was found to be a good combination to provide the initial stiffness parameters to predict the elastic settlement. The last section introduced the general equation of elastic settlement theory, that has been mentioned in the state-of-art of shallow foundation approaches. It supported the description of equation derivation in the last chapter of this thesis.

Chapter 3 presents the optimization of experimental testing of cement-treated soils induced by triaxial consolidated undrained compression test using the small-strain measurement devices. The additional small-strain measurement devices have been used that comprised of axial local deformation transducer (LDT), radial LDT and

bender element (BE) device. This chapter also explains the testing procedure including setup and configuration of devices. Finally, to compare the accuracy of small-strain measurement device with the standard devices (LVDT), which was characterized by the large-small strain ranges. The discrepancies were measured by the mean of ratio between those measurement devices, which was considered within the stress-strain relationship curves.

Chapter 4 discusses an evaluation of the mechanical behavior of CTS in large to small-strain ranges subjected to the confining pressures, curing period and cement content using triaxial testing. Considering the degradation stiffness modulus during static shearing process with low shearing speed, it requires the LDTs equipped into the triaxial testing. Through this chapter, to optimizing the LDT devices on degradation stiffness modulus under various confining pressures. A series of static test using the various of cement content and curing period were performed. Furthermore, the estimating formula of mechanical properties in small strain ranges has been proposed and evaluated by influence of confining pressures and cement content.

Chapter 5 presents the elastic settlement prediction of cement-treated clayey soils as shallow ground improvement. Through this chapter, it was mainly discussed about the influence of dynamic train loading behavior in cement-treated soil layer. Also, to enhance the prediction method within the strict allowable settlement of high-speed railway project, the influence of displacement factor and rigidity index factor of cement-treated soil is included into prediction method. Finally, the elastic settlement prediction method can be introduced with influence factor, and it has been predicted from the construction period to serviceability phase.

Chapter 6 summarizes the main findings of this thesis, delineates the remaining problem to be solved related to the practical and academical point of view. Furthermore, defines goals for the future research and scopes that need to be investigated subjected to the dynamic loading behaviors in laboratory testing.

References

Alamaa, A., 2016. High-speed railway embankments - a comparison of different regulations. KTH Royal Institute of Technology, Stockholm.

Ando, K., Sunaga, M., Aoki, H., Haga, O., 2021. Development of slab tracks for hokuriku shinkansen line. Quarterly Report of RTRI 42, 35–41.

Archer, A., Heymann, G., 2015. Using small-strain stiffness to predict the load-settlement behaviour of shallow foundations on sand. Journal of the South African Institution of Civil Engineering 57, 28–35.

Atkinson, J., 2000. Non-linear soil stiffness in routine design. Geotechnique 50, 487–508. https://doi.org/10.1680/geot.2000.50.5.487

Benz, T., Schwab, R., Vermeer, P., 2009. Small-strain stiffness in geotechnical analyses. Bautechnik 86, 16–27. https://doi.org/10.1002/bate.200910038

Evans, J., Ruffing, D., Elton, D., 2022. Fundamental of ground improvement engineering, 1st Edition. ed. CRC Press.

Fang, H.-Y., Daniels, J.L., 2006. Introductory Geotechnical Engineering: An Environmental Perspective (1st ed.)., 1st ed. CRC Press, London.

Foye, K.C., Basu, P., Prezzi, M., 2008. Immediate Settlement of Shallow Foundations Bearing on Clay. international Journal of Geomechanics 8, 300–310. https://doi.org/10.1061/(ASCE)1532-3641(2008)8:5(300

Goto, S., Tatsuoka, F., Shibuya, S., Kim, Y.-S., Sato, T., 1991. A Simple Gauge for Local Small Strain Measurements in the Laboratory. Soils and Foundations 31, 169–180. https://doi.org/10.3208/sandf1972.31.169

JETRO, 2012. Study on the high speed railway project (jakarta-bandung section), republic of indonesia (Final report (Summary)), Feasibility study for promotion of international infrastucture projects in fy2011. Yachiyo

Engineering Co., Ltd. and Japan International Consultants for Transportation Co., Ltd.

Kanazawa, H., Tarumi, H., 2010. Technical transition of earth structures for shinkansen. SOILS AND FOUNDATIONS 50, 817–828. https://doi.org/10.3208/sandf.50.817

Kitazume, M., Terashi, M., 2013. The deep mixing method, in: The Deep Mixing Method. CRC Press/Balkema, Leiden, The Netherlands.

Lee, J., Kyung, D., Kim, B., Prezzi, M., 2009. Estimation of the Small-Strain Stiffness of Clean and Silty Sands using Stress-Strain Curves and CPT Cone Resistance. Soils and Foundations 49, 545–556. https://doi.org/10.3208/sandf.49.545

Lichtberger, B., 2011. Track compendium: formation, permanent way, maintenance, economics., 2nd edition. ed. Eurail Press, Hamburg.

Liu, X., Zhao, P., Dai, F., 2011. Advances in design theories of high-speed railway ballastless tracks. Journal of modern transportation 19, 154–162.

Miura, N., Madhav, M.R., Koga, K., 1994. Introduction, in: Lowlands Development and Managements. CRC Press/Balkema, London, pp. 1–8.

Pantelidis, L., Gravanis, E., 2020. Elastic Settlement Analysis of Rigid Rectangular Footings on Sands and Clays. Geosciences 10. https://doi.org/10.3390/geosciences10120491

Putera, M.A., Yasufuku, N., Alowaisy, A., Rifai, A., 2021. Optimizing modified triaxial testing for small strain zone using local displacement transducers and bender element for cement-treated soft soil. E3S Web of Conferences 331. https://doi.org/10.1051/e3sconf/202133103003

Ranst, E.V., Utami, S.R., Vanderdeelen, J., Shamshuddin, J., 2004. Surface reactivity of Andisols on volcanic ash along the Sunda arc crossing Java Island, Indonesia. Geoderma 123, 193–203. https://doi.org/10.1016/j.geoderma.2004.02.005

Watanabe, K., Nakajima, S., Fujiwara, T., Yoshii, K., Rao, G.V., 2021. Construction and field measurement of high-speed railway test embankment built on Indian expansive soil "Black Cotton Soil." Soils and Foundations 61, 218–238. https://doi.org/10.1016/j.sandf.2020.08.008

Yamashita, S., Kawaguchi, T., Nakata, Y., Mikami, T., Fujiwara, T., Shibuya, S., 2009. Interpretation of International Parallel Test on the Measurement of Gmax Using Bender Elements. Soils and Foundations 49, 631–650. https://doi.org/10.3208/sandf.49.631

Zhai, W., Wei, K., Song, X., Shao, M., 2015. Experimental investigation into ground vibrations induced by very high speed trains on a non-ballasted track. Soil Dynamics and Earthquake Engineering 72, 24–36. https://doi.org/10.1016/j.soildyn.2015.02.002

Chapter 2
Literature Review

2.1 Introduction

Clayey soil ground can be improved with soil mixing by introducing additives into the subsurface, the soil mixing (blending) with the additives has been categorized by improving physical properties, mechanical properties and chemical characteristics. Differences of confining pressure and cement content was indicated a discrepancy for describe the mechanical properties. In this research was focused on shallow ground improvement related to the 15 m depth, it specified to the clayey soil ground in Java Island. Based on the improvement categorized of improvement series, this research had pay attention to the mechanical properties behavior and the application to prevent the settlement behaviors due to high-speed train loading.

This chapter introduces the cement-treated soil test characteristics, mechanical properties behavior within the strain ranges and summarized the elastic settlement prediction are planned to describe to ensure the main goals based on derivation of general equation formula.

2.2 Cement-treated soil test characteristics

To sufficient the sustainable improvement of the cement-treated soils, quality control and quality assurance is required before, during and after construction. The quality control for cement-treated soil mainly conducted by laboratory testing and field trial testing (Kitazume and Terashi, 2013; Probaha et al., 2000). For instance, the laboratory testing was determined normally by the element test and model test;

thus, for field testing by the geophysical tools, standard penetration test and cone penetration test, the time sequence can be shown in **Table 2.1.** In this research was mainly conducted in the testing of mechanical properties at laboratory.

Table 2.1 Quality controls and quality assurances of Cement-treated soils

Time sequence	**QA/QC**	**Remarks**
Before construction	Cement-treated soil prior laboratory testing	Select the cement content, select cement type and estimate the mechanical properties
During construction	Field trial testing for monitoring and recording the strength parameter	Maintain quality of increment stiffness of CTS by non-destructive method and destructive method. Ensure the geometric layout (plan and depth)
	Laboratory test for monitoring the strength parameter	Ensure the estimation from prior laboratory testing subjected to the development of during construction time.
After construction	Continuous laboratory test based on coring test on selected sample	Observe continuity and uniformity of long-term strength. And verify the quality of CTS

2.2.1 Cement-treated soil field trial testing

During the construction sequences, the field trial testing is become important, especially when estimating the geometric layout and took a specimen from bored sample into the laboratory testing. Also, the actual strength in the real scale of construction condition can determined and predicted for the final design by taken with destructive and non-destructive testing.

2.2.1.1 Destructive testing

Originally, the field trial testing for determine stiffness parameter was introduced by penetrating the mechanical device that produced tip stress measurement within the thickness layer of cement-treated soils, later the adaptation for estimate the bearing capacity of differences thickness layer. Based on those description, the field trial testing was categorized in the destructive testing. The field trial test machine was presented commonly by Cone Penetration Test (CPT) and Standard Penetration Test (SPT) (Schneider and Mayne, 2022).

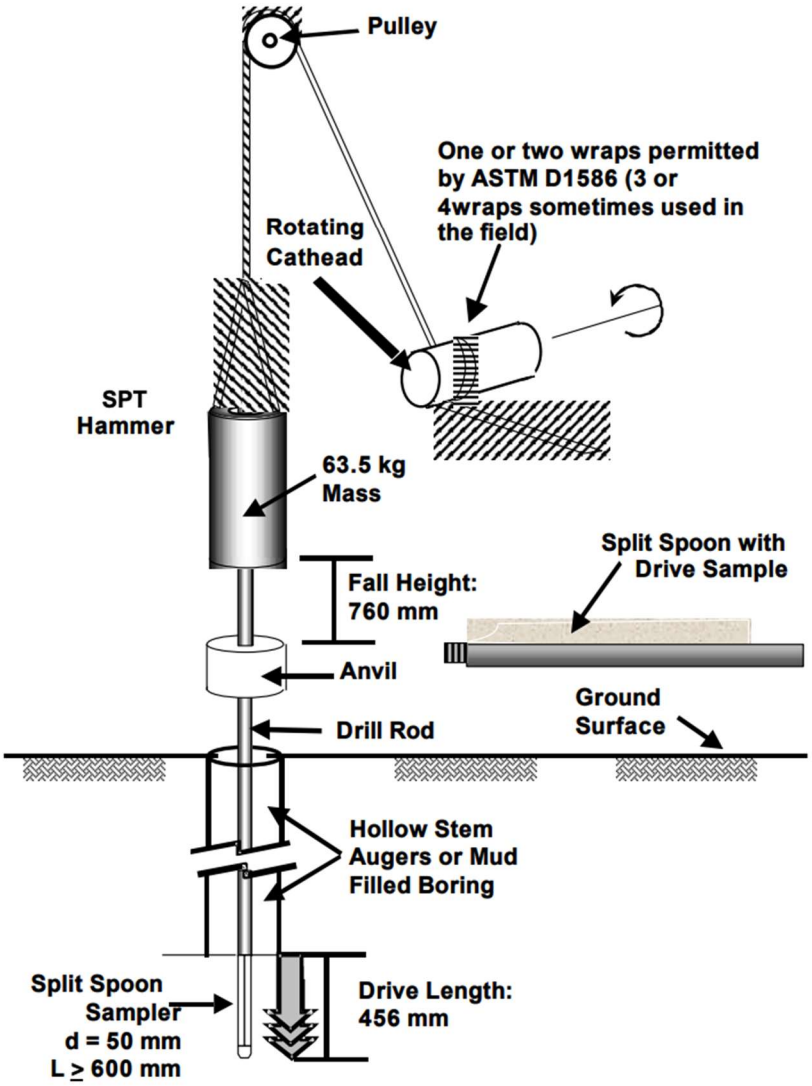

Fig. 2.1 Field method for destructive method with standard penetration test

Based on SPT had influenced that related to the numerous correction factor to estimate the numerical resistance (N-value) from the targeting of thickness layer. The machine was illustrated in **Fig. 2.1.** The effect of having many corrections factor it can be subjected to the uncertainty of estimating the stiffness parameters of soils. The advantages of this machine were included the sampling method (normally using tubes; 5 cm of diameter and 60 cm – 1 m of Height) of cement-treated in targeting layer, it can be mutual testing procedure during the measurement of N-Value. However, due to the various of influenced during the N-value measurement, there are another option such as non-destructive method for evaluating the stiffness parameter by the shear wave velocity.

2.2.1.2 Non-destructive testing

The geophysical method to evaluating the stiffness parameter has been trusted for numerous suitable methods comprises with the exploration of geological soil and rock layer (Giese, 2005; Seng and Tanaka, 2011; Yamashita et al., 2009). The non-destructive testing by shear wave velocity has transmitting the wave through the soil layer from the ground and there are receivers on the ground to record the reflecting/refracting within the soil layer, it illustrated in **Fig. 2.2**.

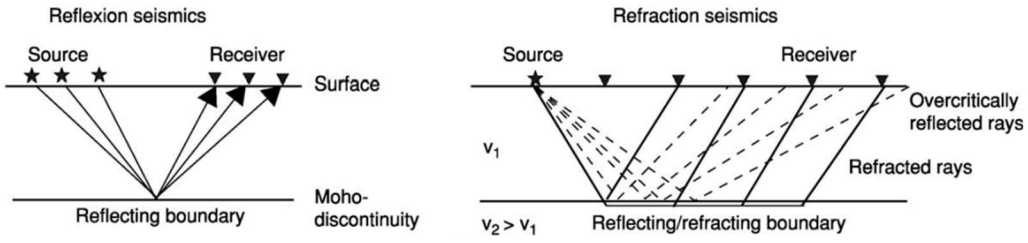

(a) (b)

Fig. 2.2 Field method for non-destructive testing to determine shear wave velocity; (a) Reflection seismic and (b) Refraction seismic.

The shear wave velocity (V_s) can be determine the Shear Modulus in small strain ranges (G_{max}) by using:

$$G_{max} = \rho \cdot V_s^2 \quad (1)$$

Where $\rho = \gamma_t/g$ is mass density by the total unit weight (γ_t) divided the acceleration due to gravity (g). Also V_s is shear wave velocity, that should be determined by the function of the depth (m), it becomes m/s. There are number of different field method to determine the cement-treated soils shear wave velocity. Recently, determination of elastic tress hold shear strain of cement-treated soil can be evaluating in laboratory testing using the bender element. It can be efficiently used for estimating the stiffness parameters subjected to the prior laboratory testing of QA/QC time sequences in cement-treated soils project development.

2.2.2 Cement-treated soil laboratory testing

Based on QA/QC, the laboratory testing is a key factor to carried out the responsibility along the time sequence (before, during and after construction), it refer to the detailed specification and performances of cement-treated soil (Evans et al., 2022; Kitazume et al., 2015). A laboratory testing should be conducted on cement-treated soil samples retrieved from all ground improvement layers, which was determined a suitable cement type and cement content to ensure the design parameters.

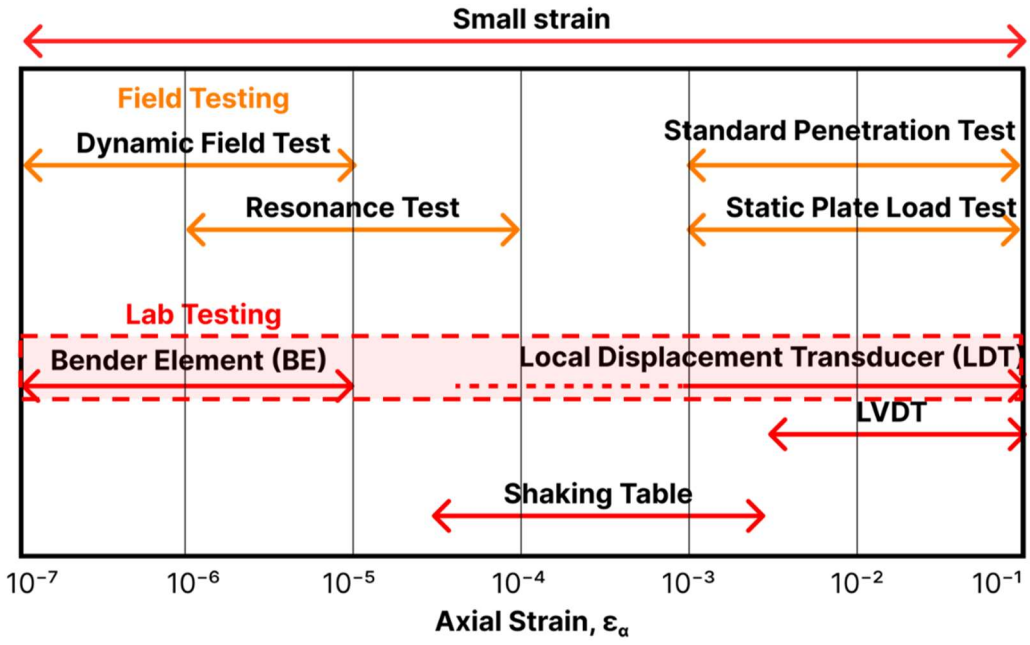

Fig. 2.3 Laboratory testing within small-large strain ranges measurement

Laboratory influenced comprises of the many factors, such as in mixing and molding phase, curing condition and testing techniques. Those factors are related to the QA/QC of cement-treated soils. To prevent the lack of QA/QC in laboratory testing, in Japan there is standards to follow such as Cement-treated soils were prepared using statically compacted stabilized soil technique based on JGS (0812-2009). However, during the measurement of mechanical properties using laboratory apparatus was significantly relied upon the test devices measurement accuracy. Most of the laboratory test was measured smaller in stiffness modulus that compared with the non-destructive method and assumed the stress-strain behavior is elastic linear, as illustrated in **Fig. 2.3.**

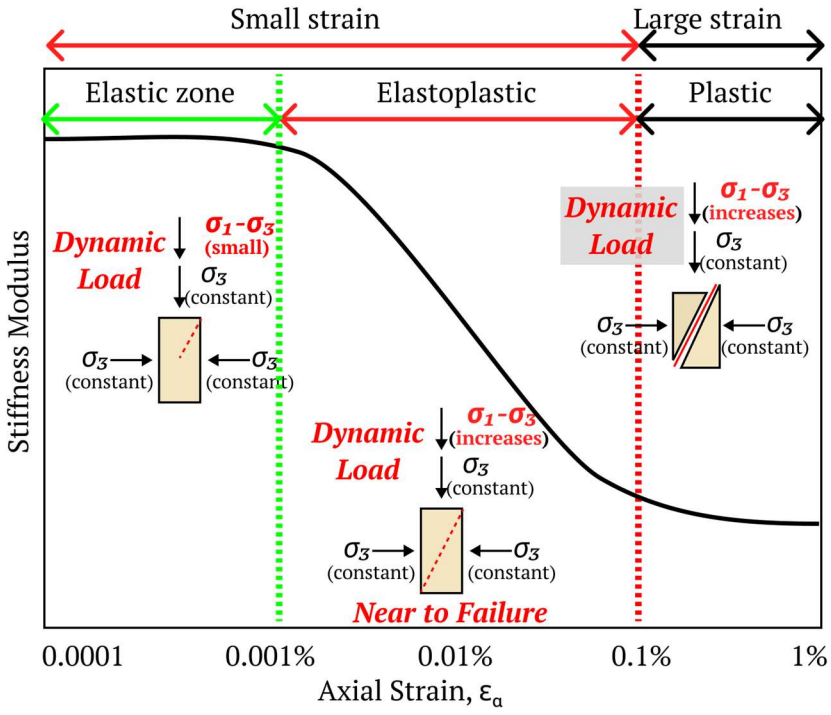

Fig. 2.4 Degradation stiffness modulus small-large strain with axial strain ranges measurement

Based on Atkinson (2000) and Viggiani and Atkinson (1995) the simple curvature for degradation stiffness modulus were found to apply generally within the small-large strain ranges, illustrated in Fig. **2.4**. Those parameters are based on the measurement devices accuracy, which make allowance for the different strain

ranges in the various of measurement devices. In order to determine small discrepancy between field trial and laboratory testing was subjected to the dynamic loading behavior, the small-strain measurement devices is required to equipped into the conventional testing method that can be measured under elastic linear to the elastoplastic curve regions (Clayton, 2011; Goto et al., 1991; Putera et al., 2021; Xiao et al., 2018). In addition to estimate the stiffness modulus in small-strain ranges can be used the Bender element test, and it was a good combination of using the Axial and Radial Local deformation transducer subjected to the elastoplastic curves.

2.3 Determination of mechanical properties based on strain measurement techniques

In this section, there would be divided into 3 section such as stress-strain curve in small-strain ranges with influence of confining pressure. The Mohr Coulomb analyses to obtain the shear strength parameter and determine the stiffness degradation modulus to obtain the mechanical behavior within the increment of axial strain.

2.3.1 Stress-strain relationship in cement-treated soils

Kitazume and Terashi (2013) was evaluated the strength characteristics of cement-treated soils in consolidated undrained test. The cement ratio was defined as 7.5% in soil-cement ratio (A_w), it was subjected to the low cement content and high consolidation pressure about 700 kN/m^2 to 8100 kN/m^2. Those are shown significant discrepancies corresponds to increment of consolidation pressure, it can be described in discrepancies of peak deviatoric stress. However, the differences of cement content and confining pressure corresponds to stress-strain relationships are somewhat confusing to evaluate, it due to the bedding error measurement of increment stress-strain has been shown within small-strain ranges. This phenomenon can be seen in high cement content and high confining pressure, where the stiffness is increasing as long as the curing period is increases.

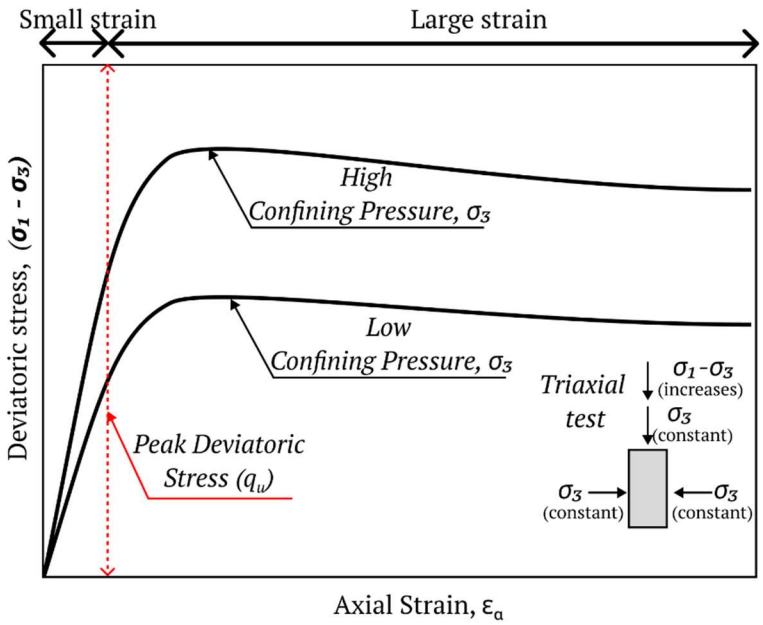

Fig. 2.5 stress-strain relationship with influence of confining pressure at small-strain ranges

Typical stress-strain curve was subjected to the peak deviatoric stress within small-strain ranges, as can be seen in **Fig. 2.5**. stress-strain relationship was described by differences in confining pressure. Increment stress-strain curve was shown significantly within small-strain ranges. the measurements were conducted in shearing process, using small-strain devices measurement has been delineated the advantages such as optimized the bedding error measurement in stress-strain curve. However, the experiment test was observed in normal shearing speed 1mm/min, it might be had variance of result corresponds to the low shearing speed process such as 0.005 mm/min. Furthermore, low shearing speed can reduce the bedding error that hypothetical based on high stiffness material testing with uniaxial apparatus (). The stress-strain relationship based on elastic theory can be expressed as below:

$$\Delta\varepsilon_x = \frac{1}{E}\left(\Delta\sigma_x - \upsilon\Delta\sigma_y - \upsilon\Delta\sigma_z\right) \quad (1)$$

$$\Delta\varepsilon_y = \frac{1}{E}\left(\Delta\sigma_y - \upsilon\Delta\sigma_z - \upsilon\Delta\sigma_x\right) \quad (2)$$

$$\Delta\varepsilon_z = \frac{1}{E}\left(\Delta\sigma_z - \upsilon\Delta\sigma_x - \upsilon\Delta\sigma_y\right) \quad (3)$$

$$\Delta\gamma_{xy} = \frac{1}{G}\,\Delta\tau_{xy} \quad (4)$$

Where ε_x, ε_y and ε_z are the strain with differences directions that can be described in perpendicular directions. $\Delta\varepsilon$ is as increment of normal strain, $\Delta\tau$ is an increment of shear stress. σ_x, σ_y and σ_z are the stress in perpendicular directions. E is Young Modulus, υ is Poisson's ratio and G is Shear modulus. However, in this research the stiffness modulus parameter of cement-treated soils to estimate in small-strain ranges was considered the small-strain measurement devices. The accuracy of measurement devices corresponds to the influence of confining pressure and differences of cement content is required to evaluated, when the others researcher had difficulties with the bending error in relationship of stress-strain curve.

2.3.2 Define Mohr Coulomb

In this study, comparison between measurement devices comprises linear variable displacement transducers (LVDT) and Axial LDT to measure the peak stress and deformation characteristic of cement-treated soils has been considered evaluating the shear strength parameter, which was subjected to cohesion and friction angle.

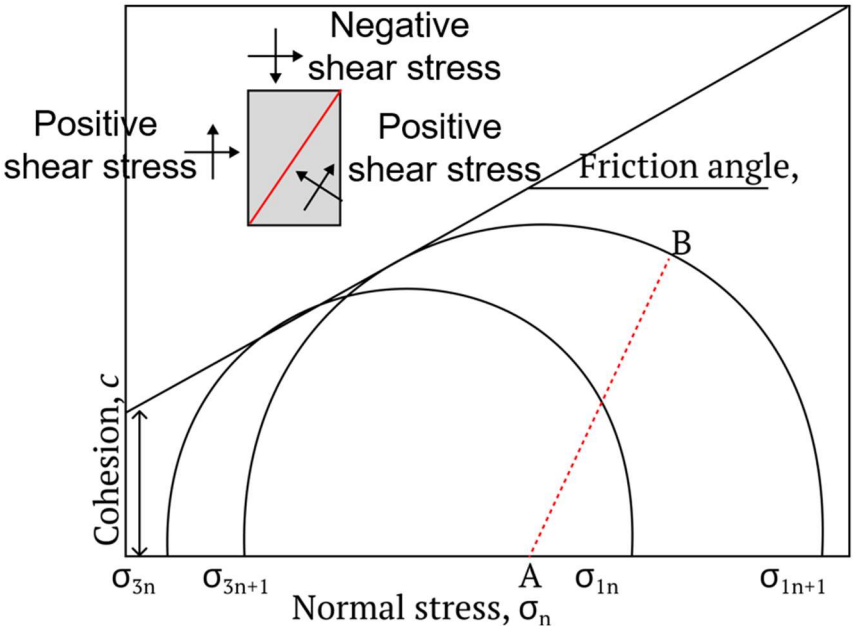

Fig. 2.6 Mohr-coulomb with differences of measurement devices

In Mohr-coulomb criterion, to evaluate the failure envelope with peak deviatoric stress, it can be determined as a linear curve as can be seen in **Fig. 2.6**. Increasing normal stress it can be described the compression behavior of the specimen, and decreasing normal stress it can be evaluated for tension. To draw a half circle of Mohr-coulomb it refers from the radius, it can be drawn as expressed as below:

$$AB = \sqrt{\left(\frac{\sigma_1 - \sigma_3}{2}\right)^2 + \tau^2} \quad (5)$$

Where AB is radius of Mohr-coulomb, $\sigma_1 - \sigma_3$ is deviatoric stress and τ is shear stress. The radius of Mohr coulomb is represented the given shear-stress and normal stress circle, differences of peak deviatoric stress can be influenced the radius of Mohr-Coulomb. In order to evaluate the differences of shear strength parameter of cement-treated soil related to the stress-strain relationship and bedding error behaviors, it could be observed by using strain measurement devices that subjected to the different cement content and confining pressure. The failure envelope should be suggested as below:

$$\tau = (\sigma_1 - \sigma_3)\, tan\varphi + c \quad (6)$$

Where τ is shear stress, $(\sigma_1 - \sigma_3)$ is deviatoric stress based on measurement in triaxial testing. The main parameter is φ for friction angle and c is cohesion, that parameter can be evaluated the failure envelope behavior in soil mechanics and evaluated the strain measurement devices.

2.3.3 Define degradation stiffness modulus

To estimate the degradation stiffness modulus, it was described approximately by the elastic zone in small-strain ranges as linear curve behavior, elastoplastic within small-large strain ranges as non-linear curve behavior and the plastic curve within large-strain ranges as equivalent linear behavior. The stiffness secant modulus relationship with axial strain ranges it can be seen in **Fig. 2.7**. To estimate Young Modulus (E) and Poisson's ratio can be calculated with the secant method, that calculation based on the origin line to the point of interest. However, influenced of

confining pressure in small strain ranges measurement has been considered that describing the discrepancies within elastic to the elastoplastic condition curves. Furthermore, the interpolation of degradation stiffness parameter modulus with axial strain can be calculated with the power function formula.

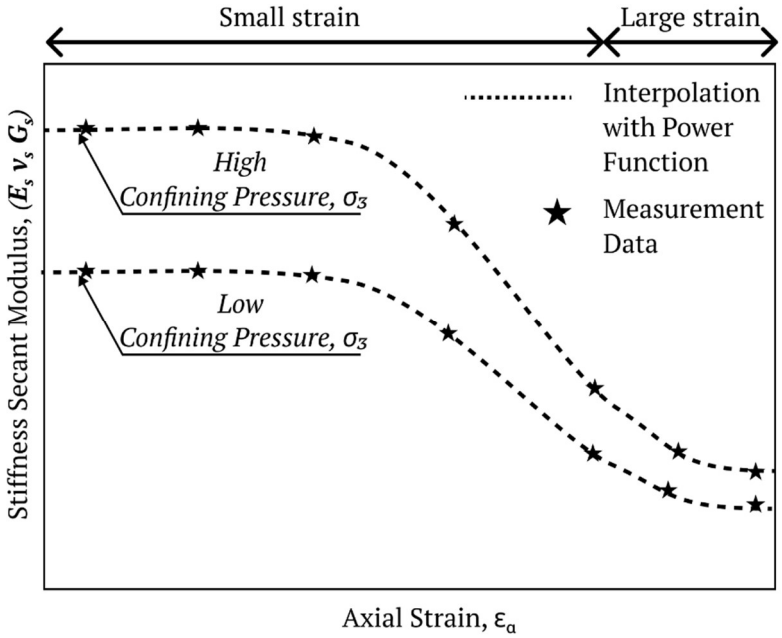

Fig. 2.7 Degradation stiffness secant modulus with influence of confining pressure at small-strain ranges

2.4 Elastic settlement prediction

In general, total settlement of soil and foundation structures comprises into elastic settlement and consolidation settlement. The elastic settlement (S_e) due to deformation at constant volume, and consolidation settlement (S_c) due to volume reduction. This research was mainly focused to calculate the cement-treated soils geometry were located below the ground and assume that during the traffic load of high-speed train in serviceability phase.

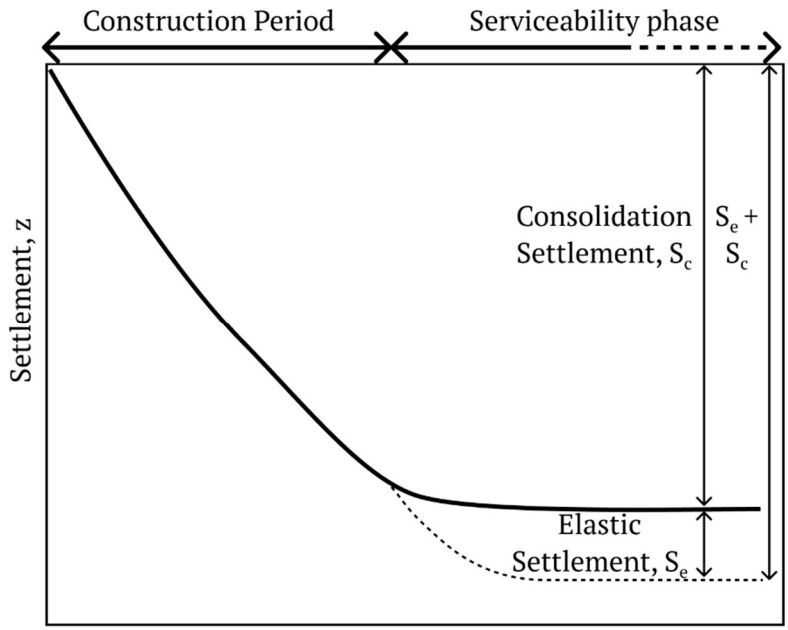

Fig. 2.8 Settlement and time period curves

Many factors are influencing the settlement behavior, based on natural soil ground type; the clayey soil with high compressibility index in the lowland area has significantly inducing with lack of bearing capacity. Another influence factor can be determined as external load, the main problem in this research such as static load can be defined by the construction period of railway track development and dynamic load induced by the high-speed train, it can be seen in **Fig. 2.8**. The influence factors based on selecting the proper cement-treated soils of mechanical properties in small strain ranges it requires, which means to predict the dynamic behavior of cement-treated soils induce by the high-speed train. Furthermore, this idea was fitted to the boundary condition and detailed discussed in chapter five.

In practice, the elastic settlement usually calculated using geometry foundation (circular) and the linearly elastic homogenous layer, which in case of the cement-treated soils with various of thickness layer and stiffness parameter did not fit to the general equation. Bowles, (1997); Das, (1985) was mentioned to the elastic settlement factor, it can describe such as below:

1. Define the boundary condition of elastic settlement based on natural soil ground geometry and sub-structures or foundation.
2. Define the external load on geometry sub-structures or foundation, it can be determined by the field investigation on load-settlement curves.
3. Evaluate the soil ground parameter using the experimental testing and field investigation, it was subjected to the strain-influence

Those settlements factor did not considered about the mechanical behavior of cement-treated soil However, general equation for elastic settlement prediction will adopt to the cement-treated soil layer, it has been evaluated in one dimensional shallow foundation geometry. It can be shown on below:

$$S_e = \left(\frac{qB}{E}\right) I \quad (1)$$

Where the S_e is elastic settlement, q is applied external load, B is width of foundation in this case it was foundation diameter, E is Young Modulus and I is influence factor. Based on those parameters, the influence factor was taken into account for geometry boundaries condition, related to the thickness and shape. For influence factor was assumed widely to the circle foundation. The assumption of external load was introduce as the uniform stress distribution on the surface. The stiffness parameter was assumed as the averages from the soil layer distribution, that was neglected assumption to compared with the increment stiffness of cement-treated soil layer. The evaluation of elastic settlement formula was expressed on below:

Table 2.2 Summary different settlement methods subjected to various of influenced factor

Settlement expression	Assumptions	Remarks	References
$S_e = q_0(\alpha B)\left(\frac{1-\upsilon_s^2}{E_s}\right) I_s I_f$	Average of Young Modulus and Poisson's ratio of the soil	This elastic settlement was considered the Point of	Bowles, 1987

q_0= Load pressure on the foundation α = Point of Interest related to the location B'= Half of foundation geometry (diameter) E_s = Young Modulus of Soil υ_s= Poisson's ratios of Soil	under the foundation I_s is Influence factor related to the shape of foundation I_f is Influence factor related to the depth foundation	interest based on the α and B'	
$S_e = \left(\frac{q \cdot B \cdot I_G \cdot I_f \cdot I_g(1-\upsilon_s^2)}{E_s}\right)$	Average of Young Modulus and Poisson's ratio of the soil under the foundation I_G is Influence factor related to the deflection of foundation I_f is Influence factor related to rigidity correction factor I_g is Influence factor related to depth of foundation	This boundary condition was considered in center location of foundation Mechanical behavior of soils and foundation was estimated using linear assumptions Mechanical behavior for soil on the ground was using the homogenous soil	Mayne and Poulos, 1999

Based on Table 2.2, it can be explained the various of elastic settlement prediction was focused mainly on geometry of the foundation and the assumption of mechanical behavior is increases linearly along the depth layer. However, in the cement-treated soils boundary condition was considered using the raft foundation, which means the rectangular position and the detailed can be explained in chapter 5. Also, the mechanical behavior was considered using the increases linear assumption, although in cement-treated soil it becomes the power function, detailed

information can be explained in chapter 4. In addition, the evaluation of influence factor for the cement-treated soil boundary condition is based on the those parameters.

2.5 Problem to be solved based on previous researcher

This chapter has been discussed about the problem is still remains with academical point of view. This research was conducted the experimental testing using triaxial test and small-strain measurement devices. In order to solve the fundamental issue in geotechnical engineering problem of cement-treated soils, the small-large strain mechanical behavior would be evaluate using the various of cement content, confining pressure and curing period. Which can be summarized as follows:

1. Optimizing the accuracy to understand the mechanical behavior in small-strain of cement-treated soil is still lacking. Due to the bedding error and the high stiffness parameter based on increasing curing period, the setup and configuration process to improve the accuracy is necessary discussed and carefully explain it in the methodology chapter.
2. The mechanical behavior of cement-treated soils in small-large strain ranges did not consider the influence of confining pressure, which was subjected to the shallow ground improvement layer.
3. The relationship between mechanical behavior in previous research mainly focus on peak deviatoric stress based on uniaxial testing. It explains the estimation of optimum mixing ratio related to the peak deviatoric stress. However, by estimating the small-strain range mechanical behavior could increase the accuracy of stiffness parameter for the dynamic properties to solve the field problem. Furthermore, the estimation of mechanical behavior corresponds to the various of cement content, confining pressure and curing periods.
4. Improving the elastic settlement prediction of cement-treated soil for high-speed railway is still lacking information. The problem could be determined by applying the differences of influence factor and dynamic loading formula.

The influences factor related to the boundaries of cement-treated soil geometry and mechanical behavior is required for improving the quality of increment stiffness by the curing period. Also, the dynamic loading is necessary to evaluated, which was the shear modulus in small strain ranges of cement-treated soils are indicated to provide an improvement of dynamic loading behavior corresponds to the spring vertical system of cement-treated soil and maximum dynamic forces of serviceability phase.

References

Atkinson, J., 2000. Non-linear soil stiffness in routine design. Geotechnique 50, 487–508. https://doi.org/10.1680/geot.2000.50.5.487

Bowles, J.E., 1997. Foundation analysis and design, Fifth Edition. ed. The McGraw-Hill Companies, Inc., Singapore.

Clayton, C.R.I., 2011. Stiffness at small strain: research and practice. Géotechnique 61, 5–37. https://doi.org/10.1680/geot.2011.61.1.5

Cuccovillo, T., Coop, M.R., 1997. The measurement of local axial strains in triaxial tests using LVDTs. Géotechnique 47, 167–171. https://doi.org/10.1680/geot.1997.47.1.167

Das, B.M., 1985. Advanced soil mechanics. McGraw-Hill, New York.

Evans, J., Ruffing, D., Elton, D., 2022. Fundamental of ground improvement engineering, 1st Edition. ed. CRC Press.

Foye, K.C., Basu, P., Prezzi, M., 2008. Immediate Settlement of Shallow Foundations Bearing on Clay. international Journal of Geomechanics 8, 300–310. https://doi.org/10.1061/(ASCE)1532-3641(2008)8:5(300

Giese, P., 2005. Moho discontinuity. Elsevier Ltd. 645–659.

Goto, S., Tatsuoka, F., Shibuya, S., Kim, Y.-S., Sato, T., 1991. A Simple Gauge for Local Small Strain Measurements in the Laboratory. Soils and Foundations 31, 169–180. https://doi.org/10.3208/sandf1972.31.169

Kang, G., Tsuchida, T., Kim, Y., 2017. Strength and stiffness of cement-treated marine dredged clay at various curing stages. Construction and Building Materials 132, 71–84. https://doi.org/10.1016/j.conbuildmat.2016.11.124

Kitazume, M., Grisolia, M., Leder, E., Marzano, I.P., Correia, A.A.S., Oliveira, P.J.V., Åhnberg, H., Andersson, M., 2015. Applicability of molding procedures in laboratory mix tests for quality control and assurance of the deep mixing method. Soils and Foundations 55, 761–777. https://doi.org/10.1016/j.sandf.2015.06.009

Kitazume, M., Terashi, M., 2013. The deep mixing method, in: The Deep Mixing Method. CRC Press/Balkema, Leiden, The Netherlands.

Probaha, A., Shibuya, S., Kishida, T., 2000. State of the art in deep mixing technology. Part III: geomaterial characterization, in: Ground Improvement. Thomas telford Ltd, pp. 91–110.

Putera, M.A., Yasufuku, N., Alowaisy, A., Rifai, A., 2021. Optimizing modified triaxial testing for small strain zone using local displacement transducers and bender element for cement-treated soft soil. E3S Web of Conferences 331. https://doi.org/10.1051/e3sconf/202133103003

Schneider, J., Mayne, P., 2022. Soil Liquefaction Response in Mid-America Evaluated by Seismic Piezocone Tests.

Seng, S., Tanaka, H., 2011. Properties of Cement-Treated Soils During Initial Curing Stages. Soils and Foundations 51, 775–784. https://doi.org/10.3208/sandf.51.775

Skempton, A.W., Bjerrum, L., 1957. A contribution to the settlement analysis of foundations on clay. Géotechnique 7, 168–178. http://dx.doi.org/10.1680/geot.1957.7.4.168

Subramaniam, P., Banerjee, S., 2014. Factors affecting shear modulus degradation of cement treated clay. Soil Dynamics and Earthquake Engineering 65, 181–188. https://doi.org/10.1016/j.soildyn.2014.06.013

Viggiani, G., Atkinson, J.H., 1995. Stiffness of fine-grained soil at very small strains. Geotechnique 45, 249–265.

Xiao, H., Yao, K., Liu, Y., Goh, S.-H., Lee, F.-H., 2018a. Bender element measurement of small strain shear modulus of cement-treated marine clay – Effect of test setup and methodology. Construction and Building Materials 172, 433–447. https://doi.org/10.1016/j.conbuildmat.2018.03.258

Xiao, H., Yao, K., Liu, Y., Goh, S.-H., Lee, F.-H., 2018b. Bender element measurement of small strain shear modulus of cement-treated marine clay – Effect of test setup and methodology. Construction and Building Materials 172, 433–447. https://doi.org/10.1016/j.conbuildmat.2018.03.258

Yamashita, S., Kawaguchi, T., Nakata, Y., Mikami, T., Fujiwara, T., Shibuya, S., 2009. Interpretation of International Parallel Test on the Measurement of Gmax Using Bender Elements. Soils and Foundations 49, 631–650. https://doi.org/10.3208/sandf.49.631

Chapter 3

System of Laboratory Testing in Small-Strain of Cement-Treated Soils with Local Deformation Transducer and Bender Element Devices

3.1 Introduction

A common problem with the railway structure underlying clayey soil ground is settlement, especially for applying the thin structures such as ballastless track. In order to optimize the settlement behavior, that can be enhanced the stiffness parameters using cement-treated soils as ground improvement ((Evans et al., 2022; Solihu, 2020; Watanabe et al., 2021). However, to evaluate the settlement prediction and stress distribution of the ground improvement subjected to the train loading, it demands a proper mechanical property from laboratory and field investigation. Many techniques for field investigation (destructive) exist from which stiffness parameter can be derived, ranging from the standard penetration test to the sophisticated self-boring pressure meter (Clayton, 2011). Also, there are non-destructive methods comprise the dynamic mechanical properties, which subjected to the geophysics investigation such as shear wave velocity on the surface ground. It is expected that the mechanical properties in the field will be different from those of laboratory-prepared samples in a controlled environment (Probaha et al., 2000; Yamashita et al., 2009).

Based on the Japan standard to get the characterization of mechanical properties was usually applied to the unconfined compressive strength (UCS). That is estimation ratios for determining the ultimate strength of the field investigation (q_{uf}) result in the laboratory (q_{ul}), which is the ratio used by the dry jet mixing associaton for japan between 1/3 and 1/4 (Probaha et al., 2000). These estimation were reflected to the numbers of experienced and project has been developed in Japan. However, to evaluate the strength should be based on the boundaries of research and regulation terms. Due to sensitivity of the high-speed project it requires the expecting level of quality control and assurance based on laboratory analysis, which can be used for the pre-design parameter. For this reason, applying the small strain devices measurement can be used to enhance the quality control in mechanical properties behavior along with the strain ranges (Goto et al., 1991).

Through this chapter, to optimizing the laboratory testing, the small strain measurement devices were equipped to the triaxial $\overline{CU}$ testing under various confining pressures. A series of static tests using various cement content and curing period were performed. Furthermore, the stress-strain relationship of the cement-treated soil was evaluated to obtain the mechanical properties.

3.2 Materials: soil and cement-treated soil preparation

3.2.1 Ariake clay engineering properties

In order to evaluate the mechanical behavior of Indonesian clay to predict the elastic settlement for HSR project in Indonesia, based on the comparison of engineering properties, it had similarity with the Ariake clay. It was collected around the Ariake Bay, in the western part of Kyushu Island, Japan. For Indonesian clayey soil, the data were collected from the oedometer and field investigation test nearby the HSR project area. The particle size distribution curve as well as the physical and mechanical properties of Ariake clay are shown in Error! Reference source not found. and Error! Reference source not found., respectively. Based on the Japanese Geotechnical Society Standard (JGS 0051-2009), Ariake clay and Indonesian clayey are classified as a cohesive soil with a high liquid limit (C.H.). The

oedometer test was conducted to determine the compressibility index and the pre-consolidated pressure. Error! Reference source not found. delineates the consolidation curve (e-log p curve), where Indonesian clayey and Ariake clay sample were indicated similarity on initial of void ratio result. Ariake clay was got the over-consolidated (OC) curve based on the increment of consolidation pressure within initial pressure. Based on engineering properties, comparison of Ariake clay and Indonesian clayey has been indicated an equivalent result on trend. Furthermore, using Ariake clay can be evaluate and estimate the mechanical behavior of Indonesian clayey soil for HSR Projects.

3.2.1.1 Determine cement content

Ordinary Portland Cement (OPC) was used as a binder material to enhance Ariake clay mechanical properties. The stiffness increment of mechanical properties subjected to the confining pressure and curing period was estimated by using three differences of cement mixing ratios (A_w). Three cement mixing ratios were used to make cement-treated soil samples, those are 15, 25, and 35%. Thus, the cement content was then determined using the following equation (Kitazume and Terashi, 2013):

$$C = \left\{ \frac{10\rho_t}{\left(\frac{1+w_n}{100}\right)} \right\} \times A_w \quad (1)$$

Where C is in (kg/m^3), ρ_t, and w_n are the wet soil density and the natural water content, respectively. The cement-treated sample preparation in laboratory was explained through the following sub-sections.

Table 3.1 Soil Parameters.

	Liquid Limit	**Soil particle density**	**Compressibility Index**	**Cement mixing ratios**	**Cement Content**
	(%)	ρs (g/cm3)	CC	Aw (%)	C (kg/m3)
Ariake clay	232-240	2.43	2.2	15, 25, 35, 50	55, 92, 128, 183

Indonesian clayey soil	120-192	1.5 – 2

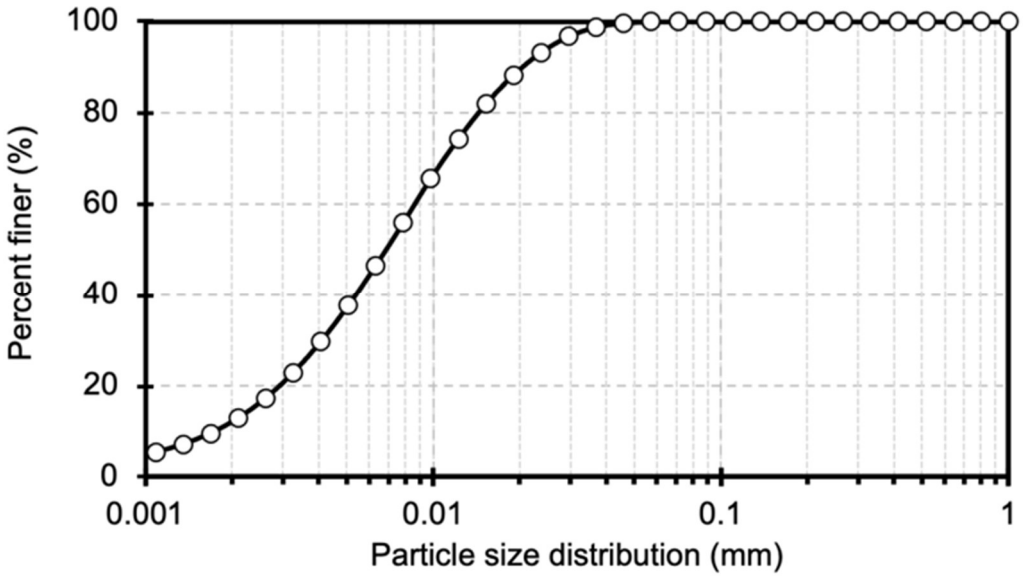

Fig. 3.1 Ariake clay particle size distribution curve.

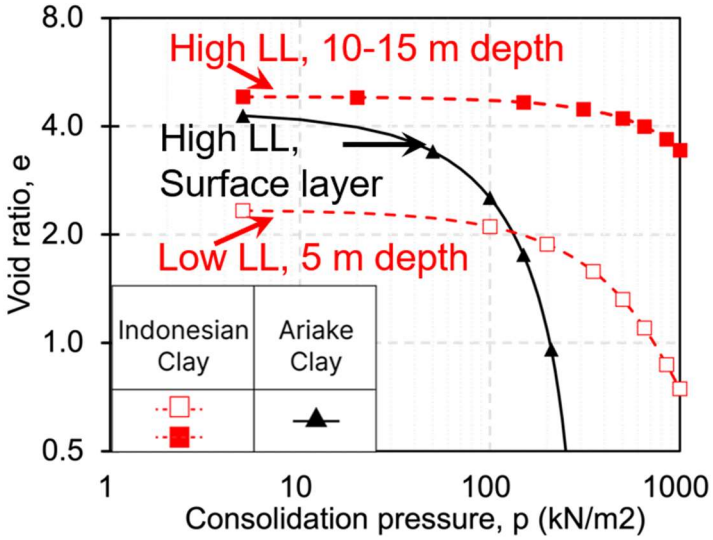

Fig. 3.2 Ariake clay consolidation curve (e-log p curve).

3.2.2 Cement-treated laboratory mixing

3.2.2.1 Dry mixing procedure

Mixing procedure was conducted following the standardized procedures and non-standardized procedure (i.e. self-arranged procedures). Kitazume and Terashi

(2013) has specified the procedures of mixing that referred to Japanese standard. Initially, Ariake clay was sieved through a 425 μm mesh diameter to remove the impurities, insects, and shrubs as well as to ensure the samples' homogeneity. It must be noted that the water content was set as two times the liquid limit of Ariake clay. Under such slurry conditions, the dry mixing method was adopted for soil-cement sample preparation (Kasama et al., 2000).

Therefore, Ariake Clay was mixed adequately with the 15, 25, and 35% dry Ordinary Portland Cement (OPC) using an electric hand mixer. The procedure of mixing was conducted until it was sufficiently homogeneous (it took typically 10 minute). A manual intervention during machine mixing is recommended by using manual hand mixer to check the binder. Eighteen cured cement-treated soil samples with different cement content and the curing period were used for testing. Cement-treated soils were prepared using statically compacted stabilized soil technique based on JGS (0812-2009).

Table 3.2 Test program for triaxial undrained test.

Test ID	**Cement Content (kg/m^3)**	**Curing Period (day)**	**Confining Pressure (kPa)**	**Total sample**	**Axial LDT max: 5 mm**	**LVDT max: 15 mm**	**Radial LDT max: 1.5 mm**	**BE**
S0101	55	7	25, 50, 100	3	✔	✔	✔	
S0102	55	28	25, 50, 100	3	✔	✔	✔	
S0201	92	7	25, 50, 100	3	✔	✔	✔	
S0102	92	28	25, 50, 100	3	✔	✔	✔	
S0301	128	7	25, 50, 100	3	✔	✔	✔	
S0302	128	28	25, 50, 100	3	✔	✔	✔	

S0401	138	7	100	3	✔	✔	✔	✔
S0401	138	28	100	3	✔	✔	✔	✔

3.2.2.2 Modified Mold for Bender Element test in cement-treated soils

The element test can successfully produce the result of soil mechanical properties by choosing a proper curing mold for cement-treated soils, when we analyzed the long-term stiffness more than 7 days. Bender Element (BE) test program as shown in **Table 3.2** requires the pilot hole for inserting the BE plate to the specimen for transmitting and receiving the shear wave velocity. The next steps for sample preparation were compacting the slurry condition into cylindrical acrylic molds (it is required to rub the mold with the grease) with dimensions of 50 mm in diameter and 100 mm in height, as depicted in **Fig. 3.3 (a).** It is defined in **Fig. 3.3 (b)** that two-stopper sided was equipped with a thin plate to make a pilot hole of BE devices. The molds were well-sealed to maintain the water content. All samples were cured at 20±3℃ for 7 and 28 days.

The preparation the LDT test program can be conducted by using the plastic molds with dimensions of 50 mm in diameter and 100 mm in height. The samples were well-sealed and cured at 20±3℃ for 7 and 28 days. In addition, the compacting process is carried out about 30 times for each layer. However, each step for preparing the cement-treated soils has to be taken in no longer than 5-10 minutes for each sample.

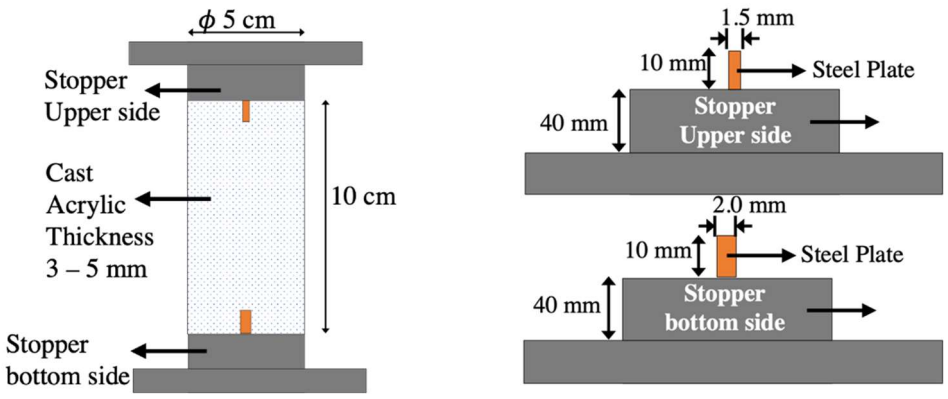

(a) (b)

Fig. 3.3 (a) Acrylic curing mold for BE test program (b) stopper geometry

3.2.3 Testing procedure of triaxial $\overline{CU}$

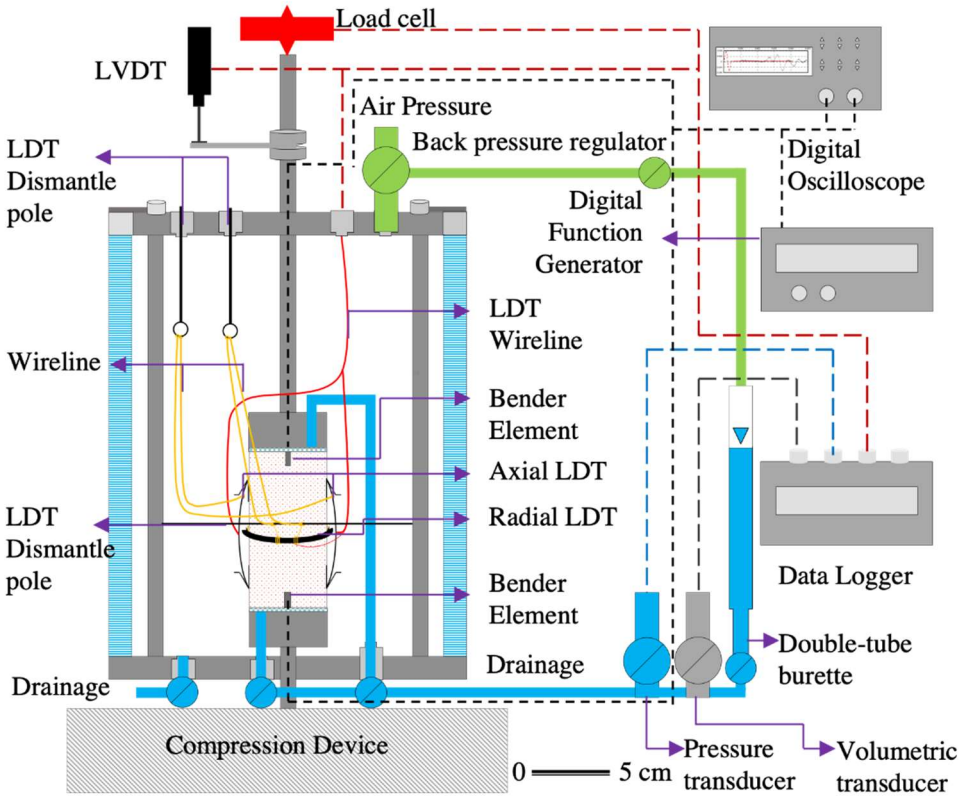

Fig. 3.4 Triaxial testing undrained using BE and LDT.

This research was using Triaxial $(\overline{CU})$ in static condition test as shown in Fig. **3.4**. The standard of testing in the conventional method on shear loading rate is about 0.005 mm/min, referred as a clay material in JGS-0821. In the conventional method, there are critical measurement devices such as linear variable displacement transducers (LVDT) to measure the deformation characteristic from the outside of triaxial chamber.

In order to use the strain measurement devices for triaxial testing, the coefficient parameters to convert the strain meter to the actual displacement were considered. In the case of the LVDT, the coefficient is about 0.005508 for 1 mm of axial displacement ranges. Load cell was contributed for getting the stress data about 5

MPa, which combined with stress-strain in axial direction to obtain the (E) Young Modulus. However, the cement-treated soils test that using conventional testing cannot determine the shear modulus (G), where the radial displacement is not measured in shearing process of undrained test. Another consequence of using the LVDT outside the chamber is the bedding error on the top and bottom on cement-treated soil. Due to this reason, the utilization of local strain measurement inside the chamber to reduce the bedding error is needed.

The accuracy of strain measurement using LVDT is about 0.01 mm, this resolution is associated with strain range measurement. For instance, the measurement with LVDT has a coverage of the strain range within 0.01 to 10%. However, this strain range measurement needs to be evaluated with the local strain measurement devices. Furthermore, the accuracies in small-strain and large strain can be defined by stress-strain relationship and determine the Poisson's ratio (ν) and Shear modulus (G).

3.2.3.1 Axial and radial local displacement transducer

LDTs was made by bronze plate and the dimension was approximately 90 mm in length, 3.5 mm in width, and 0.2 mm in thickness. The dimension of LDT can be seen in **Fig. 3.5 (a)**. The pseudo-hinged can be described as an attachment for LDT to the triaxial specimen. **Fig. 3.5 (b)** was shown the LDTs attached with Pseudo-hinged using epoxy glue and double-sided tape on the membrane, which are making a less disturbance. It had a specified angle to attach the axial LDT. The LDTs must be calibrated before setup into pseudo-hinged, the calibration can be evaluated through uniaxial testing procedure to get the strain and voltages.

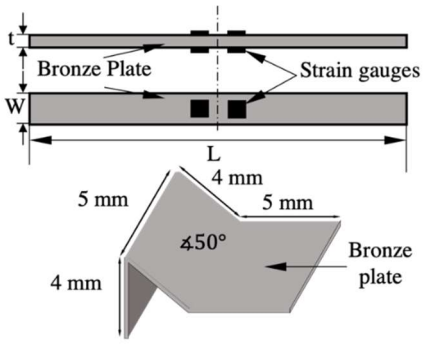

(a)

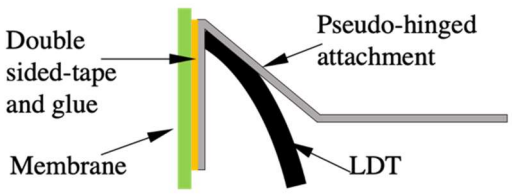

(b)

Fig. 3.5 (a) LDT geometry and (b) pseudo-hinged specification

The calibration of axial LDT is used to describe the non-linear relationship of the output voltage with the displacement as shown in **Fig. 3.6 (a)**. It informs that the limitation of the displacement is about 5 mm and 5% in the strain range. The radial LDT is used to describe the linear relationship. It can be seen in **Fig. 3.6 (b)**. The figure shows that the negative and the positive limitation of displacement ranges are about 1.5 mm and 1.5 mm. From this result, the initial condition of strain ranges can be evaluated using this equation and the maximum displacement has been determined to prevent from the broken a part of LDTs devices.

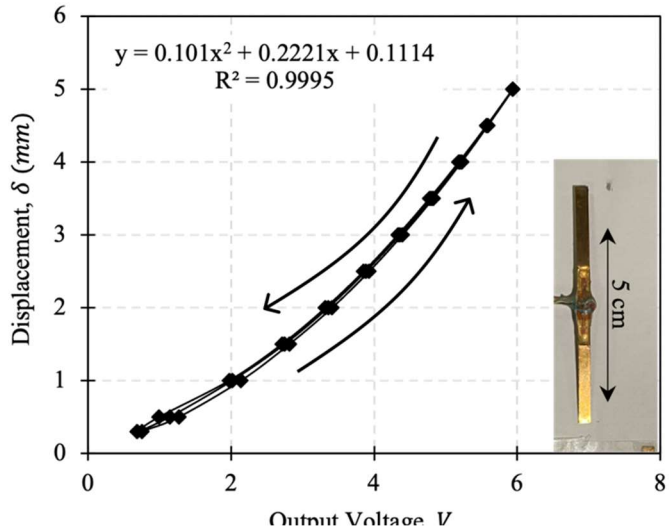

(a)

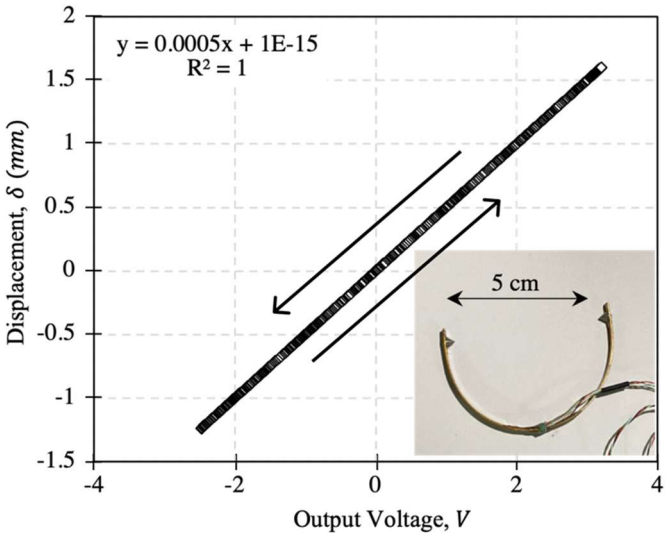

(b)

Fig. 3.6 (a) Calibration of Axial LDT and (b) Radial LDT through uniaxial test

The calibration of axial LDT is used to describe the non-linear relationship of the output voltage with the displacement that is shown in **Fig. 3.6 (a)**. It explains that the limitation of the displacement is about 5 mm and 5% in the strain range. On the other hand, the radial LDT is used to describe the linear relationship as seen in **Fig. 3.7 (b)**. This figure shows that the negative and the positive limitation is about 1.5 mm and 1.5 mm. From this result, the initial condition has been evaluated and the test condition saved in every axial and radial LDT testing.

The LDTs must be equipped into the pseudo-hinged as illustrated in **Fig. 3.5 (b)**. During the consolidation process and increasing the confining pressure, there is a problem on pseudo-hinged of LDTs that showed a detachment behavior. Therefore, it should be attached to the pseudo-hinged carefully and it requires an improvement to the system setup, such as applying the epoxy glue and double-sided tape, that used to attach it into the membrane. Both LDTs were carefully monitored during shearing and were detached from the sample using a hook line from the outside of the chamber once reaching the maximum displacement capacity.

3.2.3.2 Bender Element devices

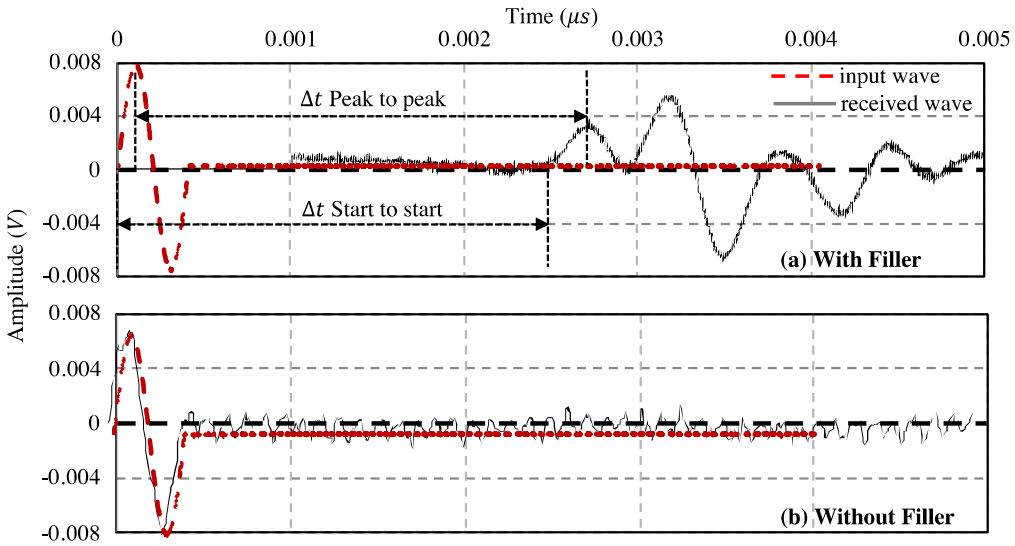

Fig. 3.7 Identification method using BE test (a) describe peak to peak and start to start method with filler and (b) describe the condition without filler.

The material of BE consists of silver, piezoelectric ceramic, and nickel as the electrode. The original dimension of BE that was used in the test is about 15 mm in length, 5 mm in width, and 1.5 mm in thickness. The dimension has been enlarged by coating the BE with special glue to protect it from the water leakage.

To prevent the measuring behavior of shear wave velocity due to the pilot hole gap, illustrate in **Fig. 3.7.** Different responses were shown in terms of the effectiveness in sample preparation that using filler and without filler. The usage of filler can reduce the discrepancies of the shear wave velocity measurement and it also protects the sample from a stress behavior of BE devices (sensitive devices, need to be limited from the stress). The maximum displacement during shearing is found to be 5 mm, it refers to casting hole maximum depth about 2.2 cm. The filler composition that was used in the test have a ratio of 1:2 between binder to water. The geometry of filler is following the **Fig. 3.8**.

The shear wave velocity can be used to calculate the shear modulus by analyzing the arrival time and amplitude of the data received from the oscilloscope. There are several methods to determine the shear modulus, such as the start-to-start method, peak-to-peak method, and cross-correlation method. This research used the peak-to-peak method to evaluate the shear modulus. The data from laboratory testing that

used a single pulse of sine wave input. Shear wave velocity was observed from the peak position of an input wave to the first peak of the received wave.

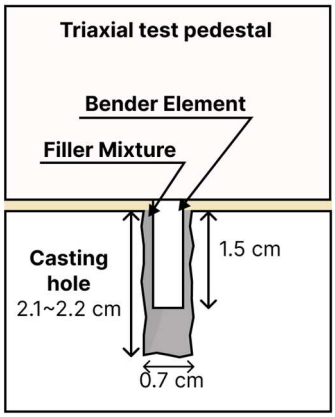

Fig. 3.8 Geometry of filler structure to improve the BE devices measurement

Shear wave velocity was observed from the peak position of an input wave to the first peak of the received wave. Shear wave velocity for transmitting the wave frequency into the specimen is about 1 – 5 kHz, and the shear wave velocity has been magnified the amplitude 5 times greater it might be a good accuracy for determine the high stiffness material such as cement-treated soils.

3.3 Local and external strain measurement devices

3.3.1 Stress-strain relationship

The evaluation of local and external strain measurement devices has been divided into two categories, large and small strain ranges. **Fig. 3.9** is mainly focused on measurements using LDTs and LVDT devices subjected to the influence of various of confining pressure. Cement contents were varied into 55 kg/m^3 for low content, 92 kg/m^3 for medium content, and 128 kg/m^3 for high content which were evaluated with 25 and 100 kPa of confining pressure. There was no significant discrepancy observed between LDT and LVDT in the low cement content although the axial and radial strain were increased. However, a significant discrepancy was observed in the medium and high cement content along the axial and radial strain axes. In small strain ranges the discrepancies of deviatoric stress was started along the

elastic to elastoplastic condition, it might be affected the large strain ranges. However, in large strain range within the plastic condition was shown converged line between LDT and LVDT measurement. Based on Japanese standard testing procedure (JGS 0523-2009) related to the maximum displacement of triaxial testing is about 15 mm or 15% of specimen height, when measuring the plastic condition it can be observed more equivalent result between LDT and LVDT measurement. A further analysis should be done by comparing the peak deviatoric stress with the peak radial-axial in the large strain range. Furthermore, for the small strain range can be analyzed by comparing the initial peak deviatoric stress and initial axial-radial in the 0.1% of each strain range.

Fig. 3.10 describes the high cement content, which was measured by stress-strain relations by bender element and LDTs devices measuring in moderate confining pressure (100 kPa). The cement content being used was 138 kg/m^3, which then were varied into 7 and 28 days. Based on the stress-strain relationship, the discrepancies of peak deviatoric stress that referred to the axial strain ranges can be described. LDTs can measure the peak of deviatoric stress under small strain ranges, although the LVDT has showed the large strain ranges behavior, that influences mainly at bedding errors between the BE pedestal into CTS specimen. Using filler in a pilot hole it can increases the reliability measurement of LVDT during shearing, which is the discrepancies was indicated decreasing if compare with the LDTs measurement. Increment of axial-radial was intercorrelated to the influences of stress-strain, which showed a good agreement that was provided between radial-axial LDTs, and it can give a less bedding error. In addition, this combination should be evaluated with the parameter studies of stress-strain relations by the specified parameters, influenced by confining pressure.

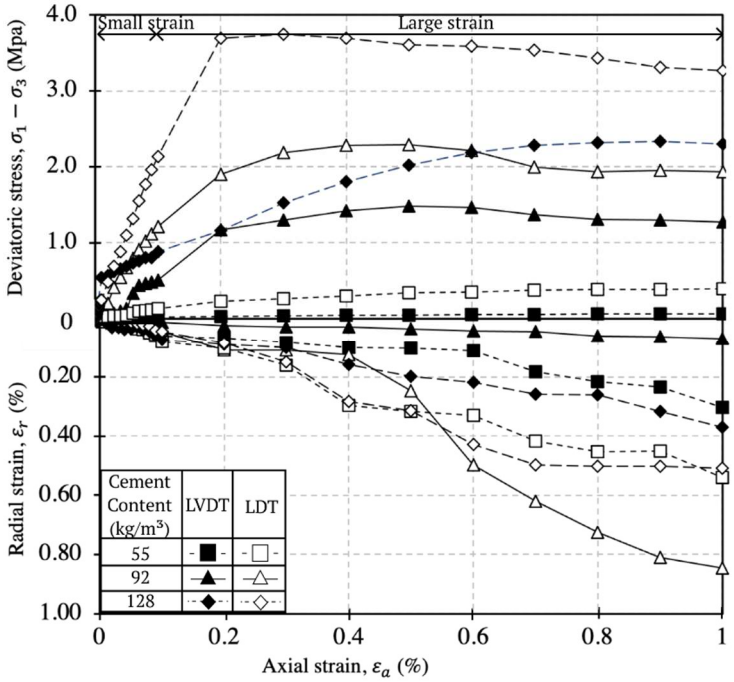

Fig. 3.9 Stress-strain relationship of cement-treated soils and influenced of cement content in 28 day curing period

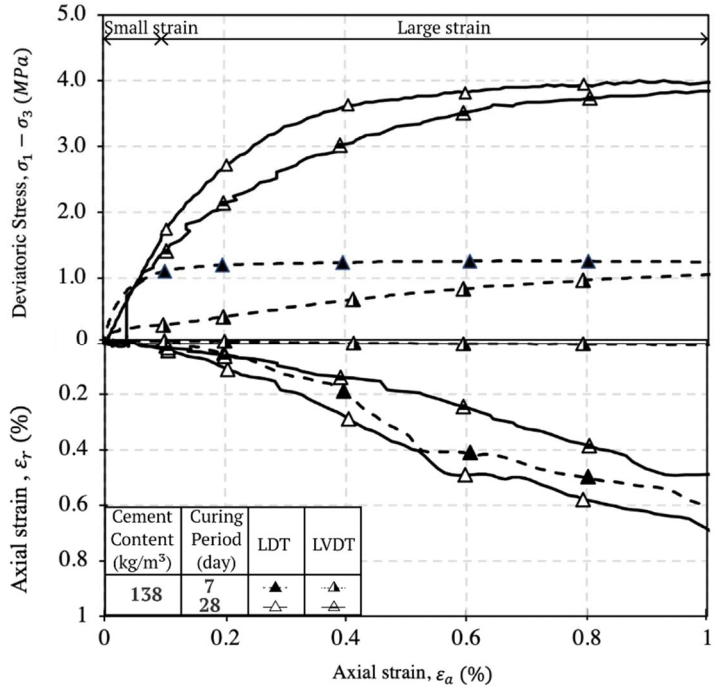

Fig. 3.10 Stress-strain relationship of high cement content with moderate confining pressure.

3.3.2 Accuracy in large strain measurement

In order to evaluate the accuracy of the strain measurement devices that consist of axial LDT, radial LDT and LVDT, the determination of influences of stress-strain measurement subjected to the different of confining pressures is required. Where it can also be used to determine the strengthening degree of CTS specimen. The estimation of peak deviatoric stress mainly focused on various large strain ranges which will be discussed thoroughly on the next sub-sections.

3.3.2.1 Influence of confining pressure related to the peak deviatoric stress

This section discusses about the peak of deviatoric stress (q_{max}) measured using LDT and then categorizes the normalized value of increment in confining pressure (σ_3/P_a) to describe the strength behavior of CTS. In **Fig. 3.11 (a)** the distribution of peak deviatoric stress with varied parameter of cement content and curing periods is shown. In low cement content (55 kg/m^3) the increasing peak deviatoric stress due to the increasing value of confining pressures was observed. A similar gradient is obtained when the curing period was increased from 7 days to 28 days in low cement content. However, in medium and high cement content (92 and 128 kg/m^3) a noticeable different in gradient between 7 and 28 days of curing period is witnessed. It can be concluded for high cement content that the hardening of CTS in large strain behavior can increase the gradient.

In **Fig. 3.11 (b)** the ratios between LDT and LVDT with varied parameter of cement content and curing period was delineated. This figure describes the discrepancies behavior at peak deviatoric stress subjected to the accuracy of measurement devices in large strain ranges. At low confining pressure was shown the small discrepancies between LDT and LVDT, those were mentioned to the various cement content and curing period. Increasing confining pressure was determined the increasing of discrepancies mainly related to the medium to high cement content (92 and 128 kg/m3). However, in low cement content (55 kg/m^3) small differences was observed in the increment of the confining pressure, which can be described from gradient angle and curing periods. Furthermore, in medium to high cement content (92 and

128 kg/m^3) was determined the high influences of discrepancies related to the increment confining pressure and curing period. In addition, LDT measurement accuracy was significantly enhancing the hardening of CTS in large strain ranges. Also, it might be influencing the undrained shear strength parameters.

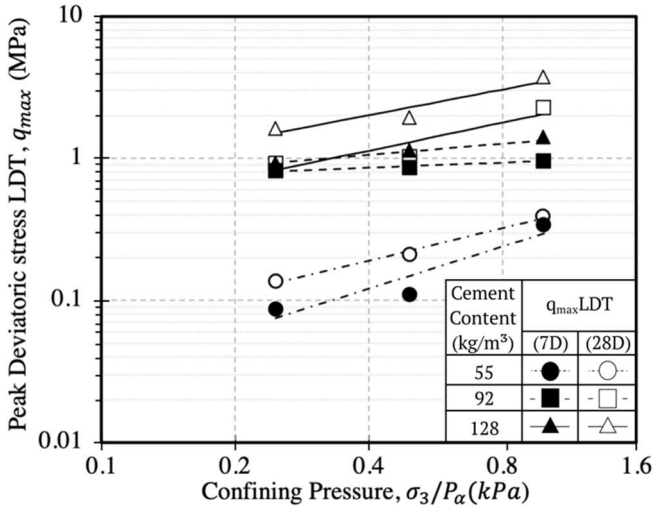

(a)

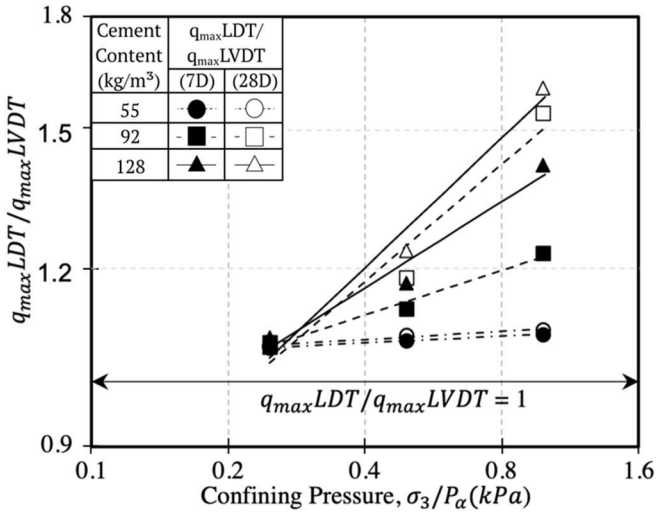

(b)

Fig. 3.11 (a) Peak deviatoric stress LDT and (b) Ratio between LDT and LVDT.

3.3.2.2 Influence of confining pressure related to the radial strain

The relations between radial strain LDT (ε_r) and confining pressures (σ_3/P_a) has been considered with various cement contents and curing periods. The

discrepancies of LDTs behaviors into maximum of radial strain LDT (ε_{rmax}) were found, where the normal test procedure of triaxial $\overline{CU}$ cannot evaluate the radial displacement. The Poisson's ratio (ν) and shear modulus (G) can be evaluated with the additional strain gauges such as the radial strain LDT that is equipped into triaxial $\overline{CU}$. Axial LDT and LVDT has been compared, the result is using LVDT had discrepancies to measuring the CTS axial-radial strain relationship. The good accuracy of the radial LDT measurement was considered to explained in this section.

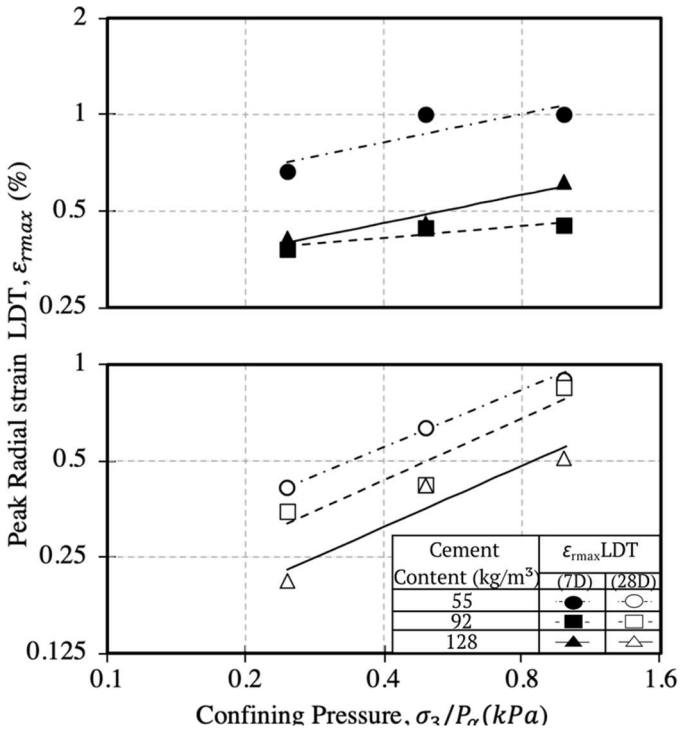

Fig. 3.12 Peak radial strain using LDT by influenced of confining pressure.

In **Fig. 3.12** the peak radial strain from LDT from 7 and 28 days of curing is shown. Based on those parameters, the radial strain produced by 7 days curing period has a larger value than those with 28 days curing period. That result was determined the decreasing of gradient of peak radial strain by increasing the curing periods. In low cement content (55 kg/m3) was determined large gradient increment of peak radial strain rather than medium to high cement content (92 – 128 kg/m3). Those parameters can be indicated to the strengthening strain by increase the curing period, which was subjected to the measurement of radial LDT device.

3.3.3 Accuracy in small strain measurement

In order to evaluate the accuracy of the strain measurement devices in small strain ranges, the LDTs, bender element and LVDT measurement device must be prepared. The influences of stress-strain measurement subjected to the different of confining pressures should also be analyzed. When determining the small strain ranges, the strain ranges shall be adjusted by using 0.1% in strain ranges. Detailed explanations are outlined as follows.

3.3.3.1 Influence of confining pressure due to the initial deviatoric stress

This section discusses about the initial of deviatoric stress (q_{max}) measured using LDT and categorized the normalized of increment confining pressure (σ_3/P_a) to describe the strength behavior of CTS. In **Fig. 3.13 (a)** the distribution of initial deviatoric stress that varied parameter of cement content and curing periods is shown. In low cement content (55 kg/m^3) it was found that the increasing initial deviatoric stress was affected by the confining pressures increment. When the curing period in low cement content was increased, a similar gradient within 7 and 28 days of curing period was obtained. In medium and high cement content (92 and 128 kg/m^3) the trend of gradient was found to be similar in every confining pressure for both 7 and 28 days of curing period. Based on initial peak of deviatoric stress, it can be explained in high cement content that the hardening of CTS is relatively higher than the medium and low cement content.

Fig. 3.13 (b) delineates the ratios between LDT and LVDT with varied parameter of cement content and curing period. It shows the discrepancies behavior at initial deviatoric stress subjected to the accuracy of measurement devices in small-strain ranges (average measurement at 0.1% of axial strain). Previously, the peak deviatoric stress shows small discrepancies in low confining pressure, although in small strain ranges was described the distinguish accuracy between LDT and LVDT, those were mentioned to the various cement content and curing period. Along with the increment of confining pressure, large discrepancies mainly occurred in the medium to high cement content (92 and 128 kg/m^3). However, in low cement

content (55 kg/m^3) was determined only small differences in gradient angle are observed by increasing the confining pressure. On the other hand, in medium to high cement content (92 and 128 kg/m^3) the ratios between LVDT and LDT were significantly influenced by the increment of confining pressure and curing period. In addition, LDT measurement accuracy was considerably enhancing the hardening of CTS in small-strain ranges. Also, it might influence to the undrained shear strength parameters.

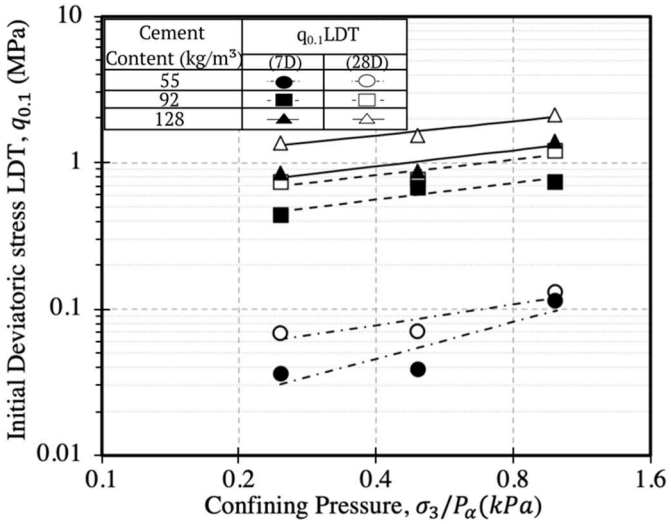

(a)

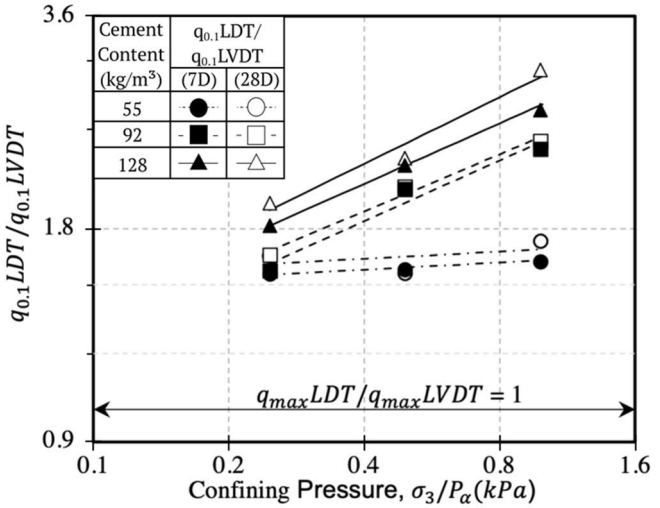

(b)

Fig. 3.13 (a) Peak Initial deviatoric stress LDT and (b) Ratio between LDT and LVDT.

3.3.3.2 Influence of confining pressure due to the initial radial strain

The relations between radial strain LDT (ε_r) and confining pressures (σ_3/P_a) in small-strain ranges was analyzed with various cement contents and curing periods. The discrepancies of LDTs behaviors into average axial strain at 0.1%, which radial strain of LDT can be useful to determine the angle of gradient ($\varepsilon_{r0.1}$). Also, to determine the initial Poisson's ratio (ν) and shear modulus (G), those can be optimized for measuring the initial stiffness using radial LDT that is equipped into triaxial $\overline{CU}$. Previously, axial LDT and LVDT was compared at the initial condition, the result of using LVDT shows discrepancies to measuring the CTS axial-radial strain relationship, the explanation was considered using radial LDT only.

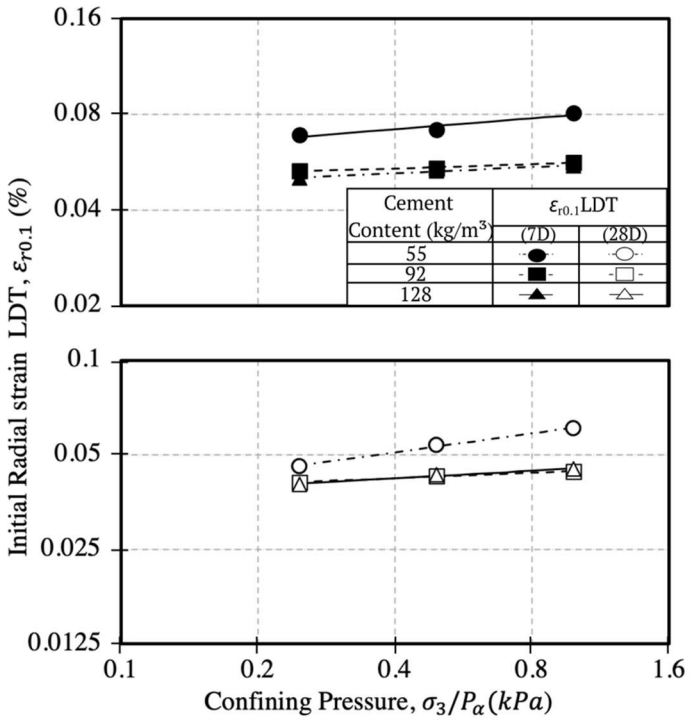

Fig. 3.14 Peak Initial of radial strain using LDT by influenced of confining pressure.

In **Fig. 3.14** the behavior of initial radial strain from LDT was analyzed in 7 and 28 days of curing. The result of low cement content (55 kg/m^3) shows that those cured in 7 days has a larger gradient compared to those cured in 28 days, for every increment of confining pressure. That result was determined the strengthening of CTS specimen by increasing the curing period. However, in medium to high cement

content (92 – 128 kg/m3) was obtained the similar trend of gradient angle within increment of confining pressure. That could be indicated the result of Poisson's ratio (ν) has similarity within the increment of strain ranges.

3.3.3.3 Influence of high cement content related to the initial shear modulus

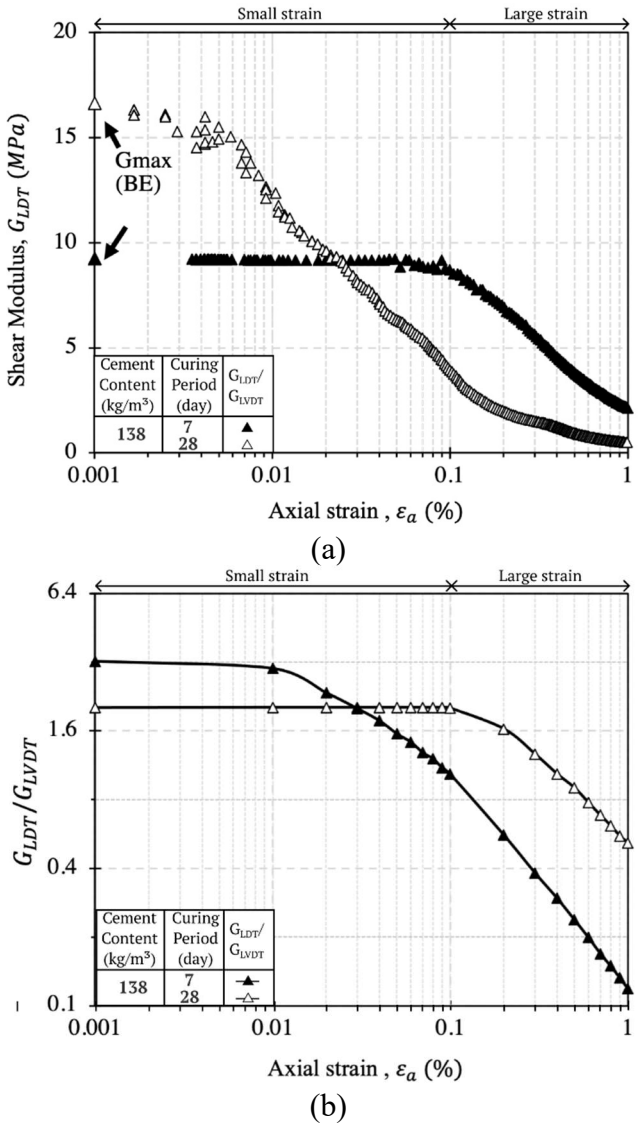

Fig. 3.15 (a) Peak Initial deviatoric stress LDT and (b) Ratio between LDT and LVDT.

The parameter of the Shear Modulus has been commonly used for the deformation characteristics in practices. Only a few researchers were focused on Shear Modulus in traffic load induced vibration to the ground improvement structure. In order to

define the Shear Modulus effect of cement treated soil in dynamic condition, the triaxial $\overline{CU}$ can be measured by applying the combination of radial and axial strain measurement devices. In addition, this application was developed on the nonlinearity of small strain range within 0.001% to 1%. However, the measurement of the static condition for obtaining the Shear Modulus in small strain range is used to optimize the system of testing, especially with moderate confined pressure and high cement content. Furthermore, the research on dynamic condition has been performed by applying the same condition on the system of testing. The Shear Modulus can be defined by the following equation.

$$\text{Shear Modulus } = -\frac{(\text{E})}{2(1+\upsilon)} \tag{3}$$

The initial shear modulus can be determined during the shearing process based on the Poisson Ratio and the Secant Modulus. The result of Shear Modulus was analyzed in association with strain measurement such as the axial strain in LDT and LVDT, as shown in **Fig. 3.10**. In 7 days of curing, the small strain range below 0.1% is relatively linear, the condition can be seen in **Fig. 3.15 (a).** The result of 28 days of curing period has to be described in non-linear condition. In small strain range (0.001%) LDT and BE are in good agreement by obtaining the initial Shear Modulus ($G_{\max}$), and differ from the modulus determined using the LVDTs. Therefore, it can be concluded that by increasing the axial strain, the Shear Modulus decreases.

The observation is made to evaluate the system of testing between LVDT and LDT from 0.01% to 1% in strain range as shown in **Fig. 3.15 (b)**. The result shows the initial Shear Modulus, which implies that the LVDT is underestimated by the axial LDT. The difference in the measured Shear Modulus was determined using the LDT and the LVDTs decrement towards larger strain ranges and converges to the same value for an axial strain equals or larger than 1%. Furthermore, the capacity of LVDT cannot be measured when the value is below 0.01%. Meanwhile, the

accuracy of the system of testing has to described a higher stiffness of material depends on the strain measurement devices and specifically in small strain range.

3.4 Summary

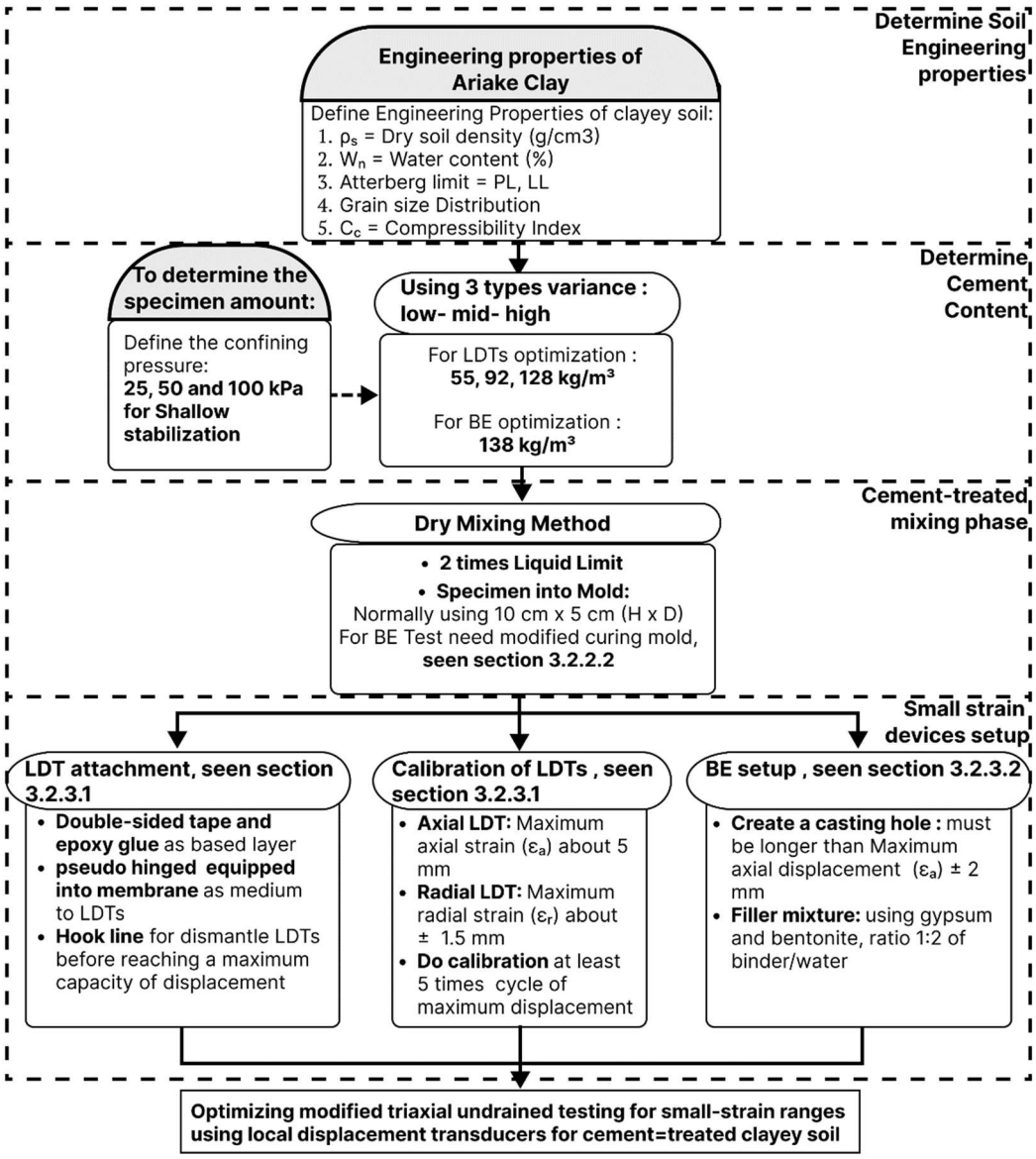

Fig. 3.16 Schematic diagram of Triaxial testing undrained using small-strain devices measurement for cement-treated soils

Through this study, the conventional Triaxial $\overline{CU}$ testing system was combined with the local and external strain measurement devices and BE system. The study aimed at optimizing the accuracy for testing the cement-treated clayey soil that mainly

focused on the small-strain range, it can be illustrated with a schematic diagram contained in **Fig. 3.16**.

The initial purpose of this chapter is to determine the engineering properties of Ariake clay which contributes to the description of the compressibility index (C_c) and Atterberg limit. The result can be considered as factors to select the variation of cement content and confining pressure. The cement contents were than categorized as low – mid – high specimen, by calculating the soil-binder ratio in kg/m^3. The method that was used in cement-treated mixing phase was following the steps for high Liquid Limit (LL) index, as the slurry condition (high water content) is dominantly found in Ariake natural ground. Using a modified mold such as acrylic mold with steel plate for BE pilot hole, was considered a good combination to protect the specimen within the curing period and it was found to be an easier way to insert the BE devices through the pilot hole.

There are several steps to do in small strain devices setup and configuration process, such as the calibration of LDTs before being equipped with the triaxial specimen. The calibration was usually conducted by using 5 times cycles until it reaches the maximum displacement. During the shearing process, a careful observation is required for limiting the displacement of LDTs, as it can protect the LDTs from getting error measurement and reach the failure state. To ensure the accuracy of the measurement and prevent the detachment behavior during the shearing process, this study suggested to apply the epoxy glue and double-sided tape to the surface of LDT's hinge-attachment.

For BE setup, it is required to keep the pilot hole gap from BE devices at least two millimeters from maximum displacement of each specimen. In addition, the gap on the pilot hole must be filled using the filler, so that the measurement of shear wave velocity of cement-treated soils sample in high cement-content and moderate confining pressure can be optimized. Moreover, the use of filler was contributed in preventing the BE from the stress behaviors in axial direction. The filler was

consisted of bentonite and gypsum; it was used the weight ratio 1:2 of binder and water.

In the small strain range (< 0.01%) for cement-treated soils with high cement content (138 kg/m^3), a significant discrepancy in the shear modulus was confirmed, which was more profound under moderate confining pressure. Finally, to ensure reliable determination of the cement-treated clayey soils shear behavior over the entire strain range, simultaneous testing using the LDT and LVDT is highly recommended.

In the small strain range (< 0.01%) for cement-treated soils with high cement content (138 kg/m^3), a significant discrepancy in the shear modulus was confirmed, which was more profound under moderate confining pressure. Finally, to ensure reliable determination of the cement-treated clayey soils under low shearing process and obtain the entire axial-radial strain range, simultaneous testing using the BE devices supporting the LDTs for evaluating the degradation stiffness modulus is highly recommended.

References

Clayton, C.R.I., 2011. Stiffness at small strain: research and practice. Géotechnique 61, 5–37. https://doi.org/10.1680/geot.2011.61.1.5

Evans, J., Ruffing, D., Elton, D., 2022. Fundamental of ground improvement engineering, 1st Edition. ed. CRC Press.

Goto, S., Tatsuoka, F., Shibuya, S., Kim, Y.-S., Sato, T., 1991. A Simple Gauge for Local Small Strain Measurements in the Laboratory. Soils and Foundations 31, 169–180. https://doi.org/10.3208/sandf1972.31.169

Kasama, K., Ochiai, H., Yasufuku, N., 2000. On the Stress-Strain Behaviour of Lightly Cemented Clay Based on an Extended Critical State Concept. Soils and Foundations 40, 37–47. https://doi.org/10.3208/sandf.40.5_37

Kitazume, M., Terashi, M., 2013. The deep mixing method, in: The Deep Mixing Method. CRC Press/Balkema, Leiden, The Netherlands.

Probaha, A., Shibuya, S., Kishida, T., 2000. State of the art in deep mixing technology. Part III: geomaterial characterization, in: Ground Improvement. Thomas telford Ltd, pp. 91–110.

Solihu, H., 2020. Cement Soil Stabilization as an Improvement Technique for Rail Track Subgrade, and Highway Subbase and Base Courses: A Review. Journal of Civil and Environmental Engineering 10:3. https://doi.org/10.37421/jcce.2020.10.344

Watanabe, K., Nakajima, S., Fujiwara, T., Yoshii, K., Rao, G.V., 2021. Construction and field measurement of high-speed railway test embankment built on Indian expansive soil "Black Cotton Soil." Soils and Foundations 61, 218–238. https://doi.org/10.1016/j.sandf.2020.08.008

Yamashita, S., Kawaguchi, T., Nakata, Y., Mikami, T., Fujiwara, T., Shibuya, S., 2009. Interpretation of International Parallel Test on the Measurement of Gmax Using Bender Elements. Soils and Foundations 49, 631–650. https://doi.org/10.3208/sandf.49.631

Chapter 4
Cement-treated Clayey Soils Mechanical Behavior in Small-Strain Ranges

4.1 Introduction

The first high-speed railway project in Indonesia is designed to connect several major cities such as Jakarta and Surabaya, covering a distance of about 700 km and operating at a maximum speed of 300 km/h (JETRO, 2012). It is planned to be constructed at the northern of Java Island, close to the Java Sea, and predominantly above lowland areas (Ranst et al., 2004), (Novico et al., 2022). The land is mainly comprised of clayey soil that characterized by a high compressibility index and a high water content. Often engineers face situations where the ground is unsuitable to hold the load on top of it and is expected to experience an excessive settlement when loaded by the planned loading due to construction and operation. Those are obstacles experienced especially in developing countries where costly techniques are not an option (Onyelowe et al., 2019). Cement-treated soil is used for structural elements such as substructures on the railway project as it could improve soft soils' engineering properties below the railway track subgrade and highway base and subbase courses (Solihu, 2020).

Generally, railway structures can be divided into ballasted and ballastless structures. The ballasted structures are characterized by high shear strength and low vertical settlement. On the other hand, the ballastless are lightweight structures, yet they endure better geometric stability, resulting in less differential settlement and lower

maintenance costs (Kumar and Singh, 2017). The ballastless track structures are generally recommended for an HSR design speed of 300 km/h and relatively weak subgrades, including lowlands (Kang, 2016). In addition to the track structure, many soil improvement techniques were utilized to improve the mechanical properties of the subsoil and reduce railways settlement. Among those are the railway superstructure (e.g., bridges and embankments) and soil reinforcement techniques, including pile foundation, drained consolidation methods, deep soil mixing (cement columns), and shallow stabilization (shallow cement-treated soils). The latter is a widely adopted technique in developing countries. However, it requires further research to prove its ability and enhance the design and assessment protocols on incremental strength related to mechanical behavior under lightweight structures.

Most studies on cement-treated soils focused on determining the initial mechanical properties at small-strain either by bender element test or resonant column (Xiao et al., 2018). Non-destructive testing methods can accurately determine the mechanical properties (Atkinson, 2000). However, a few studies focused on the initial stiffness parameters during the shearing process. The literature also mentioned that the degradation mechanical properties are predominant at a lower cement content and assessed by conducting unconfined compressive strength at a constant rate of 1.2 mm/min (Subramaniam and Banerjee, 2014). Moreover, the modified hyperbola method was developed to estimate cement-treated clayey soil's mechanical properties by evaluating the curvature parameter a, though it strongly depends on the strain rate during the shearing process (Vardanega and Bolton, 2014). For the early curing stage, it was reported that the constant parameter and slope angle on linear function could predict a relation between unconfined compressive strength and initial shear modulus (Kang et al., 2017). However, starting from 3 days of the curing period, discrepancies in the initial shear modulus that can be represented using a steep slope curve referred to as b parameter were intorduced. Therefore, it is inevitable that the undrained shear strength of cement-treated clayey soil should be evaluated as a function of confining pressure with

cement content (Kasama et al., 2006). In spite of the existing studies, the degradation of mechanical properties of cement-treated clayey soils subjected to low shearing rates and different confining pressure was not rigorously addressed.

Therefore, this chapter elaborates on the stress-strain behavior of cement-treated soil to accurately determine the mechanical properties from large to the small-strain ranges focusing on the cement content under various curing periods and confining pressures. Moreover, the intercorrelation between the confining pressure and the curing period for low and high cement mixing ratios is discussed under a low static shearing rate. This research was performed using a modified triaxial compression test equipped with LDTs and LVDTs to properly measure the small-strain ranges, where the discrepancies and reliability of the strain measurement are discussed.

4.2 Materials and testing procedure

4.2.1 Cement-treated samples

The specimens were prepared on 7 and 28 days of curing. A total of 18 samples were used to determine the mechanical behavior in small-strain ranges using triaxial consolidated undrained. Samples differ in the cement content, curing period, and the applied confining pressure during, as can be seen in **Table 4.1**.

4.2.2 Triaxial testing procedure

The testing procedure was done following the JGS 0523-2009 to determine the stress-strain development, as delineated in **Fig. 4.1**. Capturing the small-strain range and determining the soil stiffness parameters requires utilizing additional measuring devices. In this study, both the LDT and LVDT were used to capture small and large strain ranges. Moreover, the Axial and Radial LDTs were attached to the tested samples during testing to determine the Poisson's ratio and the shear modulus. The procedure of attaching the LDTs to a cement-treated soil sample was done following (Putera et al., 2021). The tests were loaded under undrained conditions and were isotropically consolidated with a 25, 50 and 100 kPa of confining pressure (σ_3).

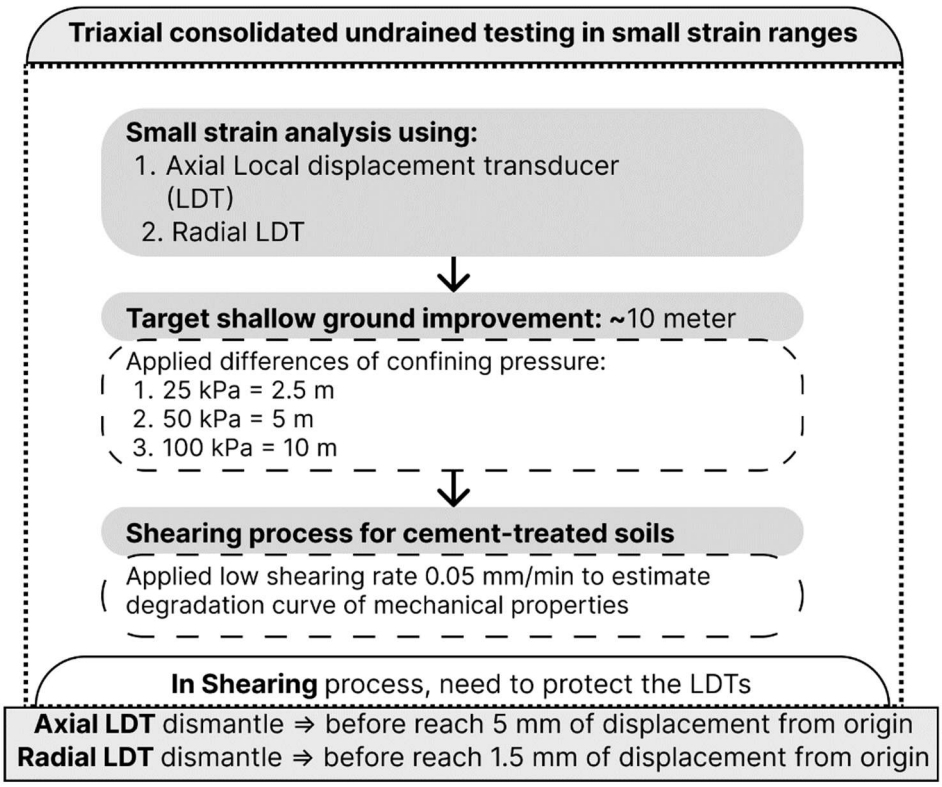

Fig. 4.1 Triaxial consolidated undrained testing program in small strain ranges

Table 4.1 Various of experimental test has been conducted in this chapter

Test ID	Cement Content (kg/m^3)	Curing Period (day)	Confining Pressure (kPa)	Total sample	Axial LDT max: 5 mm	LVDT max: 15 mm	Radial LDT max: 1.5 mm
S0101	55	7	25, 50, 100	3	✔	✔	✔
S0102	55	28	25, 50, 100	3	✔	✔	✔
S0201	92	7	25, 50, 100	3	✔	✔	✔
S0202	92	28	25, 50, 100	3	✔	✔	✔
S0301	128	7	25, 50, 100	3	✔	✔	✔
S0302	128	28	25, 50, 100	3	✔	✔	✔

This specific consolidation pressure was adopted in this study to imitate the in-situ cement-treated soil at shallow depths of around 2.5 to 10 m. The sensitivity of capturing the soil behavior under small-strain range conditions, a low shearing rate of 0.05 mm/min was applied for more accurate results. Both LDTs were carefully monitored during shearing and were detached from the sample using a hook line outside the chamber when they reached their maximum displacement capacity. For using the strain measurement result from LDTs, it requires to calculating with the calibration curve result that conversion was defined by the non-linear curve for the axial LDTs and linear curve for the radial LDTs.

4.3 Determination of mechanical properties between small to large strain ranges

4.3.1 Large strain ranges

4.3.1.1 Cohesion and friction angle

In large strain ranges, to categorize the mechanical properties was described by shear strength parameter using the Mohr-Coulomb failure criterion (Terzaghi, 1936).

$$\tau = (\sigma_1 - \sigma_3)\, tan\varphi + c \quad (1)$$

Where τ is shear stress, $(\sigma_1 - \sigma_3)$ is deviatoric stress based on measurement in triaxial testing. Two main parameters are φ for friction angle and c for cohesion. Those parameters represent the failure envelope behavior in soil mechanics. To define the friction angle, it is required to plot a (slope) tangent line at the maximum deviatoric stress (failure). The intercept line is called the cohesion and it requires various confining pressures to determine the behavior of normal stress in one variant of cement content. In this research 3 variances of confining pressure were used such as 25, 50 and 100 kPa.

4.3.2 Small-strain ranges

4.3.2.1 Initial Young Modulus

The Young Modulus (E) was determined from the deviatoric stress and axial strain curves to study the mechanical properties of cement-treated clayey soils, as shown in (2).

$$E = \frac{\sigma_1 - \sigma_3}{\varepsilon_a} \tag{2}$$

Where $\sigma_1 - \sigma_3$ is the deviatoric stress and ε_a is the axial strain. The secant method formula was used to determine the Young Modulus, it started from the small-strain ranges less than 0.1% of axial strain, that subjected to the small-strain ranges mechanical behavior (Putera et al., 2021), as explained in **Fig. 4.2.** Based on that result, it can be connected with another point of interest to create the interpolation curves. Furthermore, the large strain ranges can be included to estimate by using a similar method, which can be covered the degradation stiffness modulus from small strain range to the large strain ranges.

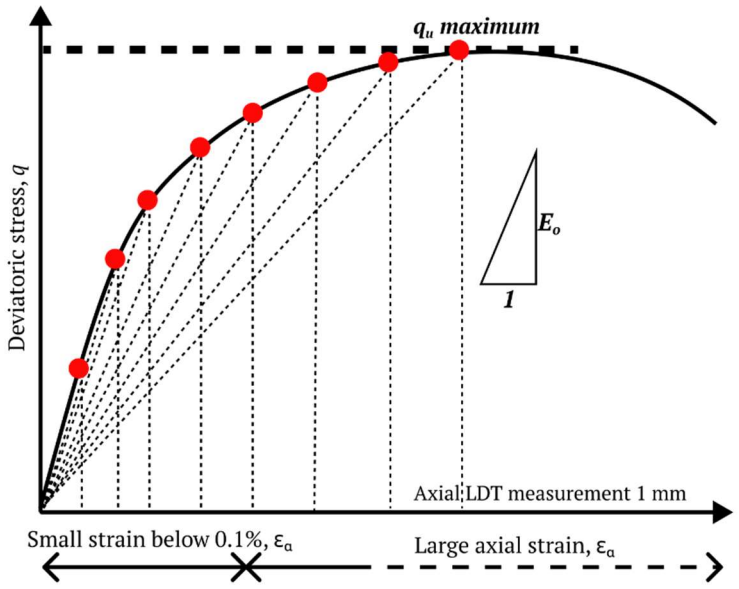

Fig. 4.2 Young Modulus from initial condition and 50 percent of maximum deviatoric stress

4.3.2.2 Initial Poisson's ratio

The initial Poisson's ratio in small-strain ranges was determined using the radial and axial strain increments. The equation is delineated as follows:

$$\nu_{sec}, \nu_o = \left[\frac{\Delta\varepsilon_r}{\Delta\varepsilon_a}\right]_{(\sigma_3=constant)} \quad (3)$$

Where $\Delta\varepsilon_r$ and $\Delta\varepsilon_a$ are the radial and axial strain increment when the deviatoric stress changes by a constant confining pressure. The Poisson's ratio can be observed by using the secant method ν_{sec} and initial strain ν_0 method. Those methods are illustrated in **Fig. 4.3**. The similar method was used to describing the behavior of Poisson's ratio in increment of axial strain ranges, which was subjected to estimate the degradation of Poisson's ratios.

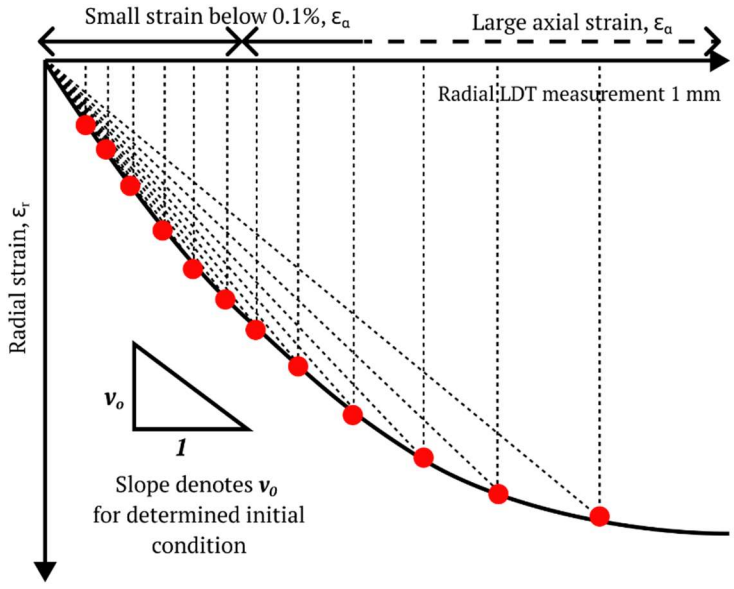

Fig. 4.3 Poisson's ratio from initial condition and 50 percent of maximum deviatoric stress

4.3.2.3 Initial shear modulus

The shear modulus degradation curve is often evaluated using the Young Modulus and Poisson's ratio. It can also be measured using the initial shear modulus (G_o) as Furthermore, it can be applied by using the equation below:

$$G = \frac{E}{2(1+\nu)} \tag{4}$$

4.4 Cement-treated soil behavior in small-large strain ranges

4.4.1 Large-strain ranges

4.4.1.1 Influence of cement content with shear strength parameter

In order to evaluate the shear strength parameter in large-strain ranges, it can be categorized as cohesion and friction angle of the cement-treated soils. Firstly, it requires drawing the failure envelope based on Mohr Coulomb, that delineated in **Fig. 4.4**. That comprise with differences of confining pressures and curing period. In **Fig 4.4 (a)**, it can be explained the low cement content (55 kg/m^3) at 7 day curing period was obtained the high influenced of confining pressure starting from 50 to 100 kPa. The maximum shear stress had high discrepancies, it can be affected the failure envelope. The discrepancies was appeared to introduce the reliable measurement in small-large strain ranges; it was explained the LDT more reliable to measure the shear strength parameter to estimate cohesion and friction angle. Small discrepancies had occurred in 28 days of curing period, as can be seen in **Fig 4.4 (b)**. That curing period was increased the shear stress of low confining pressures (25 – 50 kPa), it might be strengthening affect based on pozzolanic reaction within curing period.

To evaluate the behavior of shear strength parameter based on the result of low cement content, in this research were conducted the other variances such as 92 and 128 kg/m^3 of cement content. In **Fig. 4.5 (a)** was illustrated the influenced of

confining pressures in high cement content (128 kg/m^3), which was indicated the high cement content at 7 days of curing period can increase the shear stress rapidly

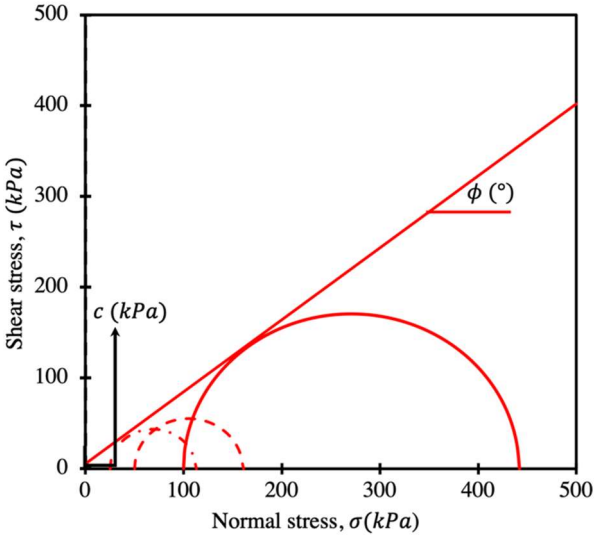

(a)

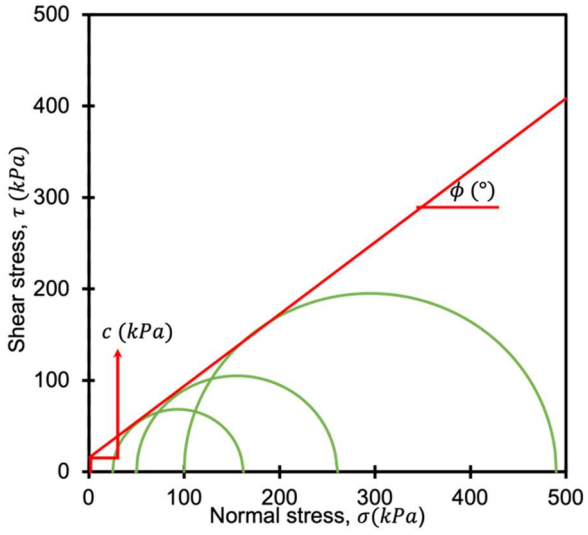

(b)

Fig. 4.4 (a) Estimating the Mohr Coulomb for 55 kg/m^3 of cement content at 7 day of curing period and (b) 28 day of curing period.

rather than the low cement content at similar curing period. The stress-strain was showed the small discrepancies between the LDT and LVDT measurement devices, it had similarity result in peak deviatoric stress distribution in previous chapters. In

Fig 4.5 (b) can be indicated the high influenced of 28 day curing periods to estimate the peak of shear stress in low confining pressure – high confining pressures. Based on the failure envelope using the LDT measurement, it was explained the LDT has obtain higher result of cohesion and friction angle. Increment of shear strength were occurred in 28 days of curing period. it might be strengthening affect based on pozzolanic reaction within the curing period. Furthermore, the influence of increment of cohesion and friction angle with cement content can be discussed more detailed in the next sub-section.

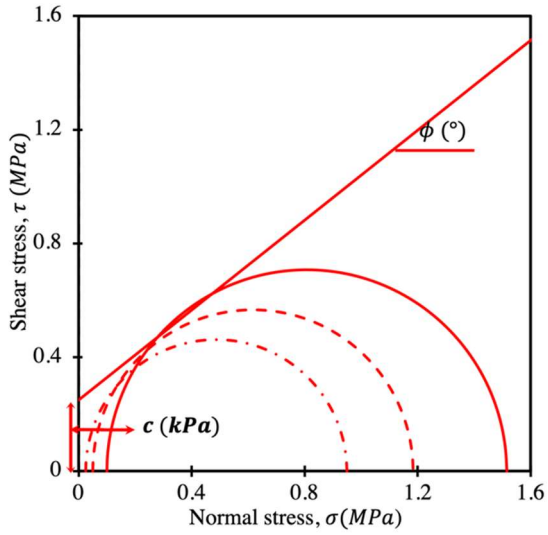

(a)

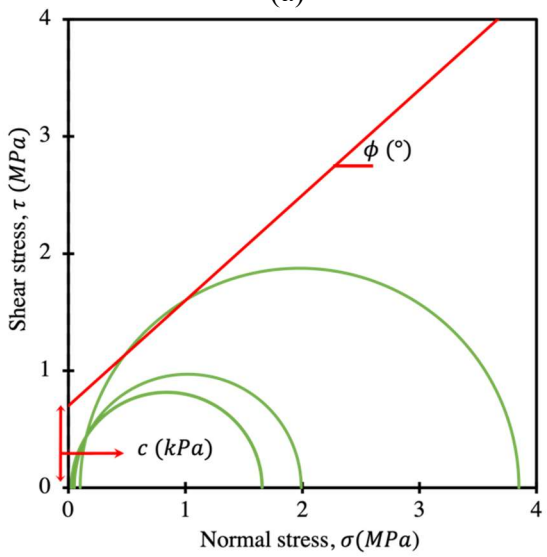

(b)

Fig. 4.5 (a) Estimating the Mohr Coulomb for 128 kg/m^3 of cement content at 7 day of curing period and (b) 28 day of curing period.

4.4.1.2 Influence of cement content with cohesion and friction angle

The basic parameter from Mohr Coulomb criterion can be evaluated using the LDT measurement devices. It has an advantage in enhancing the accuracy that mainly focuses on the failure envelope for determining the large-strain parameter such as

cohesion and friction angle parameters. In order to compare the increment of cohesion parameters with cement content, it can be seen in **Fig. 4.6**. the result was categorized by two curing periods, such as 7 and 28 days. In 7 days of curing period, the significant increment of cohesion has been occurred in 55 to 92 kg/m^3 of cement content, to describe the interpolation of the increment it was used the power function formula. That formula also fitted in 28 days of curing periods.

Friction angle can be seen in **Fig. 4.7,** there are small discrepancies related to the increment cement content and curing period with friction angle. Similar mathematical approaches have been used to define the interpolation between point such as the power function formula. Thus, the highly influences of cement-treated clayey soil mechanical behavior in large strain ranges has been significantly indicated by the increment of cohesion parameters and increment of cement contents.

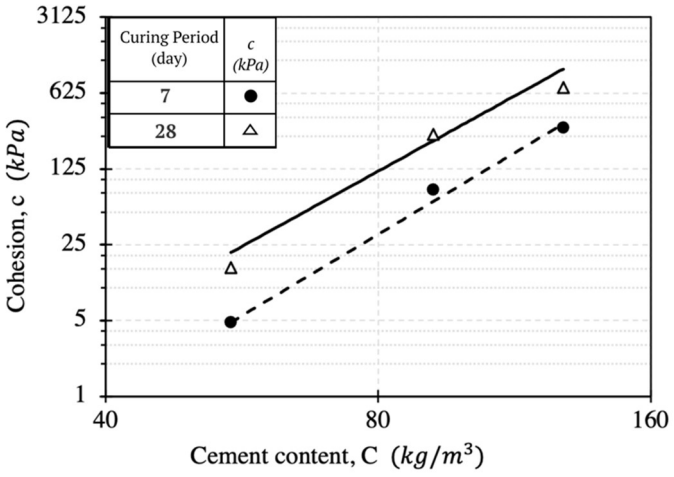

Fig. 4.6 Cohesion parameters of cement-treated soils with various cement content and curing period.

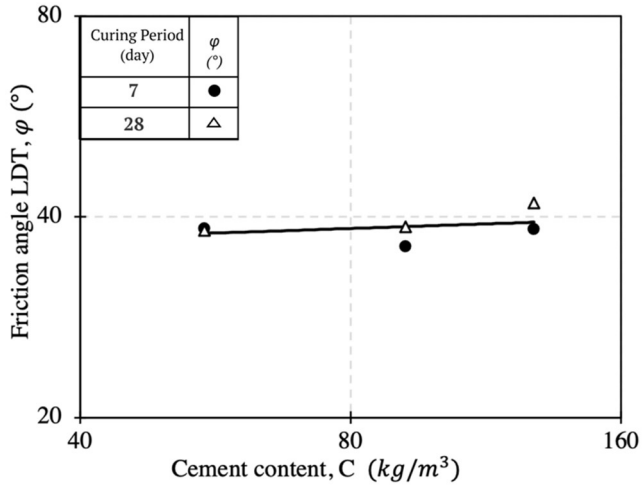

Fig. 4.7 friction angle parameters of cement-treated soils with various cement content and curing period.

4.4.2 Small-strain ranges

4.4.2.1 Influence of curing periods and mechanical behavior in small-strain ranges

The relation between the deviatoric stress and axial strain for the 55 and 128 kg/m3 cement-treated samples cured at 7 and 28 days is shown in Fig. 6. All the samples were tested at a constant confining pressure of 100 kPa under a low shearing rate.

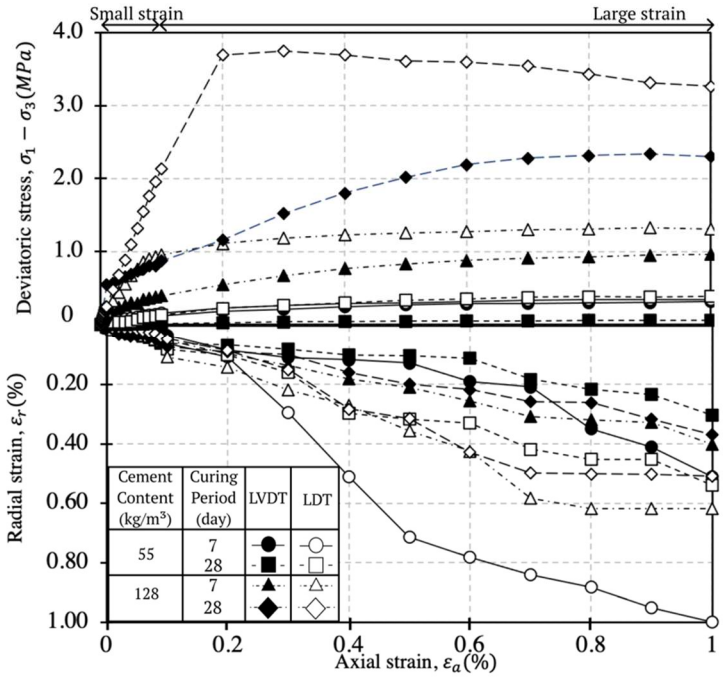

Fig. 4.8 Stress-strain relationship of low and high cement content in 7 and 28 day of curing periods.

Generally, higher cement content samples treated at 28 days showed higher maximum deviatoric stress, where the slope tends to be steeper than the other cement-treated samples. At 7 days of curing, the readings of the LVDT and axial LDT were close for the 55 kg/m3 cement content samples. However, the LVDT and radial LDT had a higher discrepancy associated with a large-strain range, which might be associated with the bedding error measurement and the accuracy difference between the inside and outside the triaxial chamber. In contrast, the higher cement content with 28 days of curing showed high discrepancies between the deviatoric stress measurement of the axial LDT and LVDT. However, the radial strain with 28 days of curing showed a similar declining curve between 128 and 55 kg/m3.

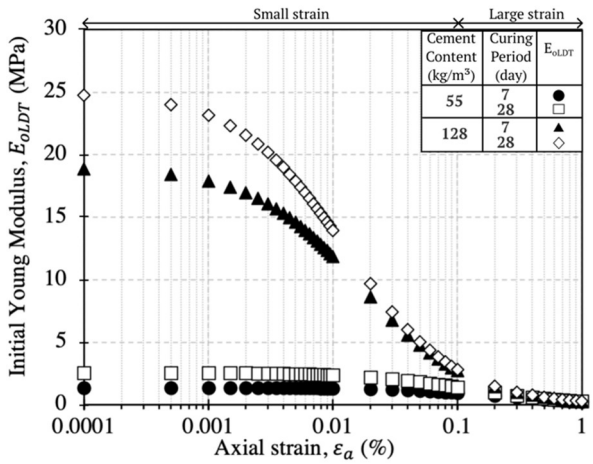

Fig. 4.9 Influenced of curing period related to the degradation of initial Young Modulus based on LDT measurement.

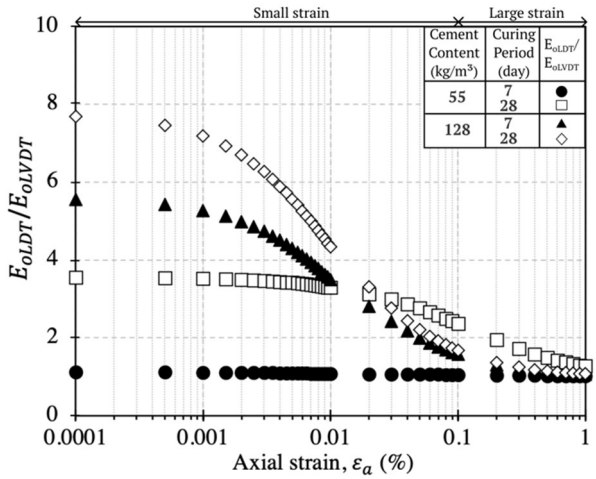

Fig. 4.10 Influenced of curing period related to the discrepancy's measurement between LDT and LVDT of initial Young Modulus.

The influence of curing period and cement content can be determined by studying the mechanical properties of the samples. As explained previously, the mechanical properties were obtained using the secant method for small-strain ranges. Based on that, it can be interpolated within small to large strain ranges. Degradation of Initial Young Modulus is represented in **Fig. 4.9** which explains that the higher Initial Young Modulus was captured at high cement content compared to low cement content and become non-linear within small strain ranges. Also, the Initial Young Modulus has been determined using the LDT and LVDT (E_{oLDT}/E_{oLVDT}), where the ratio in small-strain ranges becomes larger in LVDT measurement.

To confirm the reliability of the LDTs in measuring the initial Young Modulus, the relationship between the axial strain and E_{oLDT}/E_{oLVDT} was plotted for low and high cement content cured at 7 and 28 days, as shown in **Fig. 4.10.** For low cement content samples cured at 7 days, the LDT and LVDT shows almost similar results within the increment of axial strain ranges. That can be explained with the degradation curve of the ratios in small number (almost equal to 1). On the other hand, for high cement content cured at 28 days, higher discrepancies between the axial LDT and LVDT were shown. Similarly, the initial Poisson's ratio determined

using the LDTs were plotted for low and high cement content cured at 7 and 28 days, as illustrated in **Fig. 4.11.**

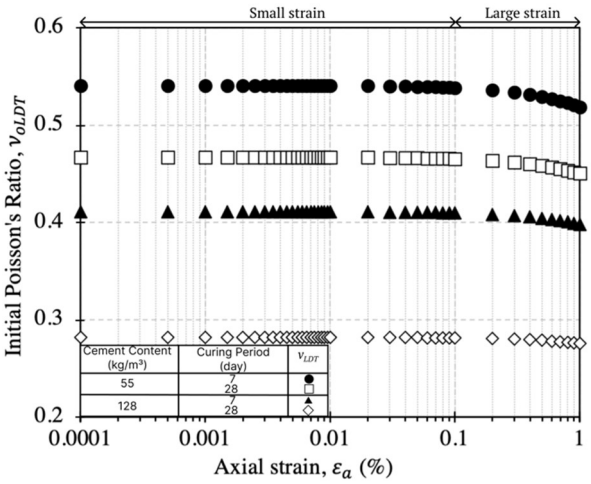

Fig. 4.11 Influenced of curing period related to the degradation of initial Poisson's ratio based on LDT measurement.

Poisson's ratio result was obtained in higher discrepancies between Axial LDT and LVDT. The reliable result was occurred by using the LDT measurement, that might be the influenced between the measurement of inside and outside of triaxial chamber. On the other hand, low cement content was obtained the lowest Poisson's ratios between Axial LDT and LVDT. The result was generated from the secant method in small strain ranges, which is the measurement of axial LDT more reliable rather than LVDT. The shear modulus calculated by empirical method shows a similar result to the initial Young Modulus ratios. Fig 4.12 evaluates the degradation of initial shear modulus. It has been shown in Fig. 4.13, wherein low cement content with 7 and 28 days of curing was obtained similar ratios between LDTs and LVDT result. That condition was influenced by initial Poisson's ratio and initial Young Modulus result.

4.4.2.2 Influence of confining pressure and mechanical behavior in small-strain ranges

In advanced the influence of confining pressure in small strain ranges during the shearing process, it can be determined using LDT and LVDT measurement devices.

The increment in stress-strain relationship must be evaluated. The measurements were conducted that used 55 and 128 kg/m3 of cement content, which can be seen in **Fig. 4.14** Based on stress-strain relations from LDT and LVDT, it has been occurred discrepancies on small strain ranges conditions, especially in high cement content. Although, low cement content with 25 kPa of confining pressure showed a small difference, which was associated with the low effect of bedding error.

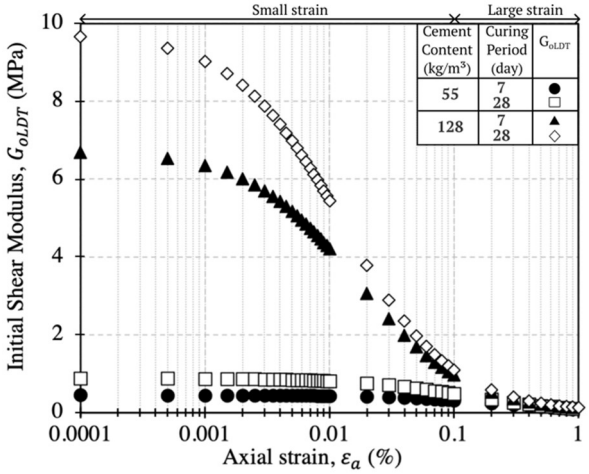

Fig. 4.12 Influenced of curing period related to the degradation of initial Shear modulus based on LDT measurement.

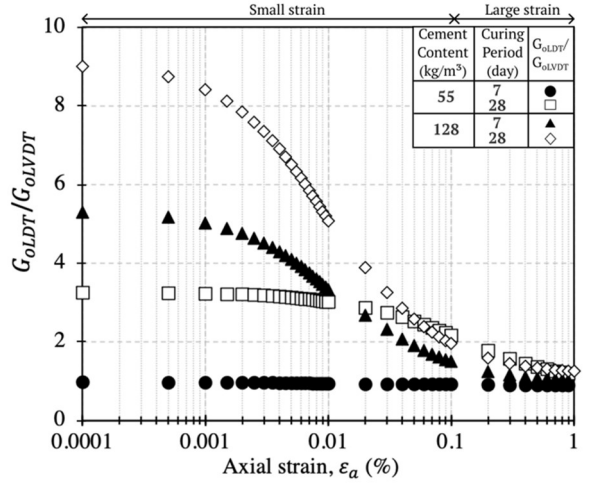

Fig. 4.13 Influenced of curing period related to the discrepancy's measurement between LDT and LVDT of initial Shear modulus.

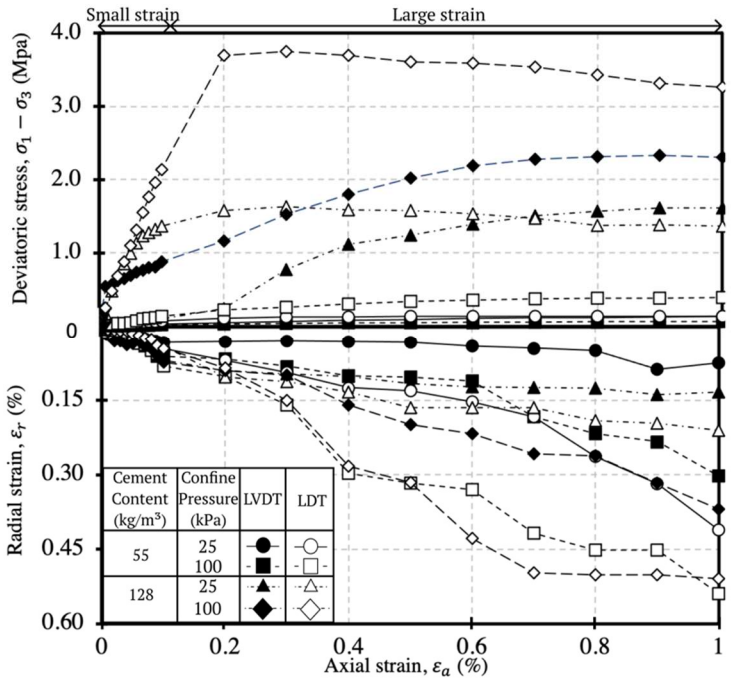

Fig. 4.14 Stress-strain relationship of low and high cement content with 25 and 100 kPa of confining pressure.

In the meantime, the increment of axial-radial strain showed a similar increment from variances of cement content and confining pressure, which can be determined by LDTs. The use of LVDT to measure the radial strain has discrepancies regarding the low increment of radial strain induced during the shearing process. That condition was manipulated by the effect of confining pressure due to strain-softening effect.

A similar method was applied to determine the influence of confining pressure and cement content within the mechanical properties of cement-treated clayey soils. It was described as a close range's ratio between Axial LDT and LVDT. Degradation of the Initial Young Modulus (E_o) as delineated in **Fig. 4.15.** It shows the influence of confining pressure were affected dominantly in high cement contents which was occurred with a non-linearity declined curve in small strain ranges. A comparison ratio measurement of LDT and LVDT was explained by significant distinctions in measurement due to increasing cement content, as shown in **Fig. 4.16.**

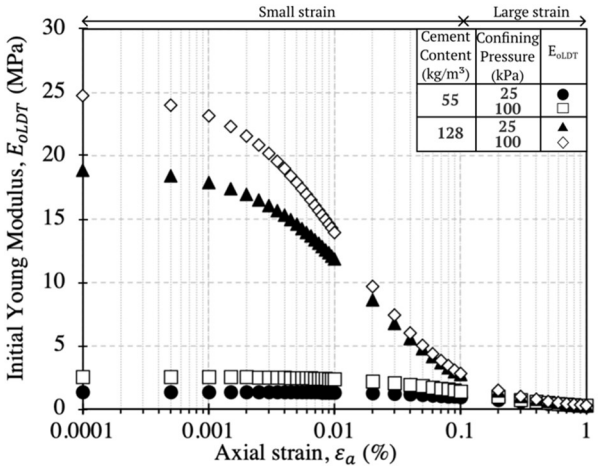

Fig. 4.15 Influenced of confining pressure related to the degradation of initial Young Modulus based on LDT measurement.

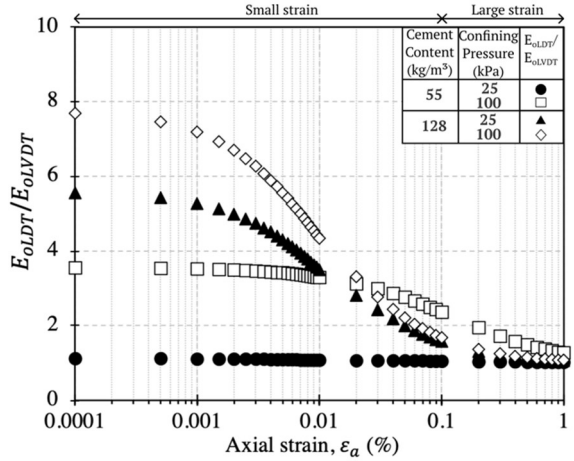

Fig. 4.16 Influenced of confining pressure related to the discrepancy's measurement between LDT and LVDT of initial Young Modulus.

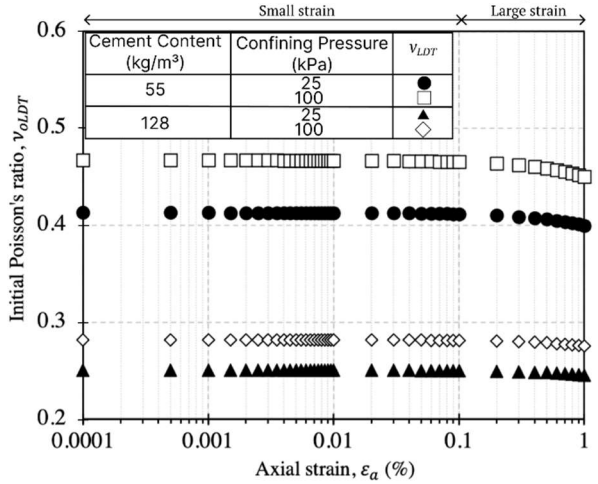

Fig. 4.17 Influenced of confining pressure related to the degradation of initial Poisson's ratio based on LDT measurement.

Moreover, the Poisson's ratio measurement had a similar trend compared to the influence of cement content as shown in **Fig. 4.17**. In small strain ranges the Poisson's ratios with differences of confining pressure, it was described the small discrepancies within 25 and 100 kPa of confining pressure. Also, a declined curve has been observed in the degradation of initial Shear modulus at 25 kPa confining pressure, as can be seen in **Fig. 4.18,** which was related to the degradation of initial Young Modulus. The degradation modulus has a similar trend between low cement content and confining pressure. It was compared with 7 and 28 days of the curing period, based on **Fig. 4.13** and **Fig. 4.19**, respectively. However, compared to the higher cement content subjected to the differences between increment of confining pressure, we can see discrepancies between low confining pressures (25 kPa) and

high confining pressure (100 kPa). That condition was derived to the measurement of increment of axial strain ranges and influence from 100 kPa of confining pressure. Furthermore, these results can discuss the gradient of coefficient parameter and increment slope of mechanical properties with different curing periods and confining pressure. In addition, through the next sub-section, evaluating the coefficient parameter of mechanical behavior in small strain ranges, it might be another process to estimate the mechanical properties using the estimation formula.

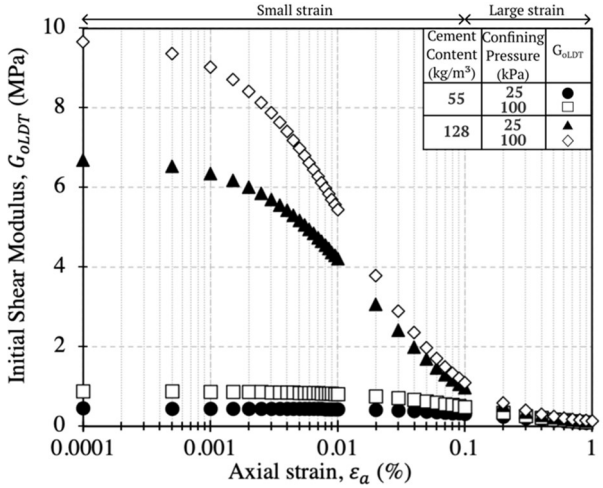

Fig. 4.18 Influenced of confining pressure related to the degradation of initial Shear modulus based on LDT measurement.

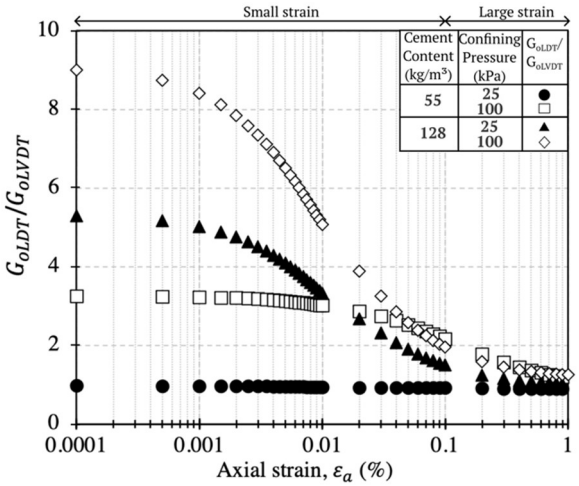

Fig. 4.19 Influenced of confining pressure related to the discrepancy's measurement between LDT and LVDT of initial Shear modulus.

4.5 Influenced of confining pressure in small-strain ranges subjected to the various of mechanical behavior

4.5.1 Relationship between confining pressure and mechanical behavior

The evaluation of the relationship between confining pressure and cement content can be characterized by the gradient slope of initial mechanical properties and the normalized confining pressure with atmospheric pressures (σ_3/P_a). The variation of logarithmic scale curvature of initial Young Modulus (E_o/P_a) was plotted in **Fig. 4.20**. that demonstrates the increment of initial Young Modulus related to the (σ_3/P_a). For low cement content (55 kg/m^3) the high discrepancies between various cement content subjected to the 7 and 28 days of curing period was experienced. In medium to the high cement content (92 – 128 kg/m^3) was occurred the small discrepancies subjected to the curing periods. To make a relationship between the measurement of initial Young Modulus and increment of confining pressure, it can be used the power function formula in logarithm scale curvature. The result was showed a good relation, and it can be applied as interpolation method to create relationship between various cement content and curing period.

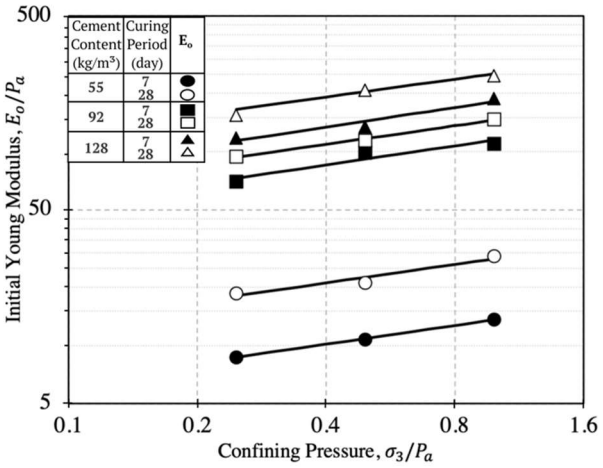

Fig. 4.20 Relationship of initial Young Modulus and confining pressure in small strain ranges.

The variation of logarithm scale curvature of Initial Poisson ratios (ν_o/P_a) was plotted in **Fig. 4.21**. It was shown the increment of initial Poisson's ratio related to the (σ_3/P_a). For low cement content (55 kg/m^3) was determined the high discrepancies between various cement content subjected to the 7 and 28 days of curing period. In medium to the high cement content (92 – 128 kg/m^3) was occurred the small discrepancies subjected to the 7 day of curing periods. For 28 day of curing period in high cement content was described the high discrepancies with various cement content. To make a relationship between the measurement of initial Poisson's ratio and increment of confining pressure, it can be used the power function formula in logarithm scale curvature. The result was showed a good relation, and it can be applied as interpolation method to create relationship between various cement content and curing period.

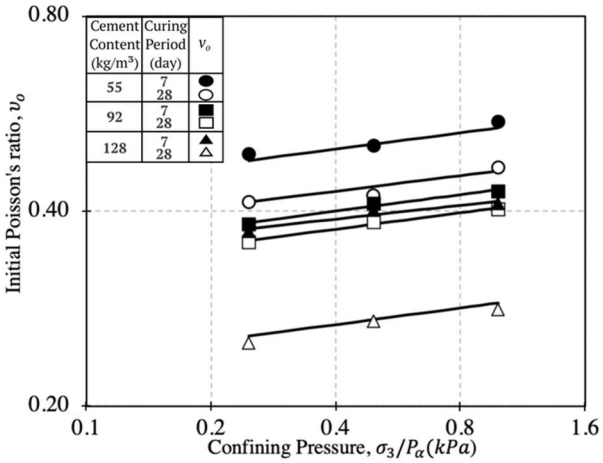

Fig. 4.21 Relationship of initial Poisson's ratio and confining pressure in small strain ranges..

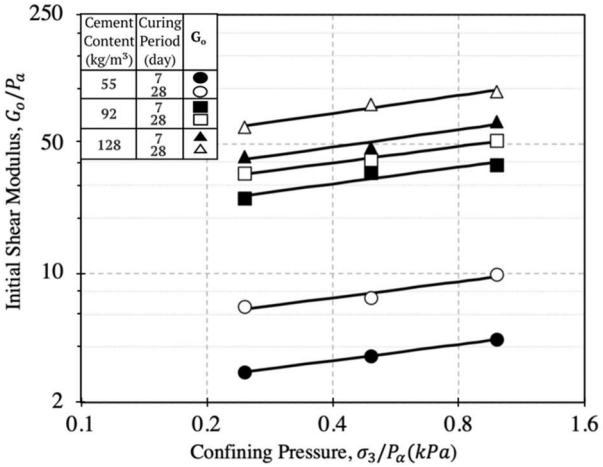

Fig. 4.22 Relationship of initial Shear modulus and confining pressure in small strain ranges..

The variation of logarithmic scale curvature of Initial Poisson ratios (ν_o/P_a) was plotted in **Fig. 4.21**. It was shown the increment of initial Poisson's ratio related to the (σ_3/P_a). For low cement content (55 kg/m^3) was determined the high discrepancies between various cement content subjected to the 7 and 28 days of curing period. In medium to the high cement content (92 – 128 kg/m^3) was occurred the small discrepancies subjected to the 7 day of curing periods. For 28 day of curing period in high cement content was described the high discrepancies with various cement content. To make a relationship between the measurement of initial

Poisson's ratio and increment of confining pressure, it can be used the power function formula in logarithm scale curvature. The result was showed a good relation, and it can be applied as interpolation method to create relationship between various cement content and curing period.

The variation of logarithmic scale curvature of Initial Shear modulus (G_o/P_a) was plotted in **Fig. 4.22**. It was shown the increment of initial Shear modulus related to the (σ_3/P_a). For low cement content (55 kg/m^3) was determined the high discrepancies between various cement content subjected to the 7 and 28 days of curing period. In medium to the high cement content (92 – 128 kg/m^3) was occurred the small discrepancies subjected to the 7 day of curing periods. To make a relationship between the measurement of initial Shear modulus and increment of confining pressure, it can be used the power function formula in logarithm scale curvature. The result was showed a good relation, and it can be applied as interpolation method to create relationship between various cement content and curing period.

Intercorrelated power function of confining pressure has been observed in this section, it subjected to the initial mechanical properties coefficient and cement content. The assumptions of constant value are based on the previous research conducted to predict the increment strength with the curing period (Kang et al., 2017). The relationship between confining pressure and mechanical properties can be suggested below:

$$\ln|E_o, \nu_o, G_o| = \ln \alpha + \beta \ \ln(\sigma_3/P_a) \tag{5}$$

$$|E_o, \nu_o, G_o| = \alpha(\sigma_3/P_a)^{\beta} \tag{6}$$

Where σ_3/P_a is confining pressure has normalized with atmospheric pressure in the same units, α is coefficient parameter of mechanical behavior subjected to the curing period and cement content. For β is gradient of slope to determine the curvature line, it subjected to curing period and cement content. The gradient was

showed a similarity slope in each relationship of mechanical behavior in small strain ranges. In this study, to estimate the relationship between parameter α and β with increment of cement content.

Furthermore, cement-treated clayey soil's determination effect at a small strain range was recommended using the axial LDT and radial LDT at a slow shearing rate. In addition, the effect of confining pressure in small-strain ranges meant the significant relationship between an increment of coefficient parameter (α) and (β) with increased mechanical properties.

4.5.2 Coefficient parameters to estimate mechanical behavior in small-strain ranges

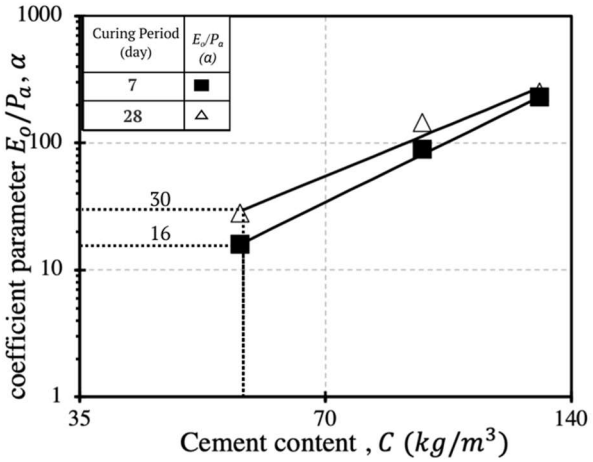

Fig. 4.23 Relationship of coefficient parameter α for estimate initial Young Modulus with increment of cement content in small strain ranges.

The applicability of power function relationship in previous section was considered to estimating the mechanical behavior of cement-treated clayey soil subjected to the shallow ground improvement in small strain ranges. When evaluated the relations between confining pressure and mechanical behavior, it has been realized to connecting the various relations with increment of cement content. For instance, the coefficient parameter can be obtained by using similar method, which was

subjected to the interpolation method that has been applied to the previous sub section.

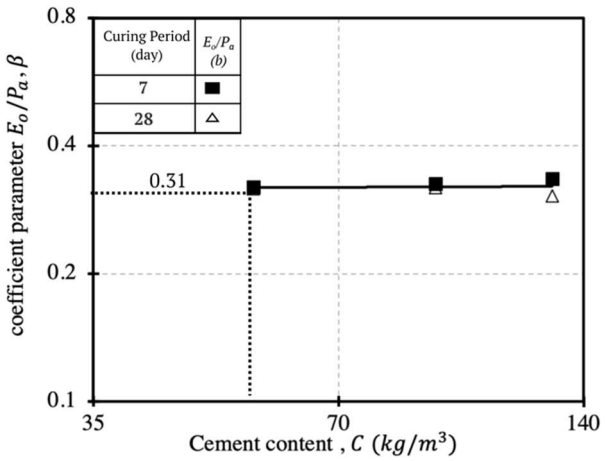

Fig. 4.24 Relationship of coefficient parameter β for estimate initial Young Modulus with increment of cement content in small strain ranges.

In **Fig. 4.23**, it represents the relationship between initial Young Modulus coefficients α and increment of cement content in logarithm scale of curvature. There are variances of curing period, it consisted of 7 and 28 days of curing period. The low cement content (55 kg/m^3) and 7 day of curing period was defined the increment of curvature has showed a good relations subjected with cement content. Its similar relations with the low cement content and 28 days of curing period. Increasing the cement content, the small discrepancies of the gradient have occurred, which was subjected to the explanation of influenced by confining pressure in the previous section. Accordingly, initial Young Modulus coefficients α can be determined as incremental of power function. For the coefficients parameters β is illustrated in **Fig. 4.24.** It can be seen as a horizontal linear curve subjected to increment cement content. In this case, has been explained in previous section related to the small discrepancies behavior for initial Young Modulus. Furthermore, the coefficients parameters β could be used the similar number for estimating the mechanical behavior in small-strain ranges. Hence, the relationship of coefficients α and β of initial Young Modulus can be suggested below.

$$E_o(\alpha) = 16\ (7\ day) \text{ and } 30\ (28\ day) \quad (7)$$

$$E_o(\beta) = 0.31 \quad (8)$$

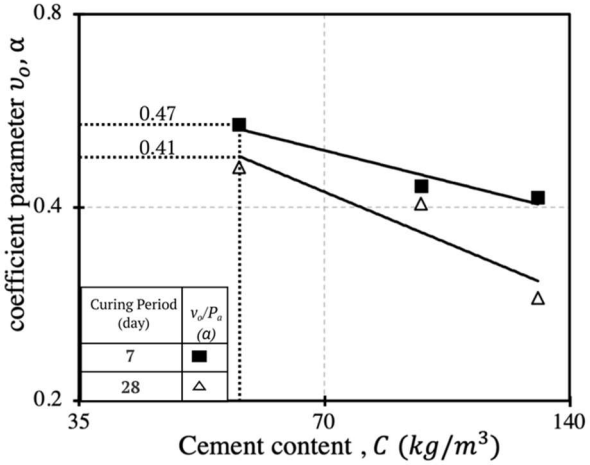

Fig. 4.25 Relationship of coefficient parameter α for estimate Poisson's ratio with increment of cement content in small strain ranges.

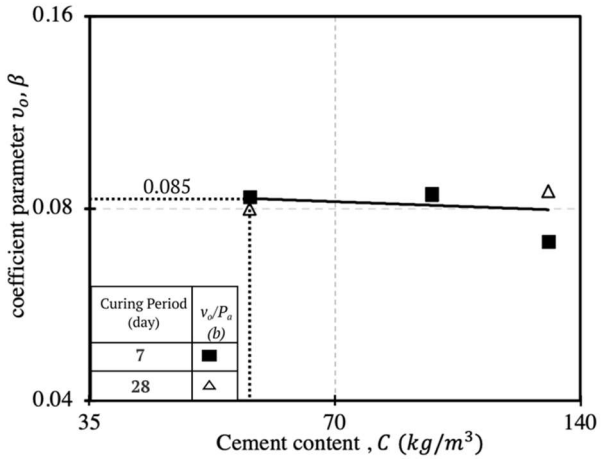

Fig. 4.26 Relationship of coefficient parameter β for estimate Poisson's ratio with increment of cement content in small strain ranges.

The relationship between initial Poisson's ratios coefficients α and increment of cement content in the logarithm scale of curvature can be seen in **Fig. 4.25**. There are variances of curing period, it consisted of 7 and 28 day of curing period. The low cement content (55 kg/m^3) and 7 day of curing period was defined the

decreasing curvature, it has been showed a good relation subjected to cement content. Its similar relations with the low cement content and 28 days of curing period. Increasing the cement content, it has to describe the discrepancies of gradient has been occurred, which was subjected to the explanation of influenced by confining pressure in the previous section. For instance, the initial Poisson's ratio coefficients α can be determined as power function, it was categorized by 7 and 28 days of the curing period. For the coefficients parameters β is illustrated in **Fig. 4.26.** It can be seen as a horizontal linear curve subjected to increment cement content. In this case, has been explained in previous section related to the small strain ranges influenced for initial Poisson's ratio, that condition could be dealt with a similar power function formula. Furthermore, the coefficients parameters β could be used the similar number for estimating the mechanical behavior in small-strain ranges. Hence, the relationship of coefficients α and β of the initial Poisson's ratio can be expressed as below:

$$\nu_o(\alpha) = 0.47\ (7\ day) \text{ and } 0.41\ (28\ day) \tag{9}$$

$$\nu_o(\beta) = 0.085 \tag{10}$$

In order to determine the initial Shear modulus coefficients α and increment of cement content in the logarithm scale of curvature, can be seen in **Fig. 4.27**. There are variances of curing period, it consisted of 7 and 28 days of curing period. The low cement content (55 kg/m^3) and 7 days of curing period was defined the increment of curvature, it has been showed a good relations subjected to cement content. Its similar trends for a good relations curve, that can be categorized by low cement content and 28 days of curing period. Increasing the cement content, it has to describe the discrepancies of gradient has been occurred, which was subjected to the explanation of influenced by confining pressure in the previous section. For instance, the initial Shear modulus coefficients α can be determined as power function, it was categorized by 7 and 28 days of the curing period. For the coefficients parameters β is illustrated in **Fig. 4.28.** It can be seen as a horizontal

linear curve subjected to increment cement content. In this case, has been explained in previous section related to the small strain ranges influenced for initial Shear modulus, that condition could be dealt with using a similar power function formula.

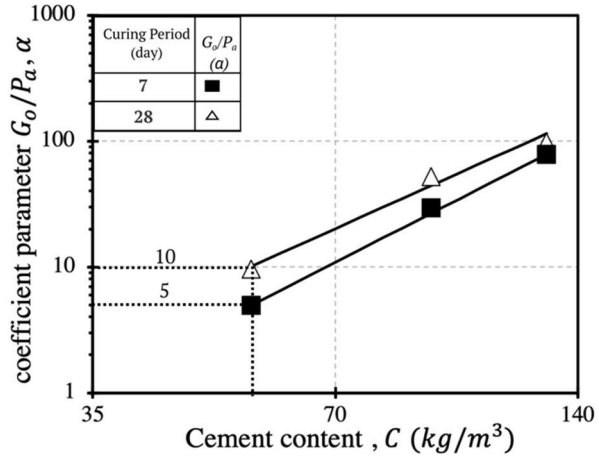

Fig. 4.27 Relationship of coefficient parameter α for estimate initial Shear modulus with increment of cement content in small strain ranges.

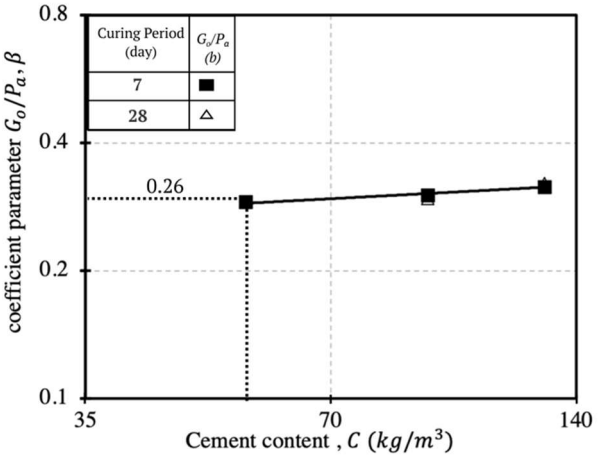

Fig. 4.28 Relationship of coefficient parameter β for estimate initial Shear modulus with increment of cement content in small strain ranges.

Furthermore, the coefficients parameters β could use the similar number for estimating the mechanical behavior in small-strain ranges. Hence, the relationship of coefficients α and β of initial Shear modulus can be outlined as follows:

$$G_o(\alpha) = 5\ (7\ day) \text{ and } 10\ (28\ day) \quad (9)$$

$$G_o(\beta) = 0.26 \quad (10)$$

In addition, the coefficient parameter can be used for evaluating the mechanical behavior subjected to the cement content and confining pressure behavior. To conduct this estimation curved, it requires at least two variances of testing sample, which were categorized by differences of cement content and confining pressure.

4.6 Summary

In this chapter, the mechanical behavior within small-large strain has been discussed. For large-strain ranges has been described using the Mohr Coulomb failure criterion and explained detailed the cohesion (c) and friction angle (φ) of cement-treated clayey soils. For small-strain ranges has been described including the initial young's modulus (E_0), shear modulus (G_0), and the Poisson's ratio for cement-treated clayey soils. Those parameters were investigated using triaxial consolidated undrained ($\overline{CU}$) equipped with small strain measurement devices (LDTs). Samples were sheared after 7 and 28 curing days. The shearing rate was set at 0.05 mm/min. A confining pressure of 25, 50 and 100 kPa was adopted for testing.

Cohesion and cement content was compared within the LDT and LVDT. It showed significant discrepancies based on increasing cement content by using the LDT measurement. This result has been proofing a similar response tend curve; it can be seen by the previous relations of the peak deviatoric stress with axial strain. To estimate the cohesion and friction angle that was analyzed using the power function formula and a good relation between the positive slope of increment of cement content was observed. However, the friction angle depicted a similar gradient slope along the increment of cement content.

A power function model was proposed to estimate the mechanical properties of the initial young's modulus (E_o), Poisson's ratio (ν_o) and shear modulus (G_o)

development with the applied confining pressure for cement treated soils under various curing periods.

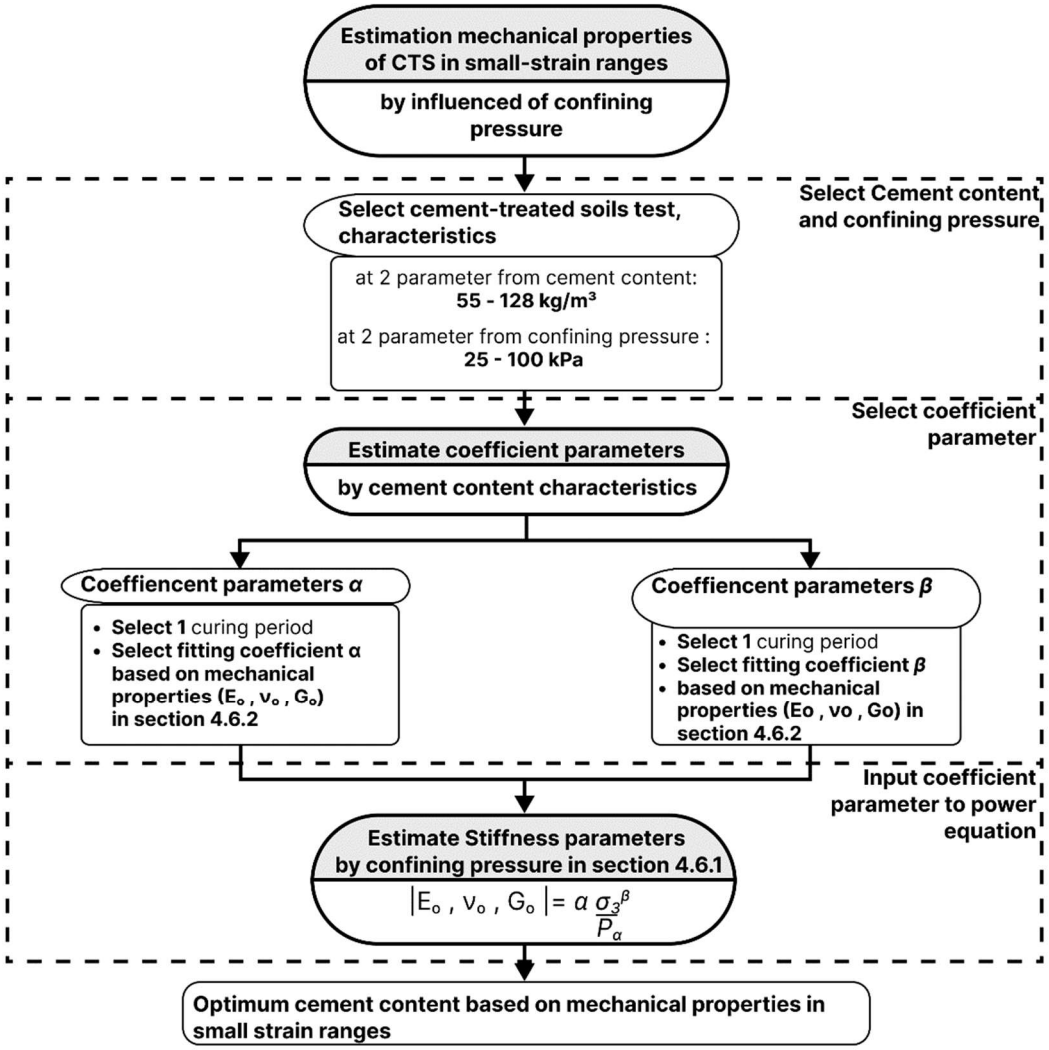

Fig. 4.29 Estimating the Mechanical properties in small strain ranges reflecting to the cement content and confining pressure

The procedure of mechanical properties estimation of cement-treated clayey soils can be seen in **Fig 4.29**. Initially, it requires selecting the variances of two cement content and confining pressures. Based on those parameters, the coefficient parameter α related to the increment of cement content behavior and β related to the gradient of curvature can be determined. For selecting the coefficient parameter, it is required to put the cement content into the curvature in Section 4.6.2, for parameter α is determine the increment of curvature and for β is relatively constant.

Finally, the requirements of coefficient parameter can be obtained, then the coefficient parameter can be used into the estimation using the power function formula.

For low cement content mixtures (55 kg/m^3) under 7 and 28 curing days, the young's modulus (E_o) and the shear modulus (G_o) degraded following a linear pattern within the small strain range before converging to a constant value. In contrast, the high cement content samples showed minor degradation in the young's modulus (E_o) and the shear modulus (G_o).

Significant discrepancies in the measured strain using the LDTs compared to the values measured using the LVDTS, which was more paramount for high cement content (128 kg/m3). Therefore, it was found that using LDTs to determine the mechanical properties of cement treated soils is necessary to ensure accurate and reliable determination of the mechanical behavior properties of cement treated soils.

References

Atkinson, J., 2000. Non-linear soil stiffness in routine design. Geotechnique 50, 487–508. https://doi.org/10.1680/geot.2000.50.5.487

JETRO, 2012. Study on the high speed railway project (jakarta-bandung section), republic of indonesia (Final report (Summary)), Feasibility study for promotion of international infrastucture projects in fy2011. Yachiyo Engineering Co., Ltd. and Japan International Consultants for Transportation Co., Ltd.

Kang, G., 2016. Influence and Control Strategy for Local Settlement for High-Speed Railway Infrastructure. Engineering 2, 374–379. https://doi.org/10.1016/J.ENG.2016.03.014

Kang, G., Tsuchida, T., Kim, Y., 2017. Strength and stiffness of cement-treated marine dredged clay at various curing stages. Construction and

Building Materials 132, 71–84. https://doi.org/10.1016/j.conbuildmat.2016.11.124

Kasama, K., Zen, K., Iwataki, K., 2006. Undrained Shear Strength of Cement-Treated Soils. Soils and Foundations 46, 221–232. https://doi.org/10.3208/sandf.46.221

Kumar, P., Singh, V., 2017. Geotechnical Aspect for Design of Track Formation System for High Speed Rail Lines on Alluvial Soil Deposited-A Review.

Novico, F., Menier, D., Mathew, M., Ramkumar, M., Santosh, M., Endyana, C., Dewi, K.T., Kurniawan, I., Lambert, C., Goubert, E., Hendarmawan, 2022. Impact of Late Quaternary climatic fluctuations on coastal systems: Evidence from high-resolution geophysical, sedimentological and geochronological data from the Java Island. Marine and Petroleum Geology 136, 105399. https://doi.org/10.1016/j.marpetgeo.2021.105399

Onyelowe, K., Van, D.B., Igboayaka, C., Orji, F., Ugwuanyi, H., 2019. Rheology of mechanical properties of soft soil and stabilization protocols in the developing countries-Nigeria. Materials Science for Energy Technologies 2, 8–14. https://doi.org/10.1016/j.mset.2018.10.001

Putera, M.A., Yasufuku, N., Alowaisy, A., Rifai, A., 2021. Optimizing modified triaxial testing for small strain zone using local displacement transducers and bender element for cement-treated soft soil. E3S Web of Conferences 331. https://doi.org/10.1051/e3sconf/202133103003

Ranst, E.V., Utami, S.R., Vanderdeelen, J., Shamshuddin, J., 2004. Surface reactivity of Andisols on volcanic ash along the Sunda arc crossing Java Island, Indonesia. Geoderma 123, 193–203. https://doi.org/10.1016/j.geoderma.2004.02.005

Solihu, H., 2020. Cement Soil Stabilization as an Improvement Technique for Rail Track Subgrade, and Highway Subbase and Base Courses: A Review. Journal of Civil and Environmental Engineering 10:3. https://doi.org/10.37421/jcce.2020.10.344

Subramaniam, P., Banerjee, S., 2014. Factors affecting shear modulus degradation of cement treated clay. Soil Dynamics and Earthquake Engineering 65, 181–188. https://doi.org/10.1016/j.soildyn.2014.06.013

Vardanega, P.J., Bolton, M.D., 2014. Stiffness of Clays and Silts: Modeling Considerations. Journal of Geotechnical and Geoenvironmental Engineering 140. https://doi.org/10.1061/(ASCE)GT.1943-5606.0001104

Xiao, H., Yao, K., Liu, Y., Goh, S.-H., Lee, F.-H., 2018. Bender element measurement of small strain shear modulus of cement-treated marine clay – Effect of test setup and methodology. Construction and Building Materials 172, 433–447. https://doi.org/10.1016/j.conbuildmat.2018.03.258

Chapter 5
Elastic Settlement Prediction using Small-Strain Mechanical Properties of Cement-treated Clayey Soils

5.1 Introduction

Indonesia is developing its infrastructure, including a high-Speed Railway (HSR) project (maximum speed of 300 km/h) that is expected to connect the Jakarta and Surabaya cities, extending for 700 km (JETRO, 2012). Along the railway, the lowland area is mainly comprised of clayey soil characterized by a high compressibility index and high water content (Novico et al., 2022; Ranst et al., 2004). Such conditions impose significant geotechnical challenges, including lack of bearing capacity, stability loss, and significant volume changes causing differential settlement. Therefore, innovative and economic techniques are needed to ensure the safety of life and properties.

Generally, railway structures can be divided into ballasted and ballastless structures. The ballasted structures are heavyweight, costly to maintain, and characterized by high shear strength and low vertical settlement. On the other hand, the ballastless is lightweight, relatively cheaper to maintain, and efficient for sites experiencing differential settlement (Kumar and Singh, 2017). Therefore, ballastless structures are commonly utilized for HSR projects in lowlands (Kang, 2016; Kumar and Singh, 2017). Despite the track structure, the subsoil mechanical properties often require

improvement to limit the railways' settlement. Several techniques are commonly used, such as superstructures (bridges and embankments), pile foundation, drained consolidation methods, deep soil mixing, and shallow stabilization. Due to the low cost, shallow stabilization is commonly practiced to prevent static and dynamic loading-induced settlement, especially in developing countries.

The total soil settlement is comprised of elastic and consolidation settlements, while in practice, mainly the latter is considered. The maximum allowable settlement for HSR associated with the dynamic loading is ≤30 mm, while it is limited to 10 mm/year for the earthquake loading (Ando et al., 2021; Kanazawa and Tarumi, 2010). In the case of HSR, combining the ballastless structure with shallow cement stabilization might be inevitable, where especially during the construction and the early operational stages, the elastic settlement with time might be of significant importance. During the construction phase, the soil stiffness of the underlying soil increases gradually, causing a reduction in the elastic settlement. However, during the post-construction (operation phase), the dynamic loading associated with the train's passage induces mainly elastic settlement (Lazorenko et al., 2019; Pantelidis and Gravanis, 2020). Therefore, the initial stiffness and the determination of the small-strain mechanical parameters are vital for analyzing the behavior and predicting the elastic settlement in the long-term operation of the HSR (Atkinson, 2000; Fang and Daniels, 2006; Foye et al., 2008).

Numerous models were proposed to predict the elastic settlement of soil profiles. However, the models mainly consider the settlement of shallow soil layers subjected to static loading under a circular foundation (Skempton and Bjerrum, 1957). Das and Ramana (2010) asserted the importance of estimating the maximum dynamic loading behavior, which can be obtained considering the load transmission to the substructure. Poulos and Davis (1968) and Mayne and Poulos (1999) proposed the influence factor in correlation with the vertical displacement. It reflects the depth of interest in the substructure embedment or the substructure geometry below the ground. Horikoshi and Randolph, (1997) derived a substructure-soil stiffness ratio for a rectangular foundation equivalent to a circular

one for predicting the elastic settlement under rectangular geometry. Razouki and Al-Zubaidy, (2010) reported the efficiency of reinforcing a specific layer thickness to reduce the elastic settlement. However, a comprehensive elastic settlement evaluation model for cement-treated soils subjected to dynamic loading that considers the thickness of the cement-treated layer is lacking.

This chapter introduces a new elastic settlement prediction model for cement-treated clayey ground focusing on the small-strain range. The model considers low-stress dynamic loading associated with the train passage and correlates it to the soil layer thickness (confining pressure). A series of undrained triaxial tests equipped with proper small strain testing devices were conducted to investigate the small strain zone behavior.

5.2 Mechanical properties of cement-treated clayey soils to predict the elastic settlement

5.2.1 Summary of triaxial testing result in small-strain ranges

In order to use the mechanical properties of cement-treated clayey soils to predict the elastic settlement in dynamic condition, the measurement of mechanical properties within small-strain ranges is required. Based on the Archer and Heymann (2015); Atkinson (2000) from field investigation measuring the geotechnical properties within small-strain ranges can provide the good accuracy for determine the dynamic properties. In the meantime, for cement-treated soils development project, the laboratory testing should be evaluated before and during the construction period, which can be subjected to get the optimum mixing ratios. Using the small-strain devices in laboratory testing can enhance the accuracy of mechanical properties. In small strain ranges, the measurement was described relatively in slight discrepancies between the result of mechanical properties of static and dynamic testing condition with cement-treated soil samples (Goto et al., 1991; Yamashita et al., 2009). Furthermore, the static condition of triaxial testing was carried out to evaluate the mechanical properties of cement-treated clayey soils.

Since the previous chapter was discussed the mechanical properties behavior in small-strain ranges and discrepancies between strain measurement devices. In this section can be a summarized of mechanical properties in small-strain ranges, which can be used to enhance the quality of elastic settlement prediction, as can be seen in **Table 5.1.**

5.2.2 To estimate the mechanical properties in small-strain ranges

A simple power equation has been described for estimating the mechanical properties relationship with confining pressure and cement content. This kind of estimation formula must be useful for determining the mechanical properties in elastic settlement prediction, which was subjected to the confining pressure as the thickness layer of cement-treated soils and cement content to define the optimum mixing ratio to improve clayey soil ground. The estimation formula of mechanical behavior based on simple power equation, can be suggested on below:

$$\ln|E_o, \nu_o, G_o| = \ln \alpha + \beta \ \ln(\sigma_3/P_a) \quad (1)$$

$$|E_o, \nu_o, G_o| = \alpha(\sigma_3/P_a)^{\beta} \quad (2)$$

Where E_o is initial Young Modulus, ν_o is initial Poisson's ratio and G_o is initial Shear modulus, which can be subjected to the measurement in small strain ranges. For coefficient parameter α and β was defined the influenced of cement content, it can be seen in the previous chapter. Therefore, the increment mechanical properties were fitted with a power curve according to increasing confining pressure. In addition, the effect of confining pressure in small-strain ranges meant the significant relationship between an increment of coefficient parameter (α) and (β) with increased mechanical properties. Based on mechanical properties relations curve of initial condition on small strain range could be used for elastic settlement prediction parameter.

Table 5.1 Summarized of mechanical properties of cement-treated soils in small strain ranges

Curing Period	**day**	**0**	**7**	**7**	**7**	**28**	**28**	**28**	**7**	**7**	**7**	**28**	**28**	**28**	**7**	**7**	**7**	**28**	**28**	**28**
Binder content	**kg/m^3**	**0**	**55**	**92**	**128**	**55**	**92**	**128**	**55**	**92**	**128**	**55**	**92**	**128**	**55**	**92**	**128**	**55**	**92**	**128**
Confining Pressure, σ_3	**kPa**		25						50						100					
Initial strain measurement	**(%)**	1×10^{-4}	1×10^{-4}	1×10^{-4}	1×10^{-4}	1×10^{-4}	1×10^{-4}	1×10^{-4}	1×10^{-4}	1×10^{-4}	1×10^{-4}	1×10^{-4}	1×10^{-4}	1×10^{-4}	1×10^{-4}	1×10^{-4}	1×10^{-4}	1×10^{-4}	1×10^{-4}	1×10^{-4}
Elastic Modulus, E_o	**Mpa**	1.0	0.9	7.3	11.4	1.8	9.3	16.5	1.1	9.2	14.4	2.3	11.7	20.4	1.4	11.5	18.2	2.8	14.6	25.2
Shear Modulus, G_o	**Mpa**	0.3	0.3	2.6	4.1	0.6	3.4	6.3	0.4	3.3	5.2	0.8	4.2	7.9	0.4	4.0	6.4	1.0	5.2	9.8
Poisson ratio, υ_o		0.5	0.5	0.4	0.4	0.4	0.4	0.3	0.5	0.4	0.4	0.4	0.4	0.3	0.5	0.4	0.4	0.5	0.4	0.3
Cohesion, c	**kPa**	10.0	5	160	250	15	260	700	5	160	250	15	260	700	5	160	250	15	260	700
Friction angle, φ	**(°)**	0.0	38.4	36.1	38.3	38.2	38.7	42.0	38.4	36.1	38.3	38.2	38.7	42.0	38.4	36.1	38.3	38.2	38.7	42.0

5.3 Elastic settlement prediction of cement-treated soils in small-strain ranges

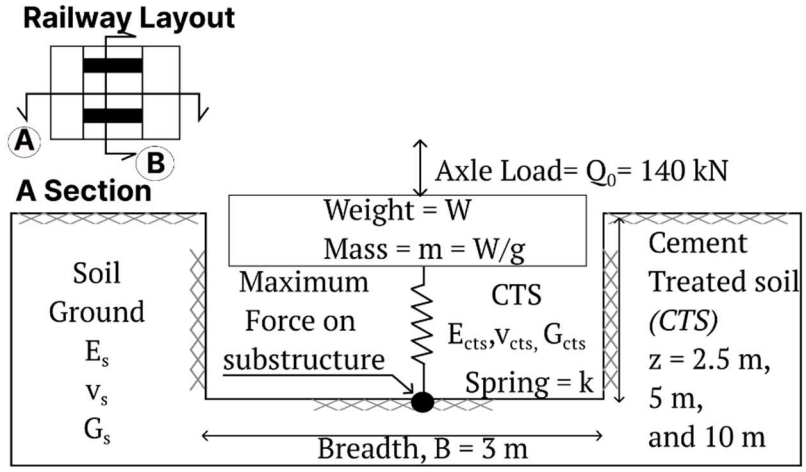

Fig. 5.1 Illustration of cement-treated soils boundaries condition for dynamic load behaviors from wheelbase in cross section.

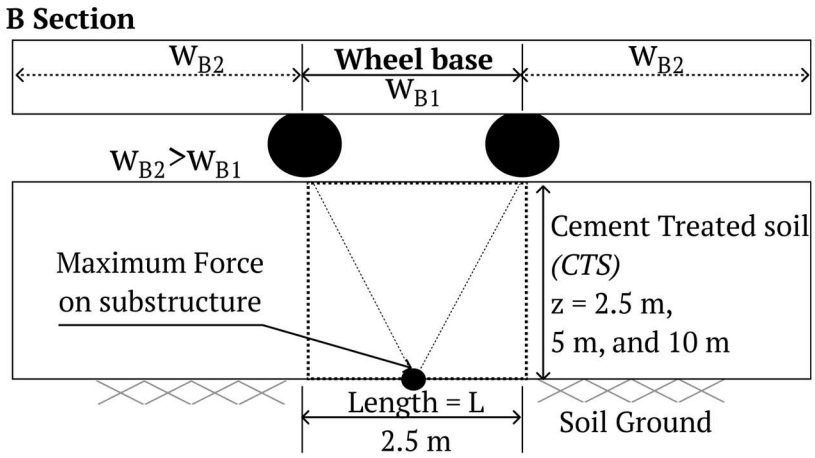

Fig. 5.2 Illustration of cement-treated soils boundaries condition for dynamic load behaviors from wheelbase in long section.

Researchers commonly adopt the following formula, which considers the displacement influence factors, to determine the elastic settlement for the shallow foundation structure:

$$S_e = qB\frac{1-\nu_{soil}}{E_{soil}}I \tag{3}$$

Where S_e is the elastic settlement of the soil ground, q is applied stress (Boussinesq formula is commonly used), B is the diameter of the foundation, (I) is a parameter that reflects the footing shape, while E_{soil} and ν_{soil} are the Young's modulus and Poisson's ratios of the underlying natural ground. Based on Poulos 1968, for circular rigid geometry, the influence factor is assumed to be 1, although the flexible geometry was considered $\pi/4$. Das (1985) reported that for a square footing the factor can be estimated using the ratio between the length and width of the rectangular geometry. However, a definite way of estimating the shape parameter for cement-treated shallow soil profile is lacking.

A simple soil profile unit is adopted in this study to estimate the elastic settlement of CTS, considering the wheelbase position as illustrated in **Fig. 5.1** for describe the cross section and **Fig. 5.2** in longitudinal section from railway track. Initially, the most severe case is considered, which is associated with the highest axial load due to the wheelbase position of the HSR (Jeon et al. 2015; Hu et al. 2015). Furthermore, The circular geometry equation of elastic settlement is generally used to estimate the equivalent rectangular shape factor under uniform loading (Horikoshi, 1997; Mayne, 1999), which can be expressed as follows:

$$B_{CTS} = \left(\frac{4BL}{\pi}\right)^{0.5} \; ; \; a = 0.5B_e \tag{4}$$

Where B_{CTS} is breadth of section from the rectangular geometry. To determine half rectangular shape, it can be described with a. This equivalent was used to determine the ratios between breadth (B) shape larger than length (L) shape. To optimize the aspect ratio of B and L, which can be suggest as follows:

$$b = \left(\frac{B_{CTS}}{L_{CTS}}\right) \tag{5}$$

Where this aspect ratio of breadth and length (b) has been considered determining the B_{CTS} is shorter than L_{CTS}. Using the aspect ratio with b parameter is defined a consistency of boundaries condition to predict the elastic settlement prediction. Based on the equivalent of rectangular shape, and b parameter, it can be used to evaluate the influence factor and dynamic load on shallow stabilization layer

5.3.1 Maximum dynamic load on shallow stabilization

The railway substructure has advantages in reducing stress transmitted load from the axle load of a train (Lazorenko et al., 2019). In this research was provided the dynamic mechanical properties of the CTS by using laboratory testing result in small strain ranges, it can be optimized the evaluation of transmitting load through the ground. In general, to determine the transmitting load that has an option such as Boussinesq method, which was used for homogeneous ground (Hu et al., 2016). However, evaluating the CTS during the construction period to the serviceability phase using dynamic load can improve with the spring mass function. Therefore, Worku (2017) was mentioned about the spring mass system of rectangular geometry on substructure, is expressed on below:

$$k_v = \frac{4 \cdot G \cdot B}{1 - \nu} \tag{6}$$

Where k_v to define the vertical spring mass system is based on the circular shape form, which should be determined using G and ν. In order to determine the equivalent geometry of the CTS aspect ratio, it can be suggested as below:

$$k_{CTS} = \frac{G_{CTS} \cdot B_{CTS} \cdot b}{1 - \nu_{CTS}} \tag{7}$$

Where k_{CTS} has been denoted to the equivalent of vertical spring mass system is based on the substituting the aspect ratios (b) on the CTS equilibrium position. Therefore, the dynamic parameters of CTS was defined by the shear modulus(G_{CTS}) and Poisson ratio (ν_{CTS}). In order to evaluate the k_{CTS} under natural response of CTS loading, which can be defined by natural angular frequency (ω_n), that can be derived as below.

$$\omega_n = \sqrt{\frac{k_{CTS}}{m}} \tag{8}$$

Natural angular frequency (ω_n) that indicate to the natural vertical vibration movement from cement treated soil above natural soil ground. Mass of cement-treated soil (m) can be calculated using the volume of CTS. In order to analyses the dynamic force on CTS, there are requirements to define angular frequency (ω) from train loading to the ground (Soomro, 2019). The requirement can be described on a frequency range, it was quite large, about 10 to 300 Hz that sources according to the train loading (Hu et al., 2016; Wang and Cox, 2012). Most often, for clayey soil the vibrational frequency has been evaluated within the ranges of 11 – 25 Hz (Lazorenko et al., 2019). In this research, train frequency was applied 11 Hz (Jones, 1994). Therefore, to determine the angular frequency (ω) from the train can be delineated as follow:

$$\omega = 2 \cdot \pi \cdot f_{train} \tag{9}$$

$$F_{dy} = W \pm \frac{Q_o}{1 - \omega/\omega_n} \tag{10}$$

Estimation of ω_n and ω has been provided the key parameter to estimating the maximum and minimum dynamic forces (F_{dy}) of axle load. Where W is the total mass of the CTS structures and Q_o is the point load based on wheelbase distribution

on the high-speed train. This study was used the 140 kN of stress above the natural ground, it represents the 2.5 m of wheel base (Hu et al., 2016).

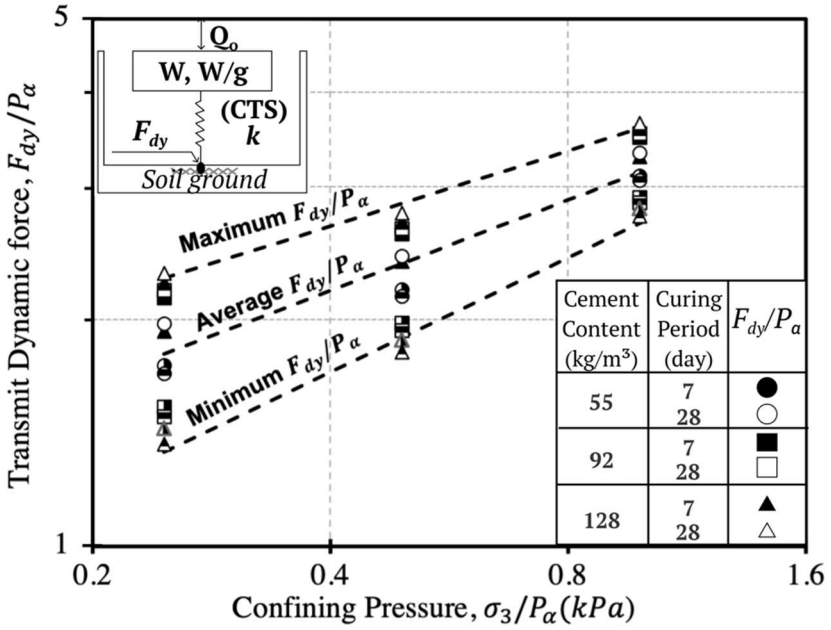

Fig. 5.3 Force vibration of mass-spring system on CTS related to increment of confining pressure.

Through this equation, it can illustrate the maximum and minimum ranges of dynamic force transmitted through the reference point, as delinated in **Fig. 5.3**. The dynamic load passing the low cement content of CTS was showed insignificant impact, which is comprises with a flexible form of substructure associating with the low mixing ratios. However, increasing the curing period at the same time by confining pressure was depicted the trend curve had showed a degrade shape form within maximum to minimum range of dynamic load.

Furthermore, dynamic force can be evaluated with the normalized confining pressure . The relationship between normalized confining pressure and dynamic forces can be suggested below:

$$F_{dy} = \alpha(\sigma_3/P_a)^{\beta} \tag{11}$$

Where σ_3/P_a is confining pressure and divided by atmospheric pressure in the same units, α and β is coefficient parameter regarding the intercorrelation between differences of dynamic load and cement content. The influences was showed through a power function, it can be obtained an intercorrelation between coefficient parameter on cement content, curing period and normalized confining pressure (σ_3/P_a) against F_{dy}.

5.3.2 Displacement influence factor of cement-treated soils layer

Displacement influence factor was considered by vertical deflection beneath the substructure within the dynamic load. To evaluate the maximum displacement at the center of CTS ground, it can be evaluated by a thickness of stabilization layer. (Poulos and Davis, 1968) and (Mayne and Poulos, 1999) was mentioned about the general derivation for influence vertical strain, in this research was derived as follow:

$$\frac{\sigma_z}{F_{dy}} = 1 - \left[1 + \left(\frac{b}{z}\right)^2\right]^{-1.5} \tag{12}$$

$$\frac{\sigma_r}{F_{dy}} = \frac{1}{2}(1 + 2\nu_{CTS}) - (1 + \nu_{CTS})\left[\left(\frac{b}{z}\right)^2 + 1\right]^{0.5} + \frac{1}{2}\left[\left(\frac{b}{z}\right)^2 + 1\right]^{-1.5} \tag{13}$$

Where $(\frac{\sigma_z}{F_{dy}})$ is vertical stress ratio with axial dynamic loading, also, the aspect of geometry in radial dimension has been considered replacing with the ratio in rectangular shape, which is parameter b. The evaluation has been expected to calculate the ratio of thickness layer (z) with parameter b. A similar replacement derivation was used to evaluate the radial stress ratio with axial dynamic loading reflect to the aspect ratio parameter b. Also, For ν_{CTS} is the Initial Poisson's ratios based on a CTS layer. Based on that estimation, it can be develop the influence of vertical strain, that is suggested as below:

$$\Delta \mathrm{I}_z = \left(\frac{1}{E_{CTS}}\right)(\Delta\sigma_z + 2\nu_{CTS}\Delta\sigma_r) \tag{14}$$

$$I_{CTSD} = \sum \Delta \mathrm{I}_z \cdot (\Delta z/b) \tag{15}$$

Where $\Delta \mathrm{I}_z$ is determined as a vertical strain at normalized depth, which can be estimated by using several parameters such as E_{CTS} as initial of Young Modulus of CTS layer and ν_{CTS}, that mechanical behavior was associated with radial and axial stress. However, to analyze the ICTSD as influence displacement factor of CTS, it requires to evaluated using the depth increment of substructure thickness and aspect ratio of rectangular shape ($\Delta z/b$). Furthermore, to validated the CTS thickness layer with ICTSD parameter at certain depth, it has been obtained by relations with σ_3/P_acan be suggested below:

$$I_{CTSD} = \alpha(\sigma_3/P_a)^{\beta} \tag{16}$$

Where α and β are varies of coefficient parameters of cement content. Those parameters were defined in small strain ranges, which show the relations in power function. **Fig. 5.4** depicts the influence factor tends to decreasing rate when σ_3/P_a ratios becomes bigger. This behavior was clarified the influences of parameters that could be control a thickness layer of CTS. The parameters behavior were plotted in logarithm scale in horizontal and vertical axis. In 55 kg/m^3 of cement content the relations were showed the discrepancies between the medium to the higher cement content, although the gradient of slope is occurs the similarity. Based on cement content behavior, 128 and 92 kg/m3 was determined in less than 1 reflect to the displacement influence factor. Furthermore, applying low cement content was categorized into the excessive influence factor, it would be a high vertical displacement induced thin layer ratios of CTS. In addition, increasing cement content and thickness layer of CTS should be reduced the I_{CTSD} and settlement behavior on the soil ground.

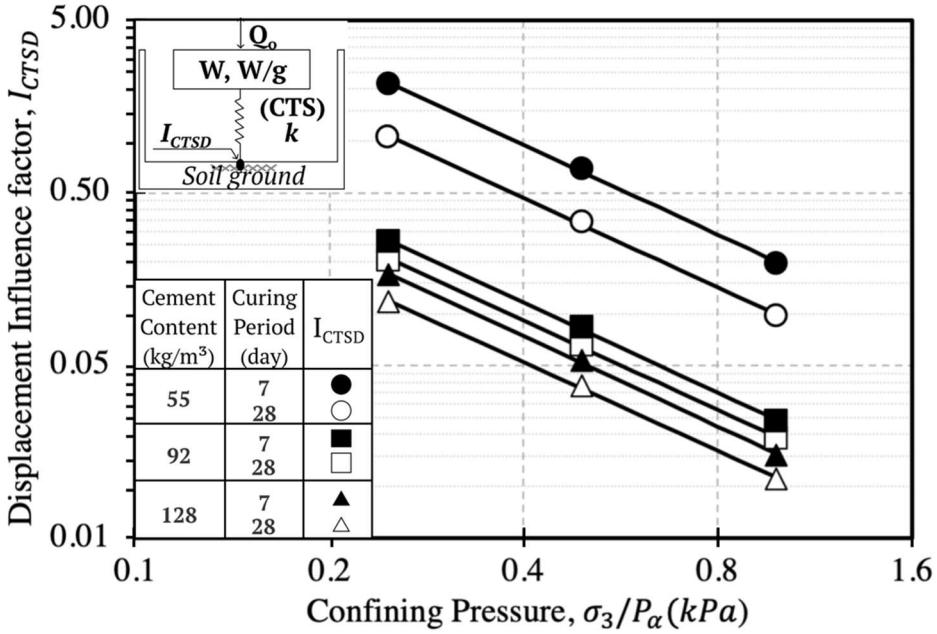

Fig. 5.4 Displacement influence factor (I_{CTSD}) of CTS related to the confining pressure (σ_3/P_a).

5.3.3 Rigidity correction factor related to stiffness ratio of cement-treated soils

Influence of increasing rigidity at CTS layer is an index to represent how properly the CTS has been improved the natural ground. Based on the mechanical properties of CTS in small-strain ranges, the strength increase is much dependent upon the curing period and cement content, which can be showed by observing into logarithm curve of mechanical properties and σ_3/P_a (Putera et al., 2022) .In order to optimized the elastic settlement prediction for CTS, it needs to showed the influence foundation flexibility factor relationship with the variants of σ_3/P_a. Refer to the classification of rigidity in shallow reinforcement structure, the factor is calculated using the equation such a below (Horikoshi and Randolph, 1997; Mayne and Poulos, 1999):

$$K_F = \left(\frac{E_F}{E_S}\right)\left(\frac{z}{a}\right)^3 \tag{17}$$

Where the K_F is describe the foundation flexibility factor, the initial form is derived with stiffness ratios between structure-soil. In order to determine an ideal solution of CTS stiffness, it should be showed the linkage between mechanical properties of CTS with increment stiffness by curing period and thickness layer. It can be suggested as below:

$$K_{CTS} = b\left(\frac{E_{CTS}}{E_S}\right)\left(\frac{z}{B_{CTS}}\right)^3 \tag{18}$$

Those assumption of CTS increment stiffness has been determined by using the Eq. 17, where using CTS aspect ratios areas (b) and evaluate the stiffness ratio between E_{CTS} with E_s from natural ground. **Fig. 5.5** has been shows the relationship between K_{CTS} and σ_3/P_a, it may contain the steep curve regarding the logarithm scale. The influence factors was showed a higher discrepancy of 128 kg/m^3 to the 55 kg/m^3, it may comprises of low stiffness ratio and higher stiffness ratios. The result for the relations K_{CTS} and σ_3/P_a has been showed as follows:

$$K_{CTS} = \alpha(\sigma_3/P_a)^{\beta} \tag{19}$$

Where α and β are varies of coefficient parameters subjected to cement content and curing period. Among those parameters it can be evaluated the influences factors related to the rigidity correction factors of CTS. That can be suggested as below:

$$I_{CTS} = \frac{\pi}{4} + \frac{1}{(4.6 + 10\,K_{CTS})} \tag{20}$$

Where K_{CTS} is stiffness factor of CTS and I_{CTS} is influelence of rigidity correction factor of CTS. Based on previous researcher the relations was defined by the curvature slope, following the analytical solutions for perfectly rigid and flexible are shown at $I = 1$ and $I = \frac{\pi}{4}$, respectively. In order to estimate the I_{CTS}, it can be observed in **Fig. 5.6**.

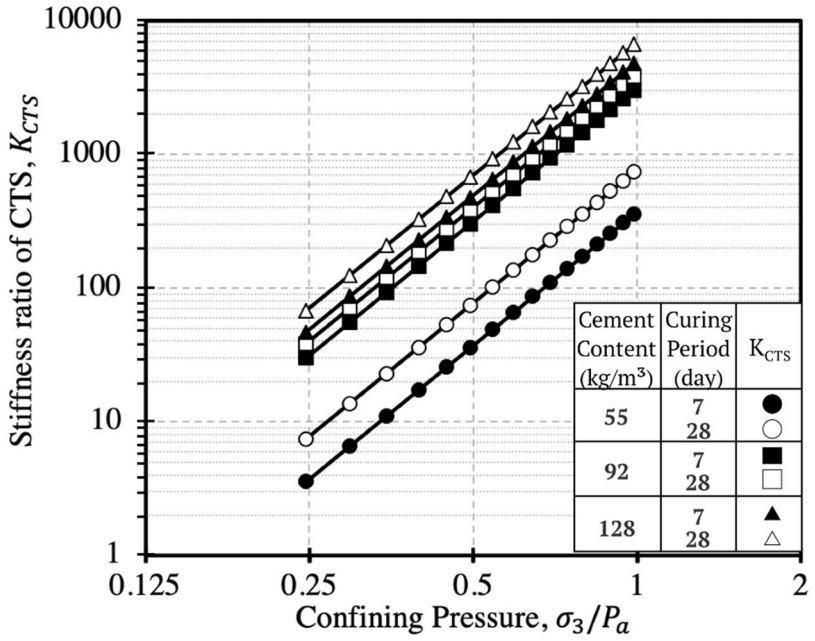

Fig. 5.5 Stiffness ratio of CTS (K_{CTS}) related to the confining pressure (σ_3/P_a).

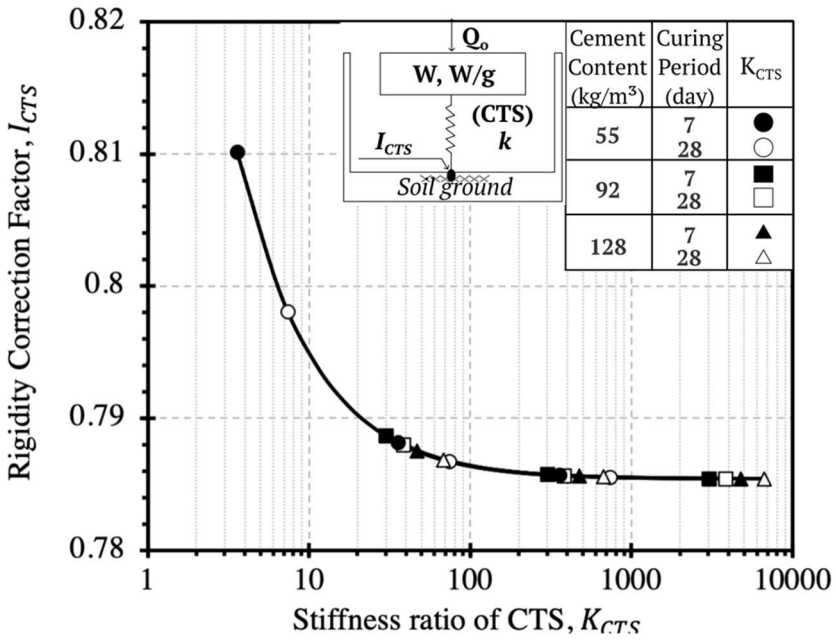

Fig. 5.6 Rigidity correction factor (I_{CTS}) of CTS related to Stiffness ratio of CTS (K_{CTS}).

For 55 kg/m3 was calculated within intermediate ranges, although the 92 kg/m3 and 128 kg/m3 had achieved to rigid structures, I_{CTS} factors becomes decreases at

the same time as increasing curing period. However, using the low cement content to the elastic settlement prediction could be affected the vertical displacement behaviors, it caused by the lacked of stiffness and slightest of increment strength respected to the curing period. In addition, the elastic settlement prediction of CTS should be estimated effectively regarding the distribution of thickness layer and curing periods behavior.

5.3.4 Elastic settlement prediction of cement-treated soils subjected to curing time in small-strain ranges

Among, many elastic settlement predictions in natural soils ground are selected and briefly introduced the influence factor using empirical approaches based on this research boundaries. Primarily, this research was focused on achieve the optimum design of settlement in high-speed railway project, it is vital for predict elastic settlement subjecting to dynamic force from high-speed train and increment strength of CTS within serviceability phase. Thus, the settlement prediction at the center for rectangular shape of CTS layer can be approximately given by:

$$S_{eCTS} = F_{dy} \cdot B_{CTS} \cdot \frac{1 - \upsilon_{soil}^2}{E_{soil}} I_{CTSD} I_{CTS} \tag{21}$$

Where the F_{dy} has been obtain using the eq (9), I_{CTSD} is normalized of displacement influence factor at certain depth, I_{CTS} is normalized of influence rigidity factor of CTS. If analyzing the variants of influence factors subjected to the boundary conditions, it was required to used a comparable variety of cement content, curing period and thickness layer. When dealt with curing time period, is required to estimate settlements against time dependent with simple interpolation formula. To calculate the discrete settlement with increment of curing period, it can be obtained using a good relations between cement content to the mechanical properties, which was estimated the settlement against time by power functions (Kang et al., 2017). Commonly, The construction period has ended at least one year, which is continuous within the serviceability phase afterward.

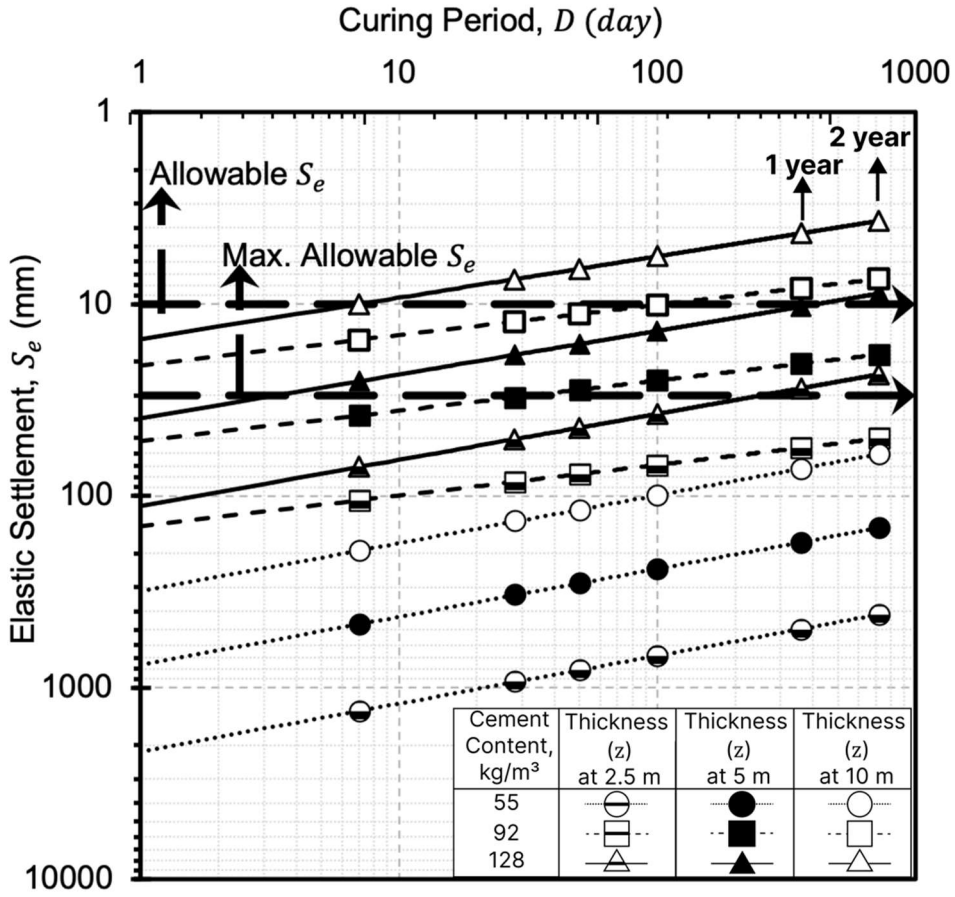

Fig. 5.7 Elastic settlement of CTS with curing period based on rigidity correction factor (I_{CTS}) and displacement influence factor (I_{CTSD}).

In **Fig. 5.7** has been described the relationship between the decent trend index on elastic settlement reflect to the curing period, it was described the effect by increasing cement content and thickness of cement-treated soil layer. When monitored the maximum allowable settlement, it was achieved the requirement of 1-year period by using 92 kg/m3 of cement content with thickness of layer about 5 m. Otherwise, in 128 kg/m3 of cement content can be cut down a time periods to obtained higher strength and low settlement induced during serviceability in advanced. Particularly, to obtaining a minimum range of allowable settlement at 10 mm should be rigorous monitor by curing time period and high cement content approaches. In order to evaluate the dynamic load behavior of High-speed railway. It has been showed the contribution of maximum dynamic load on High-speed

railway was used as a vital role in predicting elastic settlement with different variable of cement content and thickness of layer. At low cement content was showed the higher influences of maximum dynamic load, that would be cause by inadequate stiffness.

5.3.5 Elastic settlement prediction of cement-treated soils subjected to thickness layer in small-strain ranges

The elastic settlement prediction using this research boundaries was became acceptable for settlement requirements when the thickness of the cement-treated soil layer was increased. However, to obtain an optimum design related to the thickness layer is applicable with comparison on the variety of cement content parameters. To evaluate the thickness layer, it can be evaluated by plotting the various thickness reflecting to the result of the elastic settlement prediction. The relations between elastic settlement prediction with thickness layer of cement-treated soil has been suggested as below:

$$S_{eCTS} = \alpha(z)^{\beta} \tag{22}$$

Where S_e to define the elastic settlement at the center point of CTS, α and β are parameters subjected to the variety of cement content and curing period. **Fig. 5.8** was explained the elastic settlement behavior in 55 kg/m3 of cement content subjected to the thickness layers is not acceptable for maximum allowable settlement. In order to achieve the allowable settlement of low cement content, it can conduct a suitable combination of ground improvement with deep mixing and group column type. The combination should be optimized using the shallow layer of CTS (Kitazume and Terashi, 2013). In **Fig. 5.9** was delineated the influence of 92 kg/m3 of cement content with. The ranges of allowable settlement were showed the variability of thickness layers has reaching the maximum allowable settlement, it can be utilized by using 5 m of cement treated soils. On the other hand, for 10 mm of allowable settlement, it should be enhanced with 10 m thickness layer. Furthermore, it needs to 1-year period for awaiting into operation time.

In advanced, the increasing of cement content has been distinguished the curing period and thickness layer of cement-treated soil, as illustrated in **Fig. 5.10**. It can be replied by seen the curve of the maximum allowable settlement was assured within 28 days of curing time period by deploy the 5 m of thickness. Simultaneously, for the minimum allowable settlement can be achieved by 1-year period of curing time, that was considered by expand on 5 m of CTS thickness.

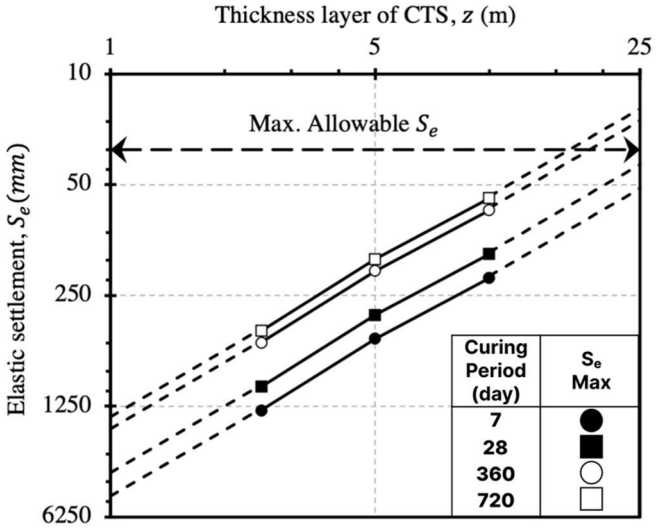

Fig. 5.8 Elastic settlement (S_e) vs thickness layer of CTS in 55 kg/m^3 of cement content under small strain ranges and maximum of dynamic forces.

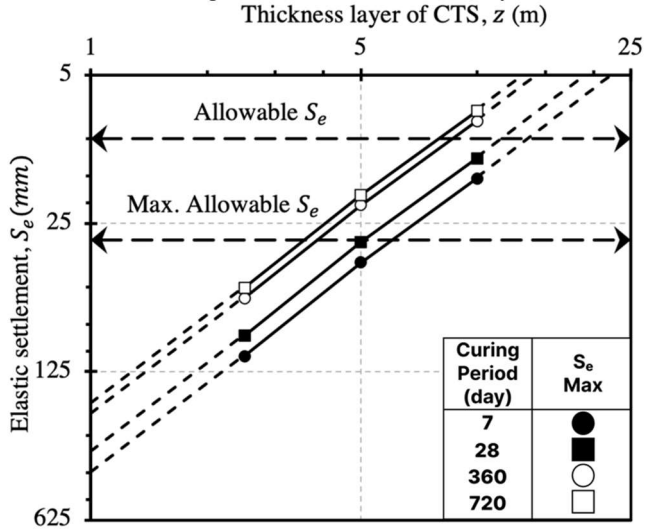

Fig. 5.9 Elastic settlement (S_e) vs thickness layer of CTS in 92 kg/m^3 of cement content under small strain ranges and maximum of dynamic forces.

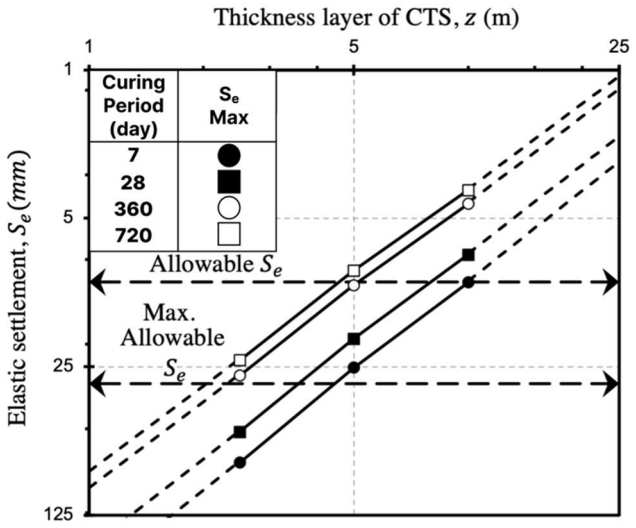

Fig. 5.10 Elastic settlement (S_e) vs thickness layer of CTS in 128 kg/m^3 of cement content under small strain ranges and maximum of dynamic forces.

Fig. 5.11 illustrates the determination process of S_e that was mainly conducted to the thickness layer of CTS, curing periods and maximum dynamic forces. The varieties of input parameters have been considered by estimation formula of CTS mechanical behaviors, It should be measured by using the small-strain measurement in the triaxial undrained testing or empirical formula by calculating the coefficient parameters of cement content and confining pressures. The essential procedure is to evaluate the maximum dynamic forces was concerned by substituting the aspect ratio, it explained the parameter b on specific derivation, which can be described to assessing the vertical spring system and transmitting force through the CTS layer. Based on those input parameters, it could be started to the evaluation of influence factors.

Estimation of the influences factors was determined by the I_{CTS} and I_{CTSD}, that account for the optimizing thickness layer and increment strength of CTS reflect to the curing period. It is worth to mentioning the evaluation of elastic settlement using the influence factors on elastic settlement prediction was enhanced the prediction method within curing time and thickness layer of CTS. However, the limitations of elastic settlement prediction are necessary to extend the further curing period of

CTS sample, especially for long-term serviceability phase estimation on the maintenance periods.

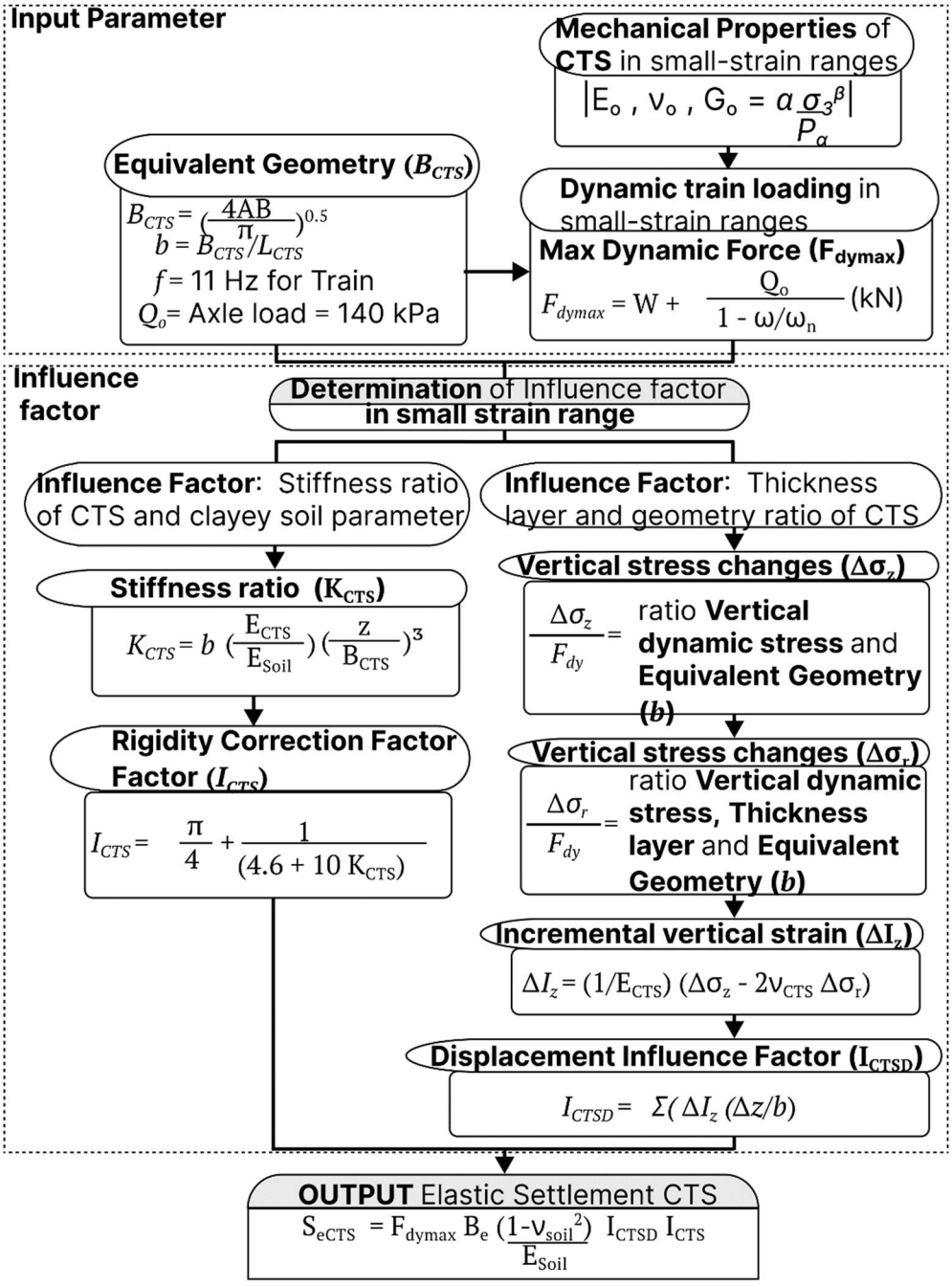

Fig. 5.11 Elastic settlement (S_e) determination process reflecting to the result of mechanical properties within small-strain ranges.

5.4 Summary

Through this chapter, the mechanical characteristics of cement-treated clayey soil underlying a high-speed train railway were experimentally investigated to elaborate on the elastic settlement behavior, considering the influence of the cement content and the confining pressure. Focusing on the small strain range, a series of triaxial undrained testing equipped with local displacement transducers (LDT) was carried out to optimize the cement mizing ratio and curing time aiming at supressing the elastic settlement within the standard requirements. Furthermore, a model was proposed to estimate the settlement of cement-treated clayey soil. The main findings of this study can be outlined as follows:

A simple power formula that captures the initial mechanical properties parameters (Young's modulus, Poisson's ratio, shear modulus) as a function of the confining pressure, cement content, and curing periods was proposed. It was found that the Young's and shear moduli for a straight line on a log-log scale versus the cement content and confining pressure.

A simple elastic settlement prediction model was proposed for cement-treated clayey soil subjected to dynamic loading (high-speed train), focusing mainly on the small strain range. The model included three main factors to reflect the applied dynamic force (F_{dyn}), displacement influence factor (I_{CTSD}) and rigidity correction factor (I_{CTS}). A power formula was emperically intorduced to express the new factors as functions of the confining pressures. The model can estimate the time-dependent elastic settlement of cement-treated soils based on the measured small strain mechanical properties of at least two curing periods, assuming an extrapolation using the proposed power formula.

The prediction model optimized the mixing ratio at a specific curing period, reflecting the wheel-base loading on the cement-treated soil layer. For example, using Ariake clay, subjected to dynamic loading of 140 kN force spanning over 2.5 m wheel-base, the elastic settlement can be minimized using high cement content

> 100 kg/m3, While the curing period should not be less than 100 days to ensure achieving the aimed hardening of the cement.

References

Ando, K., Sunaga, M., Aoki, H., Haga, O., 2021. Development of slab tracks for hokuriku shinkansen line. Quarterly Report of RTRI 42, 35–41.

Archer, A., Heymann, G., 2015. Using small-strain stiffness to predict the load-settlement behaviour of shallow foundations on sand. Journal of the South African Institution of Civil Engineering 57, 28–35.

Atkinson, J., 2000. Non-linear soil stiffness in routine design. Geotechnique 50, 487–508. https://doi.org/10.1680/geot.2000.50.5.487

Benz, T., Schwab, R., Vermeer, P., 2009. Small-strain stiffness in geotechnical analyses. Bautechnik 86, 16–27. https://doi.org/10.1002/bate.200910038

Das, B.M., 1985. Advanced soil mechanics. McGraw-Hill, New York.

Das, B.M., Ramana, G.V., 2010. Principles of soil dynamics, Second edition. ed. CL Engineering.

Fang, H.-Y., Daniels, J.L., 2006. Introductory Geotechnical Engineering: An Environmental Perspective (1st ed.)., 1st ed. CRC Press, London.

Foye, K.C., Basu, P., Prezzi, M., 2008. Immediate Settlement of Shallow Foundations Bearing on Clay. international Journal of Geomechanics 8, 300–310. https://doi.org/10.1061/(ASCE)1532-3641(2008)8:5(300

Goto, S., Tatsuoka, F., Shibuya, S., Kim, Y.-S., Sato, T., 1991. A Simple Gauge for Local Small Strain Measurements in the Laboratory. Soils and Foundations 31, 169–180. https://doi.org/10.3208/sandf1972.31.169

Horikoshi, K., Randolph, M.F., 1997. On the definition of raft—soil stiffness ratio for rectangular rafts. Géotechnique 47, 1055–1061. https://doi.org/10.1680/geot.1997.47.5.1055

Hu, J., Bian, X., Jiang, J., 2016. Critical Velocity of High-speed Train Running on Soft Soil and Induced Dynamic Soil Response. Procedia Engineering 143, 1034–1042. https://doi.org/10.1016/j.proeng.2016.06.102

JETRO, 2012. Study on the high speed railway project (jakarta-bandung section), republic of indonesia (Final report (Summary)), Feasibility study for promotion of international infrastucture projects in fy2011. Yachiyo Engineering Co., Ltd. and Japan International Consultants for Transportation Co., Ltd.

Jones, C.J.C., 1994. Use of numerical models to determine the effectiveness of anti-vibration system for railways. Proceedings of the Institution of Civil Engineers - Transport 105, 43–51. https://doi.org/10.1680/itran.1994.25706

Kanazawa, H., Tarumi, H., 2010. Technical transition of earth structures for shinkansen. SOILS AND FOUNDATIONS 50, 817–828. https://doi.org/10.3208/sandf.50.817

Kang, G., 2016. Influence and Control Strategy for Local Settlement for High-Speed Railway Infrastructure. Engineering 2, 374–379. https://doi.org/10.1016/J.ENG.2016.03.014

Kang, G., Tsuchida, T., Kim, Y., 2017. Strength and stiffness of cement-treated marine dredged clay at various curing stages. Construction and Building Materials 132, 71–84. https://doi.org/10.1016/j.conbuildmat.2016.11.124

Kitazume, M., Terashi, M., 2013. The deep mixing method, in: The Deep Mixing Method. CRC Press/Balkema, Leiden, The Netherlands.

Kumar, P., Singh, V., 2017. Geotechnical Aspect for Design of Track Formation System for High Speed Rail Lines on Alluvial Soil Deposited-A Review.

Lazorenko, G., Kasprzhitskii, A., Khakiev, Z., Yavna, V., 2019. Dynamic behavior and stability of soil foundation in heavy haul railway tracks: A review. Construction and Building Materials 205, 111–136. https://doi.org/10.1016/j.conbuildmat.2019.01.184

Lee, J., Kyung, D., Kim, B., Prezzi, M., 2009. Estimation of the Small-Strain Stiffness of Clean and Silty Sands using Stress-Strain Curves and CPT Cone Resistance. Soils and Foundations 49, 545–556. https://doi.org/10.3208/sandf.49.545

Mayne, P., Poulos, H., 1999. Approximate Displacement Influence Factors for Elastic Shallow Foundations. Journal of Geotechnical and Geoenvironmental Engineering - J GEOTECH GEOENVIRON ENG 125. https://doi.org/10.1061/(ASCE)1090-0241(1999)125:6(453)

Novico, F., Menier, D., Mathew, M., Ramkumar, M., Santosh, M., Endyana, C., Dewi, K.T., Kurniawan, I., Lambert, C., Goubert, E., Hendarmawan, 2022. Impact of Late Quaternary climatic fluctuations on coastal systems: Evidence from high-resolution geophysical, sedimentological and geochronological data from the Java Island. Marine and Petroleum Geology 136, 105399. https://doi.org/10.1016/j.marpetgeo.2021.105399

Pantelidis, L., Gravanis, E., 2020. Elastic Settlement Analysis of Rigid Rectangular Footings on Sands and Clays. Geosciences 10. https://doi.org/10.3390/geosciences10120491

Poulos, H., Davis, E., 1968. The Use of Elastic Theory for Settlement Prediction Under Three-Dimensional Conditions. Geotechnique 18, 67–91. https://doi.org/10.1680/geot.1968.18.1.67

Putera, M.A., Yasufuku, N., Alowaisy, A., Ishikura, R., Hussary, J.G., Rifa'i, A., 2022. Evaluating the small-strain mechanical properties of cement-treated clayey soils based on the confining pressure. (unpublished).

Putera, M.A., Yasufuku, N., Alowaisy, A., Rifai, A., 2021. Optimizing modified triaxial testing for small strain zone using local displacement transducers and bender element for cement-treated soft soil. E3S Web of Conferences 331. https://doi.org/10.1051/e3sconf/202133103003

Ranst, E.V., Utami, S.R., Vanderdeelen, J., Shamshuddin, J., 2004. Surface reactivity of Andisols on volcanic ash along the Sunda arc crossing Java Island, Indonesia. Geoderma 123, 193–203. https://doi.org/10.1016/j.geoderma.2004.02.005

Razouki, S.S., Al-Zubaidy, D.A., 2010. Elastic settlement of square footings on a two-layer deposit. Proceedings of the Institution of Civil Engineers - Geotechnical Engineering 163, 101–106. https://doi.org/10.1680/geng.2010.163.2.101

Skempton, A.W., Bjerrum, L., 1957. A contribution to the settlement analysis of foundations on clay. Géotechnique 7, 168–178. http://dx.doi.org/10.1680/geot.1957.7.4.168

Soomro, Z.A., 2019. Analysis for angular velocity of railway wheelset measurement and creep error estimation. International Robotics & Automation Journal 5, 63–67. https://doi.org/10.15406/iratj.2019.05.00175

Wang, A., Cox, S.J., 2012. High-Speed Rail: Excitation Frequencies and Track Stiffness, in: Maeda, T., Gautier, P.-E., Hanson, C.E., Hemsworth, B., Nelson, J.T., Schulte-Werning, B., Thompson, D., de Vos, P. (Eds.), Noise and Vibration Mitigation for Rail Transportation Systems. Springer Japan, Tokyo, pp. 151–158.

Worku, A., 2017. The use of springs in static analysis of structures to account for short-and long term subgrade deformations. Journal of Experimental Aircraft Association 24.

Yamashita, S., Kawaguchi, T., Nakata, Y., Mikami, T., Fujiwara, T., Shibuya, S., 2009. Interpretation of International Parallel Test on the Measurement of Gmax Using Bender Elements. Soils and Foundations 49, 631–650. https://doi.org/10.3208/sandf.49.631

Chapter 6
Conclusions and Future Work

6.1 Conclusions

This thesis was aimed to evaluate the empirical method for elastic settlement prediction of cement-treated clayey soil in relation to the dynamic load in small-strain ranges. Focusing on the mechanical behavior in small-strain ranges, it can be evaluated by triaxial testing that equipped with axial-radial LDTs. To enhance the prediction of elastic settlement of cement-treated soils during the experimental test was developed by the various of cement content for evaluate the optimum mixing ratio, confining pressure for define the thickness layer and curing period for predict the long term of settlement. This means to elaborate the small-strain mechanical behavior with the prediction model, it is required to keep the boundaries condition that reflected to geometry were located on the highest axial stress within the wheel-base. The main conclusions can be drawn as follows:

1. It was found the consideration of cement-treated clayey soil preparation method to getting the good accuracy of evaluating the initial stiffness modulus. The step need to consider is determining cement content by natural soil ground engineering properties and the boundary condition of the element test (ranges of evaluating the confining pressure). In determining cement content to the mixing phase, it has been paying attention to preparing the soil-mixing binder into the acrylic mold with stopper for the Bender Element specimen and normal plastic mold for the LDTs specimens.

2. To maintain the accuracy of LDTs and BE, there are several configurations before doing the test. Those devices are sensitive to the stress-strain behavior, regarding the high deviatoric stress is induced during a shearing process in triaxial test that are carefully handled is required. To calibrate the LDTs with a good accuracy in small-strain ranges, it considered the uniaxial test evaluating the axial strain with voltage relationship by non-linear curves and radial strain with voltage in linear curves. To ensuring the accuracy of measurement and prevent the detachment behavior during the shearing process, it suggested the surface of LDT's hinge-attachment needs apply the epoxy glue and double-sided tape. For BE test the ranges of transmitting the wave frequency was obtained within the 1 – 5 kHz, the protection of BE devices was considered carefully using the filler and create the pilot hole $\pm$ 2 mm of maximum strain ranges, it contains the gypsum and bentonite (with 1:2 ratios of binder and water based on weight).
3. The accuracy in large-small strain ranges was discussed a significant discrepancy in the deviatoric stress-axial strain and axial-radial strain relationship, increasing cement content and confining pressure, the discrepancies become larger that was confirmed in increment of axial strain. BE test was measured the shear wave velocity and successfully evaluated the shear modulus using the filler, which was more profound under moderate confining pressure and low shearing process. Finally, to ensure reliable degradation stiffness modulus of the cement-treated clayey soils over the entire strain range, simultaneous testing using the combination of BE devices for determining elastic linear and LDTs for elastoplastic curves is highly recommended.
4. The result of shear strength of cement-treated soil using LDTs and LVDT was observed, through the large strain ranges is obtained a good accuracy in LDT measurement devices, especially in high cement content. To estimate the relationship between cohesion-cement content and friction angle-cement-content, it was determined by the power function formula. The positive slope of cohesion and cement content has been shown a good

relations. However, the friction angle was shown a similar gradient slope along the increment of cement content.

5. Mechanical properties (Young's modulus, Poisson's ratio, shear modulus relationship with confining pressure was described as good relations within small-strain ranges. That relationship was captured using the power function formula in logarithm scale.
6. Estimation of mechanical properties (Young's modulus, Poisson's ratio, shear modulus) as with cement content and confining pressure was proposed with a simple power function formula. In order to estimate the mechanical properties, parameter coefficient α related to the increment of mechanical properties and β correspond to the gradient of slope of the cement content has been evaluated with power function. Finally, the requirements of coefficient parameter can be obtained, then it can be using the coefficient parameter into estimation power function formula.
7. Prediction method of elastic settlement was empirically proposed for cement-treated clayey soil subjected to dynamic loading (high-speed train), various of thickness layer and cement content, which were focusing mainly on the small-strain range. It has been evaluated with a good relations using power function formula to estimate the post construction period. For example, using Ariake clay, subjected to dynamic loading of 140 kN force spanning over 2.5 m wheel-base, the elastic settlement can be minimized using high cement content > 100 kg/m3, While the curing period should not be less than 100 days to ensure achieving the aimed hardening of the cement.

6.2 Future work

In this thesis have been accomplished the objectivities and necessities of elastic settlement prediction method using triaxial testing result in small strain ranges. To enhances the final results from element testing and prediction method are required some validation method. Those are listed in future work as follows:

1. Based on the optimizing system of triaxial testing, it can be obtained the bender element test and filler materials combined with the LDTs. Using those small strain devices can improved the estimation of cement-treated soil mechanical behavior in small strain ranges especially in high cement content. This research did not consider the cyclic loading in shearing process, it can be a new approach to evaluate the dynamic loading mechanical behavior in small-strain ranges.
2. Evaluation mechanical properties of cement-treated soils that subjected in the small strain ranges was tested between 7 and 28 days curing period has been done. The result can predict the 2 year period using power function formula. However, to validate the long-term strength using power function formula, that requires more experimental testing conducted at least in serviceability phase (post construction period) after 1 year period.
3. The recommendation to validate the empirical method of elastic settlement prediction should be evaluated with finite element method, such as 3-dimensional method, which means the boundary condition could adjust using similar boundaries in the empirical model. The failure criterion in the finite element method should be evaluated more comprehensively. Furthermore, elaboration of mechanical behavior in small strain ranges with power function formula is necessary to be included in validation method, which has been captured the result shown a good of correlation the increment stiffness subjected to the confining pressure and cement content.